

LEGIBILITY NOTICE

A major purpose of the Technical Information Center is to provide the broadest dissemination possible of information contained in DOE's Research and Development Reports to business, industry, the academic community, and federal, state and local governments.

Although a small portion of this report is not reproducible, it is being made available to expedite the availability of information on the research discussed herein.

1987-01-16

Los Alamos National Laboratory is operated by the University of California for the United States Department of Energy under contract W 7405 ENG 36

LA-UR--87-2464

DE87 013164

TITLE Food for Thought: Five Lectures on Lattice Gauge Theory

AUTHOR(S) Rajan Gupta, Theoretical Division, Los Alamos National Laboratory, Los Alamos, NM 87545

SUBMITTED TO Proceeding of the CCAST Workshop on Lattice Gauge Theory Using Parallel Computers, Gordon Breach (1987)

DISCLAIMER

This report was prepared as an account of work sponsored by an agency of the United States Government. Neither the United States Government nor any agency thereof, nor any of their employees, makes any warranty, express or implied, or assumes any legal liability or responsibility for the accuracy, completeness, or usefulness of any information, apparatus, product, or process disclosed, or represents that its use would not infringe privately owned rights. Reference herein to any specific commercial product, process, or service by trade name, trademark, name, or otherwise, does not necessarily constitute or imply endorsement, recommendation, or favoring by the United States Government or any agency thereof. The views and opinions of authors expressed herein do not necessarily state or reflect those of the United States Government or any agency thereof.

By acceptance of this article, the publisher recognizes that the U.S. Government retains a nonexclusive, royalty-free license to publish or reproduce the published form of this contribution, or to allow others to do so, for U.S. Government purposes.

The Los Alamos National Laboratory requests that the publisher identify this article as work performed under the auspices of the U.S. Department of Energy.

MASTER

Los Alamos Los Alamos National Laboratory Los Alamos, New Mexico 87545

**FOOD FOR THOUGHT:
FIVE LECTURES ON LATTICE GAUGE THEORY**

RAJAN GUPTA[†]

MS-B285, Theoretical Division
Los Alamos National Laboratory
Los Alamos, N.M. 87545

ABSTRACT

The topics covered in these lectures are the heavy $q\bar{q}$ potential, glueballs, the chiral transition with dynamical fermions, Weak interaction matrix elements on the lattice and Monte Carlo renormalization group. Even though for the most part these lectures are reviews, many new results and ideas are also presented. The emphasis is a on critical analysis of existing data, exposing bottlenecks and a discussion of open problems.

[†] *J. Robert Oppenheimer Fellow*

INTRODUCTION

The comparison between QCD as the fundamental theory of strong interactions and experiments has so far been hampered by our inability to incorporate the low frequency modes in analytic calculations. Since quarks and gluons are not observed as asymptotic states, even the most energetic processes require an understanding of what is happening at the length scale of confinement. Thus the problem of strong interactions has to be addressed in a fundamental way. At present, the only technique with promise is Monte Carlo simulations of Lattice regularized QCD. As with any other calculation technique, the ingenuity lies in setting up the problem. In these lectures I will try to bring through the flavor that these calculations require the same type of cleverness, insight and analytical skills as a good phenomenologist calculating multi-loop Feynman diagrams. The execution of these calculations is following the path of experiments.

The topics I will cover are

- 1] The heavy $q\bar{q}$ potential.
- 2] The glueball Spectrum.
- 3] QCD with dynamical fermions: The Chiral transition.
- 4] Weak Interaction Matrix Elements on the Lattice.
- 5] Monte Carlo Renormalization Group.

The attempt is to make each lecture a self sufficient unit. The style of the lectures is critical and probably terse. I am allowed this liberty due to the excellent introductions by John Kogut and Mike Creutz. So, I will explore techniques, ideas and their virtues. The focus at all time will be on physics goals and how to obtain hard numbers.

My original contributions to this set of lectures are a product of many enjoyable collaborations. The support of Los Alamos, DOE (MFE) and Pittsburgh Supercomputer Center in providing time for the calculations is gratefully acknowledged. I thank Philippe de Forcrand, Greg Kilcup and Steve Sharpe for a critical reading and for many discussions, and Kim Maltman for helping me make the lectures readable.

These lectures are a result of T. D. Lee and Norman Christ's invitation to participate in the Lattice Gauge Symposium/Workshop Using Parallel Computers held in Beijing, 1987. To write them has lead to many sleepless nights, mainly because I wanted to emulate their style of clarity and depth. I hope they find them as insightful as was my journey into a wonderful land.

1) THE HEAVY $q\bar{q}$ POTENTIAL

The very attempt to construct a potential to describe the interaction of quarks restricts our focus to heavy fermions. It is only when the mass m is large that we can formulate the bound state of a $q\bar{q}$ system as a non-relativistic problem, with binding energies calculable from a potential via the Schrödinger equation. There exist two systems, charmonium and bottomonium that are made up of heavy quarks. The precision to which we can already measure their levels is shown in figure 1 [1]. Our goal is to derive a potential, check it against these levels, and then with it predict the anticipated toponium spectra.

The lattice calculations are non-perturbative but the potential we derive from them is "from first-principals" in a restricted sense only. There are two reasons a) we ignore dynamical quarks and b) we have to decide before hand what terms contribute to it. The lattice calculations do not predict a functional form. We have to make a trial ansatz and use the data from lattice calculations to fix the unknown parameters. So, if this lecture shows a certain lack of rigor, and has a certain flavor of phenomenology, do not be disappointed. As you will see, even with the modelling it is non-trivial to extract a potential and in any case this is the best option we have at the moment.

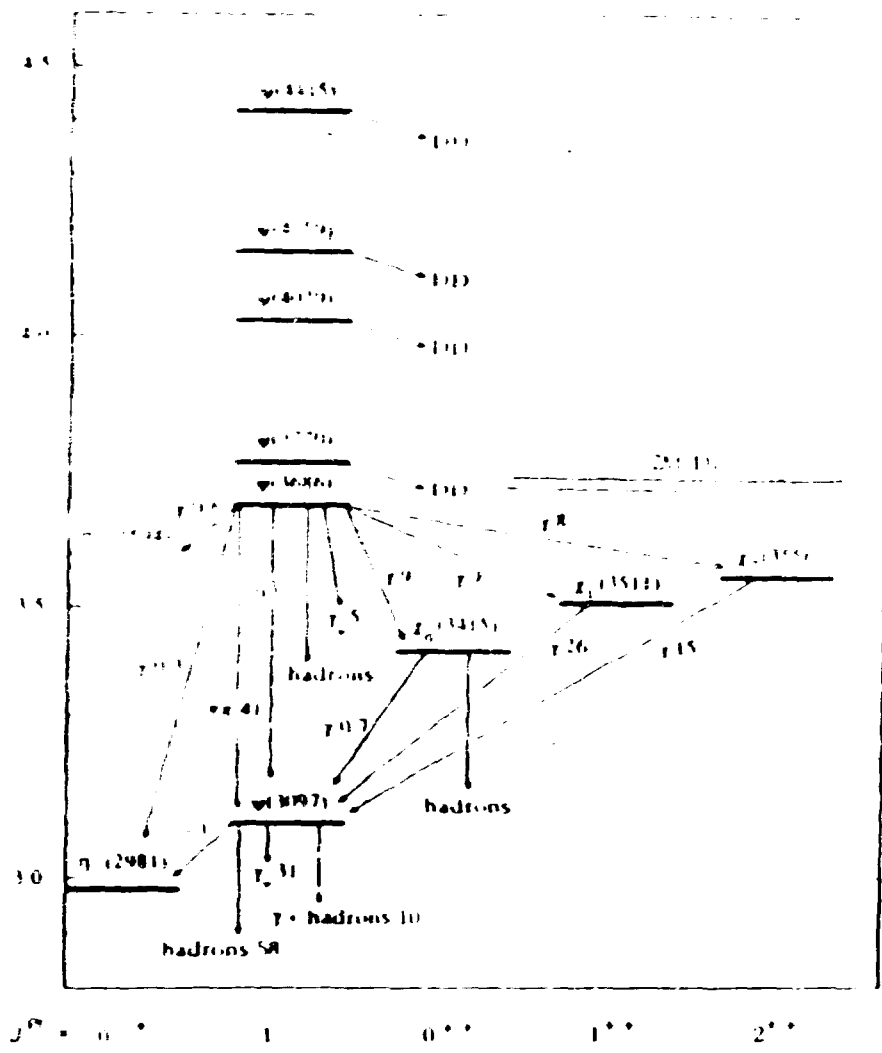
The discussion of the $q\bar{q}$ potential is broken into two parts. I will start with the spin-independent part of the potential which is also better understood.

1.1) Spin-Independent Potential: Phenomenology

General theoretical arguments provide the behavior of the spin independent potential in the two extreme regions. At large separations ($r \rightarrow \infty$), confinement dominates and the physical picture is of a "chromo-electric flux tube". The potential $V(r)$ behaves as a linear function of the distance:

$$V(r) \rightarrow \sigma r . \quad (1.1)$$

A good estimate of the string tension derived from the Regge slope is $\sigma \approx (420 \text{ GeV})^2$.



At the other end of the distance scale, *i.e.* short distances, the running coupling constant can be evaluated in perturbation theory. To leading order it is

$$\alpha_s(q^2) = \frac{\alpha_s(\mu^2)}{1 + \frac{33-2n_f}{12\pi} \alpha_s(\mu^2) \ln \frac{q^2}{\mu^2}} \quad (1.2)$$

With increasing q^2 it becomes weak, with a zero at $q^2 = \infty$. This property is called asymptotic freedom. In this weak coupling limit we expect the effective potential to approach the one gluon exchange result (Coulomb potential)

$$V(r) \rightarrow -\frac{4}{3} \frac{\alpha_s}{r} \quad (1.3)$$

where $\frac{4}{3}$ is the color factor and α_s is the QCD running coupling constant.

A simple form for the full effective potential is to take a linear combination, $a r + \frac{b}{r}$, parameterized by two independent constants a, b . Physically, these constants represent the scales at which an individual term begins to dominate. They can be fixed using the charmonium or bottomonium spectrum. This logic is a simple motivation for the Cornell potential [2]

$$V_c(r) = -\frac{0.48}{r} + (0.427 \text{Gev})^2 r \quad (1.4)$$

The constants are determined by fitting to charmonium. The predictions for bottomonium are pretty good.

Richardson [3] modified the perturbative running coupling constant so that it has built into it a linear long distance part. This ansatz restricts the number of free parameters to one. The potential is simple in momentum space:

$$V_r(q^2) = -\frac{4}{3} \frac{12\pi}{33-2n_f} \frac{1}{q^2 \ln(1 + \frac{q^2}{\Lambda^2})} \quad (1.5)$$

Again fixing Λ from charmonium, V_r does a good job on bottomonium also.

The last potential I consider is a totally heretical solution proposed by Martin [4]

$$V_m(r) = 5.82 \text{ GeV } r^{0.104} . \quad (1.6)$$

It too reproduces the data.

The three potentials are shown in figure 2 along with the mean charge radius of the onium states. Do we have any chance of finding the correct form when these three solutions, which are radically different, work as well as they do? The answer to the question is very simple: The range of r over which the potential has to be fixed to reproduce the charmonium and bottomonium spectrum is $r = 0.2$ to 1 fermi. In this interval the three potentials can be made to coincide by adjusting a single parameter as shown in the figure. They begin to deviate at $r > 1$ or < 0.1 fermi. The region $r > 1$ is the domain of light quarks, and there a simple potential model is hard to justify even if it seems to work at times. The only test of these potentials is toponium. For a top quark mass = 50 GeV, the charge radius, wavefunction at the origin and the binding energy are significantly different for the three cases. Estimates by Gilman [5] are shown in Table 1. The predictions for the three are very different. It should therefore be easy to distinguish between these potentials and maybe even constrain the parameters, or suggest if new terms are required. For the time being, to extract a potential from the lattice, we shall assume the form $(r + \frac{1}{r})$.

Potential	E_{1s} (GeV)	$\langle r_{1s} \rangle$ (fermi)	$E_{2s} - E_{1s}$ (GeV)	$\Psi(0)_{1s}$ (GeV ^{3/2})
Cornell	97.1	0.028	2.2	23.3
Richardson	96.3	0.048	1.0	8.5
Martin	98.6	0.084	0.5	2.7

Table 1: Characteristics of toponium states assuming a top quark mass of 50 GeV for the three potentials discussed [5].

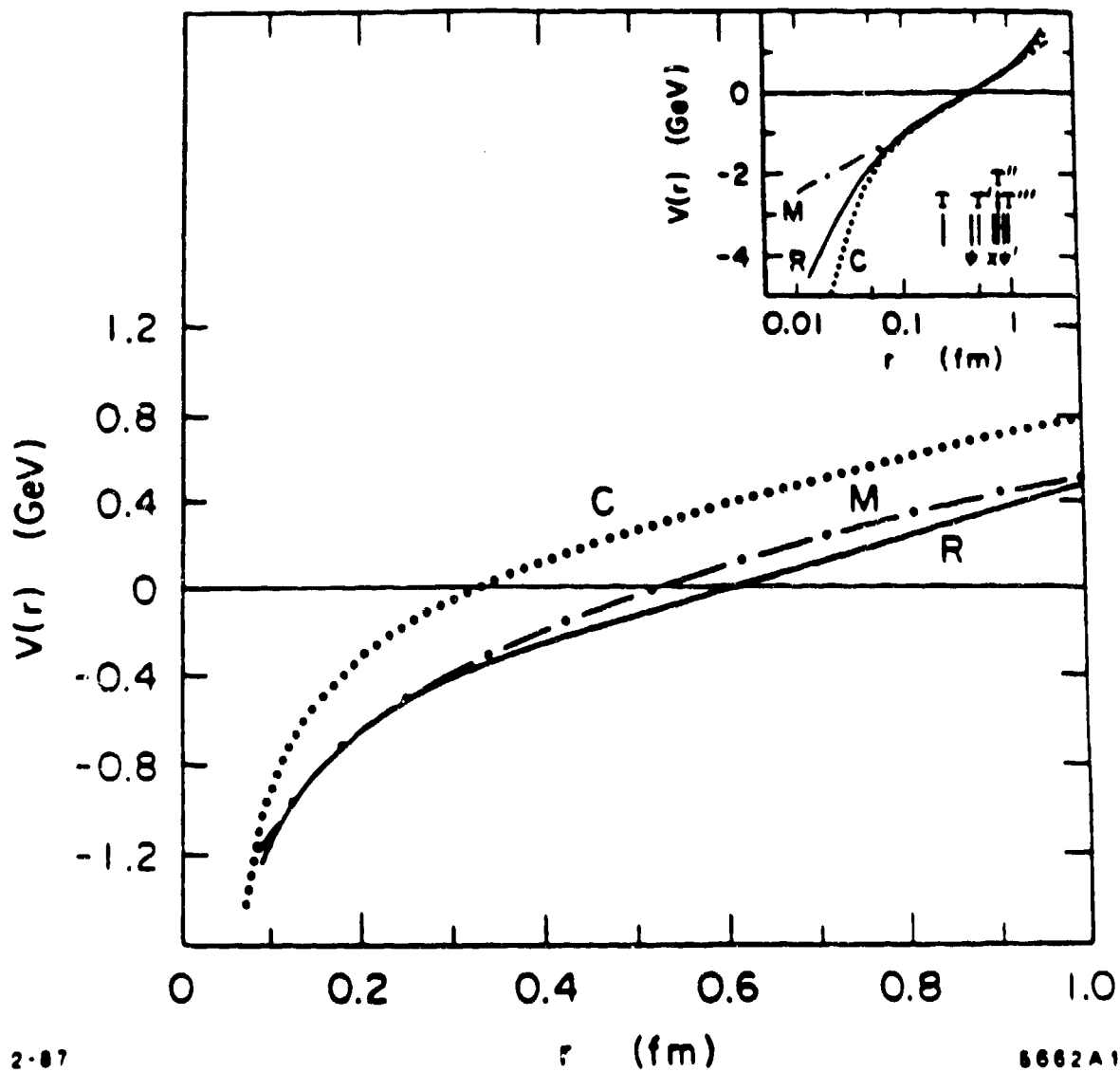


Fig. 2: Comparison of the shape of the Cornell [2] (dotted curve), Richardson [3] (solid curve), and Martin [4] (dash-dot curve) potentials. Also shown are the mean radii of some charmonium and bottomonium states.

1.2) Extracting the Spin-Independent Potential from the Lattice

To fix the parameters of the simple $(r + \frac{1}{r})$ potential, I break up the separation r between $q\bar{q}$ into three regions: 1) Confining, characterized by the linear term at large r ; 2) Perturbative, where the $\frac{\sigma}{r}$ potential with a running coupling constant is manifest and 3) intermediate r , for which we don't have a good handle. The attempt will be to work in a given region and fix one or more parameters. Then we have fewer free parameters when making fits in other regions. Now onto the lattice.

Let us for starters assume that we have at our disposal extremely good data for arbitrarily large Wilson loops. Then to extract the spin independent potential one defines

$$V(R) = - \lim_{T \rightarrow \infty} \frac{1}{T} \ln W(R, T) . \quad (1.7)$$

A quick derivation of this potential is as follows: The term in the action representing the interaction of a scalar charge with the gauge field is $\int j_\mu A^\mu$. Let the current j_μ be due to a heavy external charge propagating in a closed loop, then the extra action is the path ordered product of the gauge field along the loop, $P \int A^\mu dx_\mu$. This is exactly what the expectation value of a Wilson loop measures. On the lattice let this loop be planar $R \times T$. Then the physical process described by this loop can also be thought of as to create a $q\bar{q}$ pair, separate it by distance R , propagate it for time T and let it annihilate. The extra action for doing this is the potential energy \times the time T for which the potential acts. This leads to the definition in eqn. (1.7). To get the physical potential we have to isolate lattice artifacts, like those caused by sharp corners *etc.* Thus we need a functional form for V to which we fit the data. This is where one is forced to make some assumptions about what terms contribute to V . Let me start with large r where confinement (linear potential) dominates to first extract σ .

1.2a) Wilson String Tension σ_W

If the potential contains a linear term, then σ_W is in principal given by the Creutz ratio

$$\begin{aligned}\sigma_W &= \lim_{R,T \rightarrow \infty} \chi(R,T) \\ &\equiv \lim_{R,T \rightarrow \infty} -\ln \frac{W(R,T)W(R-1,T-1)}{W(R,T-1)W(R-1,T)}\end{aligned}\tag{1.8}$$

or by

$$\sigma_W = \lim_{R \rightarrow \infty} (V_L(R) - V_L(R-1)) .\tag{1.9}$$

In both methods, it is necessary to have correlated errors in the Wilson loop expectation values for a good estimate. Otherwise a 1% error in one of the loops would change σ by ± 0.01 . Recall that at $\beta = 6$ the value of σ is ≈ 0.05 .

How large should R and T be to extract the asymptotic value? Since the finite temperature transition is a measure of the confinement scale, it is natural to assume that the size of the loops necessary to isolate σ , at a given value of β , is $\geq N_f^\xi$. We have very good estimates for this scale ξ : $\xi = 8$ at $\beta = 6$, $\xi \approx 10$ at $\beta = 6.2$, $\xi \approx 12$ at $\beta = 6.3$ and 14 at $\beta \approx 6.4$ [6][7]. For larger β it is reasonable to use asymptotic scaling to determine ξ . To convert this into physical units, I use the cumulative lattice data at $\beta = 6.0$ for $\frac{1}{a}$, to get $\xi \approx 1$ fermi, a very reasonable value for when the linear term should predominate.

If we assume this is the correct length scale then what Wilson loop data is adequate? At present, Phillippe De Forcrand [8] alone has good statistics for up to 7×7 loops at $\beta = 6.0$ on a 16^4 lattice and 8×12 and 9×10 loops at $\beta = 6.3$ on a $24^3 \times 48$ lattice (10,000 data sweeps). From these, he extracts $\sigma = 0.046$ and 0.0173 at $\beta = 6.0$ and 6.3 respectively. There are no errors quoted by him on purpose because the systematic errors are huge. Taking these numbers seriously, we find a violation of asymptotic scaling; the scale is still changing too fast.

I would like to highlight the magnitude of systematic errors. I have done an analysis of the global data and for illustration again pick de

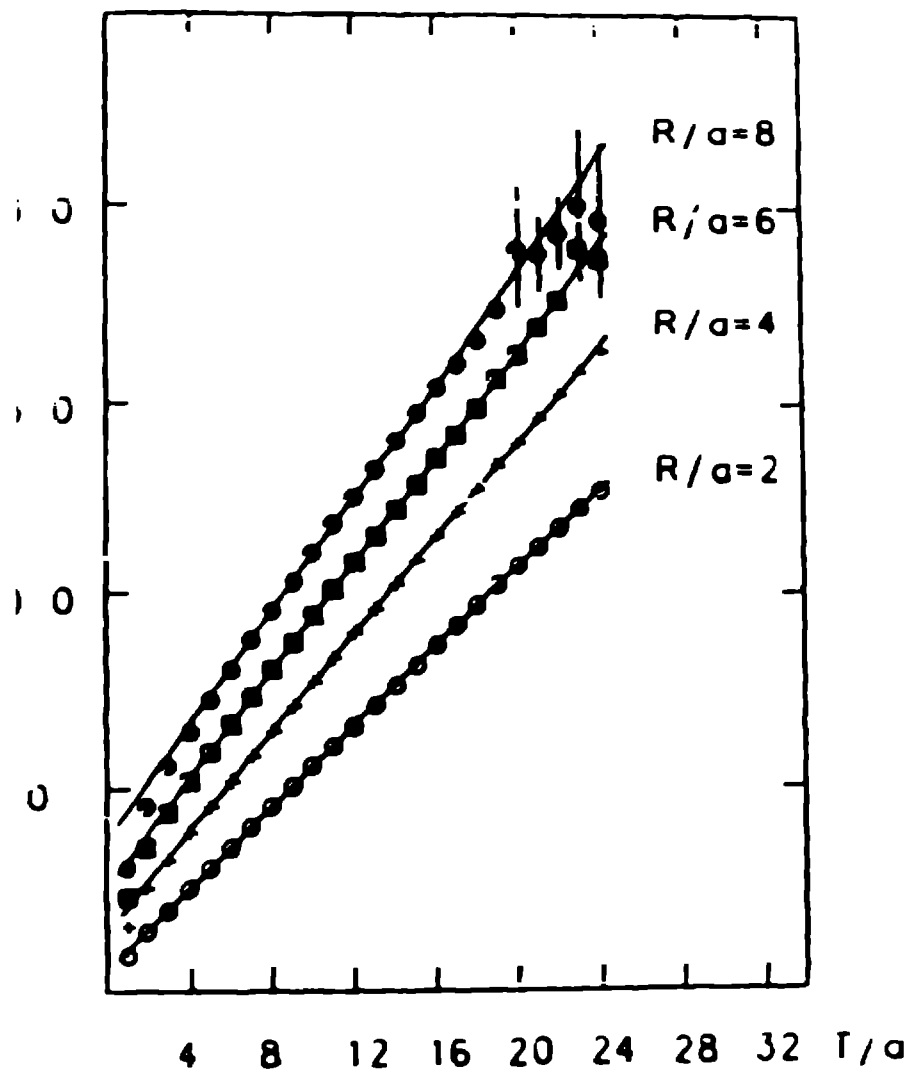
Forcrand's data at $6/g^2 = 6.0$. A fit using eqn(1.10) to all loops in the range (3,3) to (7,7) gives $\sigma = 0.059$. Also, $\chi(6,6) \approx \chi(7,6) \approx 0.064$. Compare these numbers with 0.046 obtained by de Forcrand using a fit to eqn(1.7) for r between 2 and 6 (a three parameter fit to 5 points !!). Next let me indicate the role of statistical errors at this level of sophistication. The 7×7 loop has 2% errors. This makes $\chi(7,7)$ vary between 0.051 and 0.094. I hope I have made the point. The bottom line is that we may still have 50% errors in the determination of σ from Wilson loops already at $6/g^2 = 6$. The data and results at $\beta = 6.3$ on a $24^3 \times 48$ lattice are reproduced from [8] in figures 3a and 3b.

The results which are at least as reliable as the above are compiled in Table 2 along with the σ_t extracted from Polyakov loops as discussed below. An analysis of the scaling of this data has been done by M. Fukugita in his lectures.

$\frac{6}{g^2}$	σ_W [9]	σ_W [10]	σ_t [11]	σ_W [8]
5.5			0.340(15)	
5.6	0.279(9)			
5.7			0.135(5)	
5.8	0.111(3)	0.099(1)		
5.9			0.061(2)	
6.0	0.061(2)		0.042(3)	0.046
6.1		0.046*		
6.2	0.036(2)*			
6.3				0.0173

Table 2: The Wilson (σ_W) and 't Hooft (σ_t) string tension from Barkai *et al.* [9], Otto *et al.* [10], de Forcrand *et al.* [11] and de Forcrand [8]. The * against values indicates that the estimate is not asymptotic. Note the systematic error when more than one group has extracted σ at the same coupling, and also the difference between σ_W and σ_t .

$W(R, T)$



3A

Plots of the measured Wilson loops $W(R, T)$ versus T , on a $24^1 \times 48^3$ lattice. The slope for large T measures the potential $V(R)$

$V(R)$

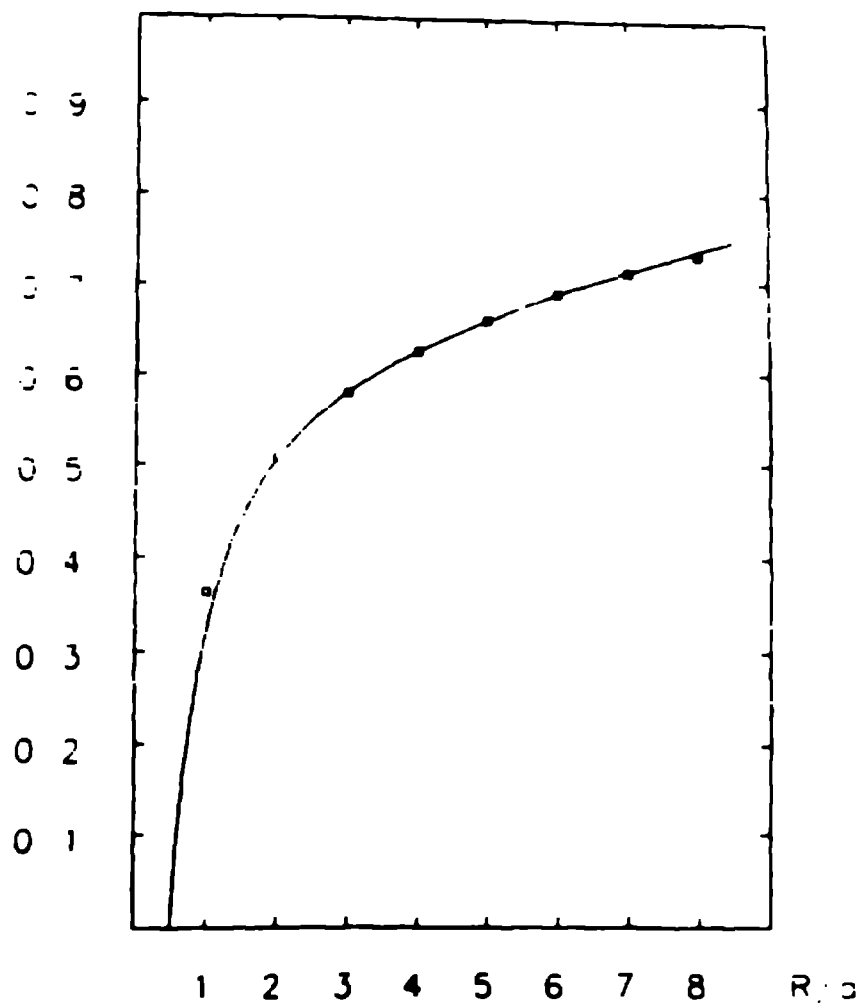


Fig 3B

Potential $V(R)$ extracted from the fitting procedure of Fig 3A. The solid line is (Coulomb + linear) fit to the points $R = 3$ to 8

1.2b) Does the Wilson Loop Data Support the Effective String Picture?

An alternative way to parameterize the lattice data in the large r region is to assume a simple long distance picture of QCD; one of chromo-electric flux confined to a tube. Under this assumption, one can study the modes of a scalar gaussian string to derive what terms contribute to V . It has been shown that such scalar string theories have a roughening transition [12] arising from fluctuations perpendicular to the plane of the loop. The leading behavior of a $R \times T$ Wilson loop is

$$\begin{aligned}
 -\ln W(R, T) &= \sigma RT + p(R + T) + c \\
 &- (d - 2) \left\{ \frac{\pi T}{24 R} + \frac{\ln R}{4} + \frac{1}{2} \sum_{n=1}^{\infty} \ln(1 - e^{-\frac{2n\pi T}{R}}) \right\} .
 \end{aligned}
 \tag{1.10}$$

The last term is universal and depends only on the number of transverse dimensions $(d - 2)$. The coefficients σ, p, c depend on g . Again, to extract σ we need to know what region to trust this string picture in. The answer is given by Alvarez [13] from a $1/d$ expansion of the Nambu-Goto string:

$$V(R) = \sigma R \left\{ 1 - \frac{R_c^2}{R^2} \right\}^{\frac{1}{2}}
 \tag{1.11}$$

where

$$R_c^2 = \frac{\pi(d - 2)}{12\sigma} \approx \frac{0.52}{\sigma}
 \tag{1.12}$$

is the lower bound on r . This gives $T > R > 3$ at $\beta = 6$. An analysis of Wilson loop data within this framework was done by Flensburg and Peterson [14]. They fit the then existing loop data in terms of eqn. (1.10) and found reasonable consistency with the model independent coefficients. Their work is still a good description of the status. I show their results in figure 4. The only relevant new numbers are from de Forcrand [8] for the coefficient of the $\frac{1}{2}$ term. He gets ≈ -0.34 at both $\beta = 6.0$ and 6.3 which is to be compared with the predicted universal

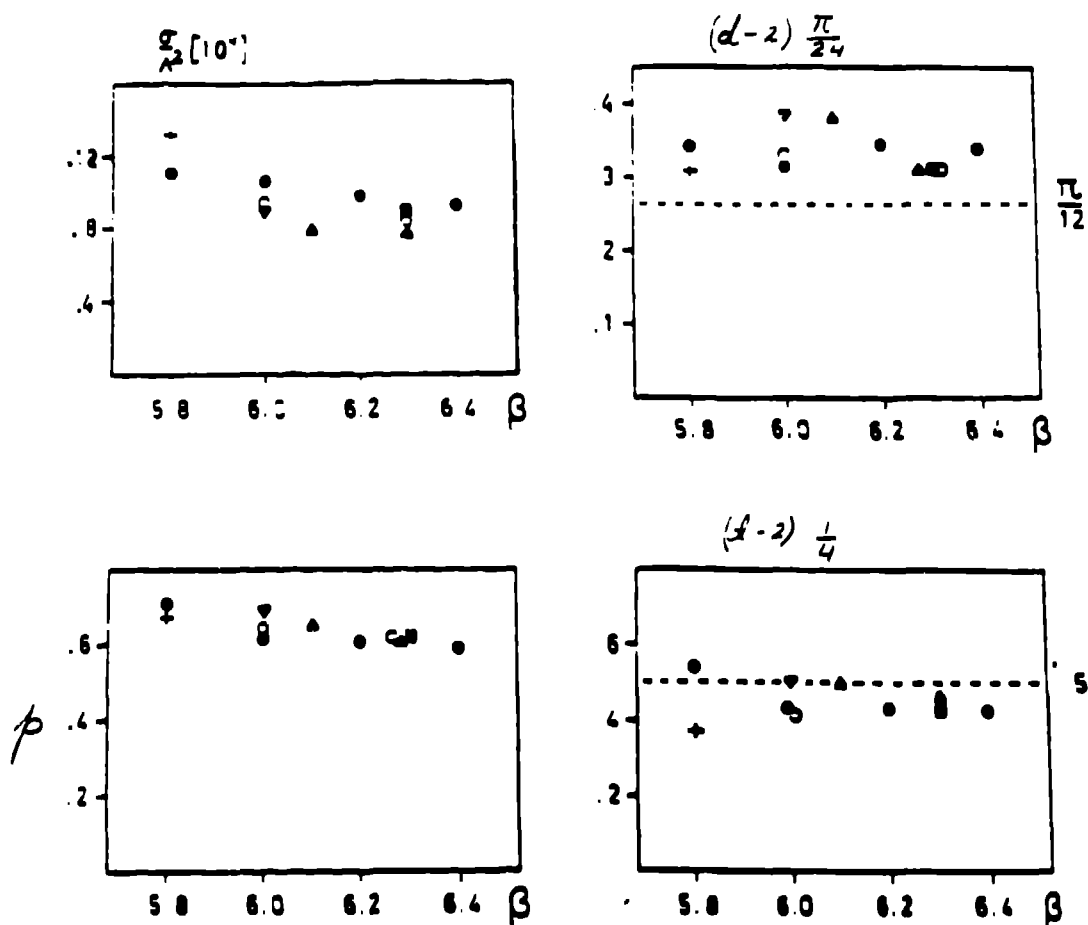


Fig. 4: Comparison of the Wilson loop data with the effective scalar string model (see eqn. (1.10)) at different β [14]. a) string tension, $\sigma/\Lambda^2 (\times 10^4)$, should approach a constant. b) p , which is the coefficient of the perimeter term. c) $1/r$ term with a universal coefficient $\pi/12$. d) $\ln R$ term with a universal coefficient $1/2$.

value $-\frac{r}{12} = -0.26$. Clearly, more work needs to be done especially if one wants to distinguish between various string models.

1.2c) 't Hooft String Tension

The 't Hooft string tension is determined from the connected 2-

point correlation function of the Polyakov-Wilson line P [15]

$$\Gamma(\tau) \equiv \langle P^\dagger(\tau) P(0) \rangle - \langle P \rangle^2 = \sum c_\alpha e^{-E_\alpha \tau} \quad (1.13)$$

where $E_0 = \sigma_t(L)L$ and L is the transverse size of the lattice.

In the last two years, most measurements of the string tension have been made using Polyakov loop correlations and are usually supplemented with the source method [16]. While the inequality $\sigma_t \leq \sigma_W$ is true, it is believed that equality holds for all β and not just in the continuum limit [17]. The only data that supports equality is from de Forcrand [8] at $\beta = 6$, i.e. $\sigma_t = 0.042$ versus $\sigma_W = 0.046$. However, the errors in the evaluation of σ_W are large as discussed above. So, this question is not yet settled.

In Table 2, I have listed the published values of σ_t along the Wilson axis. A remarkable feature of these calculations is the verification of the universal finite volume term

$$\sigma(\infty) = \sigma(L) + \frac{\pi}{3L^2} \quad (1.14)$$

with a large coefficient $\frac{\pi}{3}$. The agreement is in much better shape than the universal term in Wilson loops.

There is a depressing side to the method too. As β is increased, the transverse dimensions have to be increased to preserve the signal out to large r . It is not clear whether this alone will guarantee that the signal extends to the same physical distance. In present calculations, the r_{max} to which the signal extends changes from 7 to 9 in going from $\beta = 5.5$ to 6.0. This is not fast enough. Also, the auto-correlations grow significantly. So, to go beyond $\beta \approx 6.1$, new tricks will be needed. I discuss some in my talk on glueballs.

A second relevant point is that two such 't Hooft excitations can have the quantum numbers of glueballs with energy $2\sigma L$. Thus when measuring glueball masses L should be selected so that $2\sigma L \gg m$.

1.3) The Full Spin-Independent Potential

The standard assumption made to extract a potential is that the major contamination in $V(r)$ from Wilson loop data comes from the

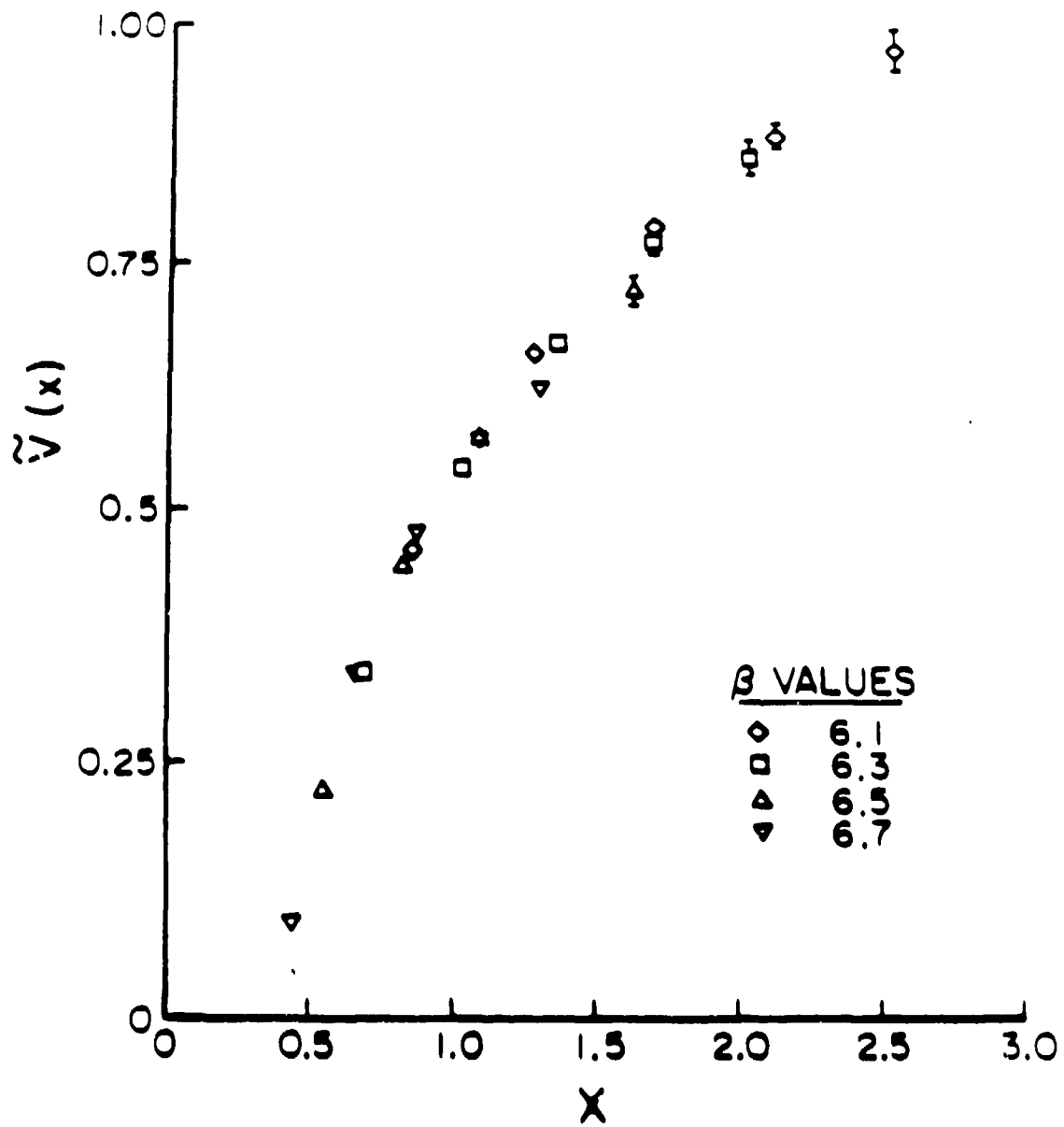


Fig. 5: Constructing the potential using asymptotic scaling to combine data at different values of β [18]. The curve is not universal in spite of appearances.

perimeter term. Thus one parameterizes V_L , defined in eqn (1.7), as

$$V_L(R) = \sigma R + p + \frac{c}{R} . \quad (1.15)$$

The constant p is from the perimeter term in the loops and to get $V(r)$ we subtract p obtained from the fit. At this stage the potential $V(r)$ and the distance r are measured in lattice units. To convert them in to physical units we need a mass scale. Let me call this m , which could be $\sqrt{\sigma}$ or a hadron mass calculated at each value of the coupling. Then, the data at different values of the coupling (with any action) can be put on the same plot, $\frac{V}{m}$ versus rm . If scaling holds and the data and fits are good, then all the points should fall on a single universal curve. This is the physical potential. Note that by using m calculated at corresponding couplings I do not rely on asymptotic scaling but just on scaling.

The problem with existing data is that we do not know the scale m very well for $\beta > 6$ as shown above by the string tension measurements. One option is to use asymptotic scaling having determined m at one reliable point. We know asymptotic scaling does not work for at least $\beta < 6.15$ (see section 4 of my talk on MCRG). Second, the range of r available so far at any given β is small. Flower and Otto [18] showed that because of this, and in spite of appearances, we don't have a universal curve. In their data (shown in figure 5) too, the problem is hidden by the fact that the distance scale over which the potential is measured at any given coupling is small.

1.4) Comparing the Lattice and Phenomenological Potential

As I have already stressed, both lattice and phenomenological potentials have uncertainties. However, the phenomenological potential is tuned to fit the spectrum, so it is meaningful to compare the lattice and the Cornell potential. This is shown in figure 6.

The unambiguous statement for the present is that the lattice potential does a very poor job at short distances. Is this a problem due to the quenched approximation? One does not know. Certainly, we have

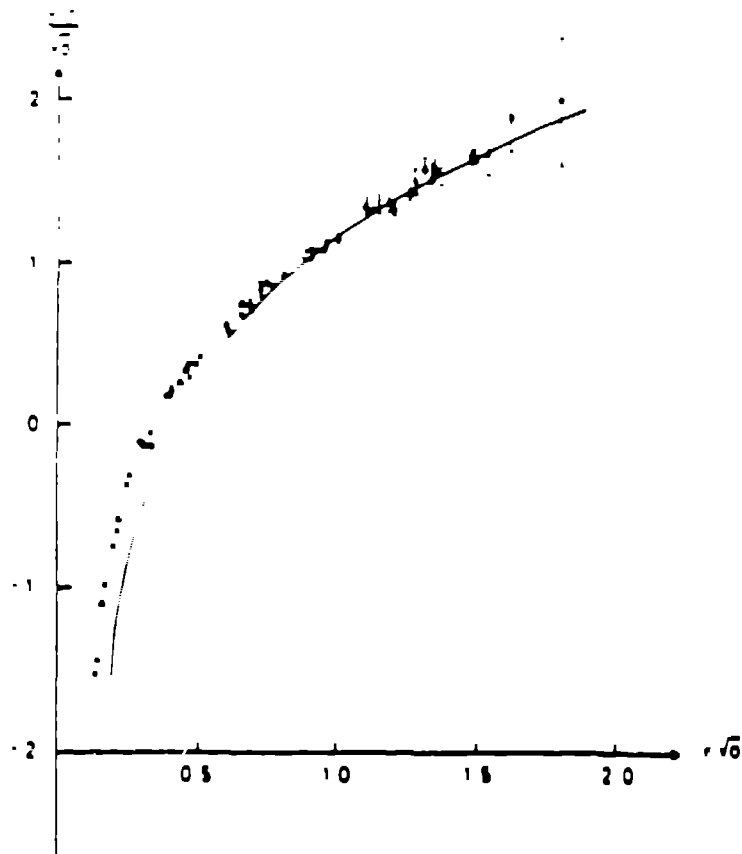


Fig. 6: Comparison of the Monte-Carlo determined potential with the Cornell potential. The normalization is chosen to make the two agree at $r/\sigma = 1$.

to wait for the next generation of dedicated super computers to start addressing these details.

To summarize, the lattice calculations give the correct qualitative picture of the spin-independent potential. However, the systematic and statistical errors are large so quantitative comparison is not good. At this point it might be appropriate to define our goal. To cover the range of charmonium, bottomonium and toponium, we would like to map the potential from 0.02 to 1 fermi. Let us optimistically assume that scaling begins at $6/g^2 = 6$. Then to achieve the goal we have to

measure $V(r)$ for at least $r = 10$ all the way from $6/g^2 = 6$ to ≈ 7.4 . This is a Herculean task without a breakthrough in algorithms. Let the brave of heart proceed.

Calculating the expectation value of large Wilson loops (or the correlation of two Polyakov lines) is central to extracting the potential. The bottlenecks are 1) critical slowing down and 2) removing the short distance fluctuations from the loops. I can only offer suggestions for there is a desperate need for a breakthrough. To overcome the first there are two proposals, fourier acceleration and multigrid. The status of fourier accelerations is discussed by John Kogut in his lectures. A proposal for a multigrid update algorithm is presented in section 7 of my lecture on MCRG. These techniques are being tested. For the second we need "fat" loops. Improved actions and DLR variance reduction techniques as applied today are some help but are too limited to achieve the final goal.

1.5) The Spin-Dependent Potential

To go beyond the simple central potential for heavy quark systems, it is natural to include spin-orbit and spin-spin interactions. This full potential was first derived by Eichten and Feinberg as an expansion in $\frac{1}{m}$. It is reviewed in two excellent SLAC summer school lectures by M. Peskin [19] and F. Gilman [5] and in this lecture I shall follow their notation and recapitulate the parts pertinent to lattice calculations. In exact analogy with the hydrogen atom, the spin-dependent potential is

$$\begin{aligned}
 V_s(r) = & \left[\frac{\vec{S}_1 \cdot \vec{L}}{2m_1^2} + \frac{\vec{S}_2 \cdot \vec{L}}{2m_2^2} \right] \left[\frac{-dV(r)}{rdr} + 2 \frac{dV_1(r)}{rdr} \right] \\
 & + \frac{(\vec{S}_1 + \vec{S}_2) \cdot \vec{L}}{m_1 m_2} \frac{dV_2(r)}{rdr} \\
 & + \frac{1}{3m_1 m_2} (3\vec{S}_1 \cdot \hat{r} \vec{S}_2 \cdot \hat{r} - \vec{S}_1 \cdot \vec{S}_2) V_3(r) \\
 & + \frac{2}{3m_1 m_2} \vec{S}_1 \cdot \vec{S}_2 V_4(r)
 \end{aligned} \tag{1.16}$$

where $V(r)$ is the spin independent term we have already discussed. The terms V_1, V_2 , and V_3 are spin-orbit interactions while V_4 is the hyperfine interaction. To relate these to quantities that can be calculated on the lattice, we start with the extra action in the path integral due to a heavy external source with spin. This is

$$\int A_\mu J^\mu + \frac{g}{4} \int \Sigma_{\mu\nu} F^{\mu\nu} \quad (1.17)$$

where $\Sigma_{\mu\nu} = \frac{-i}{2}[\gamma_\mu, \gamma_\nu]$ is the spin operator. In the non-relativistic limit, eqn (1.17) is

$$\int i v_\mu J^\mu + \frac{g}{2m} \int \vec{\sigma} \cdot (\vec{B} - \vec{E}). \quad (1.18)$$

The functional integral (expectation value) we wish to perform is in presence of these extra terms. The first term defines an external current source which is our old familiar Wilson loop. We treat the second term in eqn(1.18) as a perturbation i.e. an expansion in $\frac{1}{m}$. Note that the E or B fields that are brought down by expanding the exponential can be anywhere along the world line of the quark or anti-quark. This will give rise to integrals over the t part of the loops since the spatial parts of the loop correspond to instantaneous separation. There are two types of terms that can be generated; 1) that comes from a straight expansion of which the only non-zero term (to lowest order) is due to the magnetic field of the q interacting with that of \bar{q} . This is the third term below. 2) The interaction of one $\vec{\sigma} \cdot \vec{B}$ with the velocity operator of either the q or the \bar{q} . This gives the first two terms below:

$$\begin{aligned} \hat{p}_k \frac{dV_1}{dr} &= \lim_{T \rightarrow \infty} \frac{1}{T} \int \int_{-T/2}^{-T/2} dt_1 dt_2 \frac{t_1 - t_2}{2} \epsilon_{ijk} \frac{g^2 \langle E_i(\vec{0}, t_1) B_j(\vec{0}, t_2) \rangle}{\langle W(R, T) \rangle} \\ \hat{p}_k \frac{dV_2}{dr} &= \lim_{T \rightarrow \infty} \frac{1}{T} \int \int_{-T/2}^{-T/2} dt_1 dt_2 \frac{t_1 - t_2}{2} \epsilon_{ijk} \frac{g^2 \langle E_i(\vec{0}, t_1) B_j(\vec{R}, t_2) \rangle}{\langle W(R, T) \rangle} \\ (\hat{p}_i \hat{p}_j - \frac{1}{3} \delta_{ij}) V_3 + \frac{1}{3} \delta_{ij} V_4 &= \\ & \lim_{T \rightarrow \infty} \frac{1}{T} \int \int_{-T/2}^{-T/2} dt_1 dt_2 \frac{t_1 - t_2}{2} \frac{g^2 \langle B_i(\vec{0}, t_1) B_j(\vec{R}, t_2) \rangle}{\langle W(R, T) \rangle} \end{aligned} \quad (1.19)$$

where for example $E_i(\vec{0}, t_1)$ is an insertion of an electric field at location $(\vec{0}, t_1)$. To lowest order in the lattice spacing a , the fields are defined by

$$U_{\mu,\nu} - U_{\nu,\mu} = 2iga^2 F_{\mu,\nu} \quad (1.20)$$

where $U_{\mu,\nu}$ is the untraced plaquette in the (μ, ν) plane. An example of the insertions for the first two terms is shown in figure 7. The division by $W(R, T)$ removes the contribution of the spin-independent potential to the extra action, leaving only the spin-dependent part.

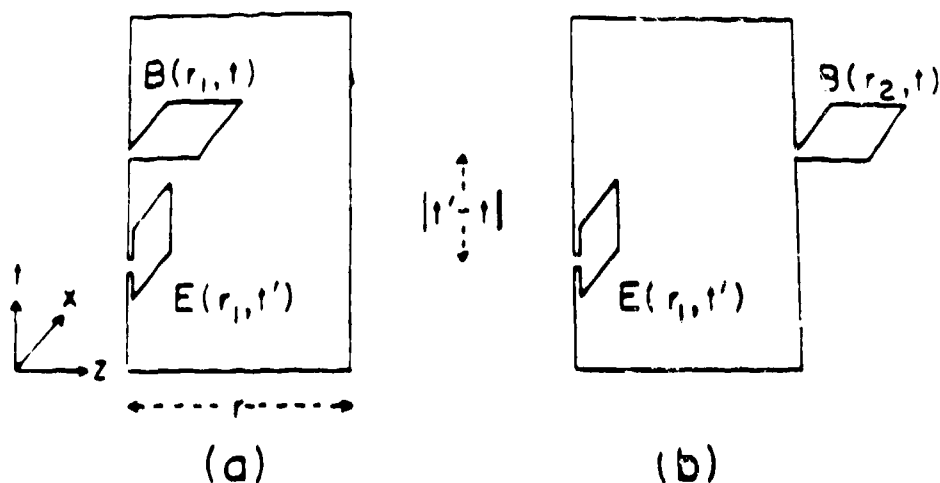


Fig. 7: Examples of insertions of plaquettes in Wilson loops that contribute to the evaluation of spin-orbit potentials. a) V_1 and b) V_2 .

The first computational task then is to formulate these insertions on the lattice. This is not unique and at finite β the arbitrariness will have important consequences for the normalization of the V_i , in addition to the practical concern of the statistical signal. Secondly, these insertions on the lattice will themselves consist of small loops. Thus different insertions will have different small R behavior. In figure 8, I give an example of a B field insertion. There are four possible plaquettes attached to a given point \vec{r} defining the field at

$$B(\vec{r} + \frac{\hat{\mu} + \hat{\nu}}{2}), B(\vec{r} + \frac{\hat{\mu} - \hat{\nu}}{2}), B(\vec{r} + \frac{\hat{\nu} - \hat{\mu}}{2}), B(\vec{r} - \frac{\hat{\mu} + \hat{\nu}}{2}) \quad (1.21)$$

Each of them individually is an insertion. A better solution is the sum. This has two advantages, it improves the statistical signal and second it is the average field defined at \bar{r} .

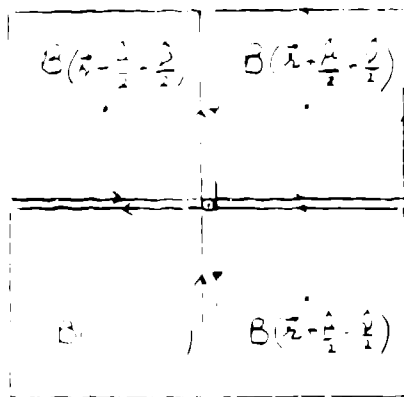


Fig. 8: A $B(\bar{r})$ field insertion defined as an average of four plaquettes to improve the statistical signal.

The first physics question is whether all the spin-dependent interactions are short ranged. Michael and Rakow [20][21] showed by lattice calculations that the tensor (V_3) and the spin-spin (V_4) terms are short ranged. This was soon confirmed for SU(3) by de Forcrand and Stack [22] who also found that V_2 was short ranged. Their result for V_1 is wrong due to an oversight. Phenomenological analysis of the heavy-quark spectra indicates a need for a long range spin-orbit component [23]. More important, Gromes [24], using simple Lorentz invariance, derived the identity

$$V(r) = -V_1(r) + V_2(r) \quad (1.22)$$

Thus, the question now reduces to determining which of the two, V_1 or V_2 is long range. The answer for SU(2), provided by Michael [25], is V_1 . The result was confirmed for SU(3) by Campostrini, Moriarty and Rebbi [26] [27]. Their data for the force, dV/dr , taken on a $16^3 \times 32$ lattice at $\beta = 6.0$ and 6.2 , are reproduced in figure 9. The normalization

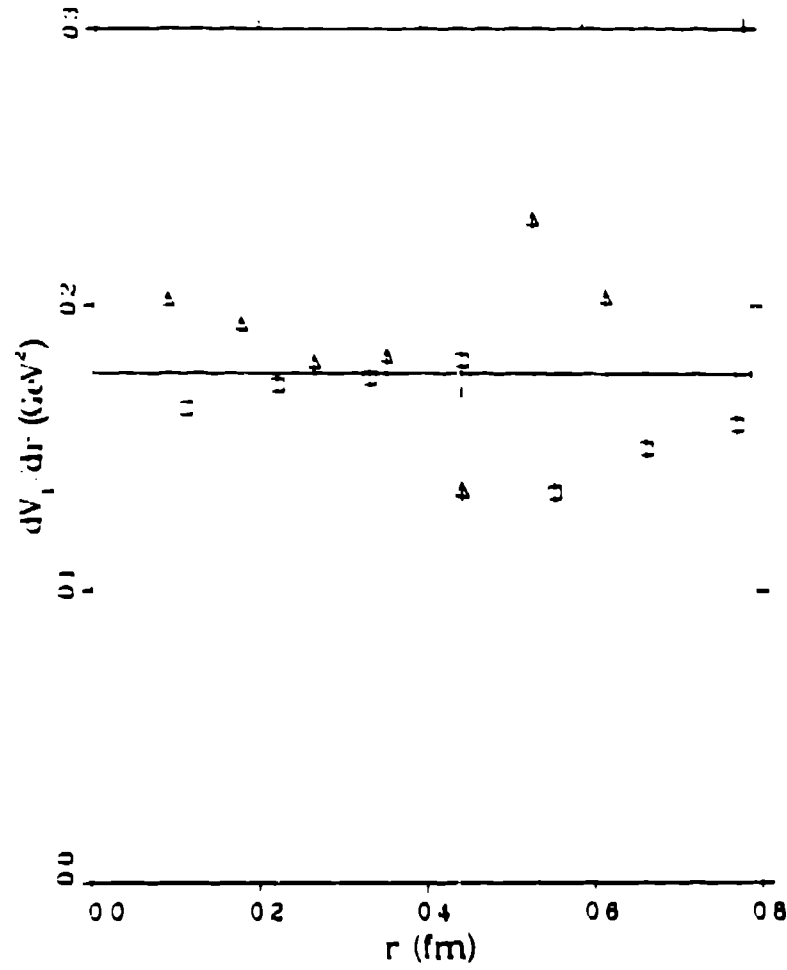


Fig. 9a: Spin-dependent Potential [26]. a) $\frac{dV_1}{dr}$ converted to physical units using asymptotic scaling including a renormalization discussed by the authors. The squares and triangles represent data at $\beta = 6.0$ and 6.2 respectively.

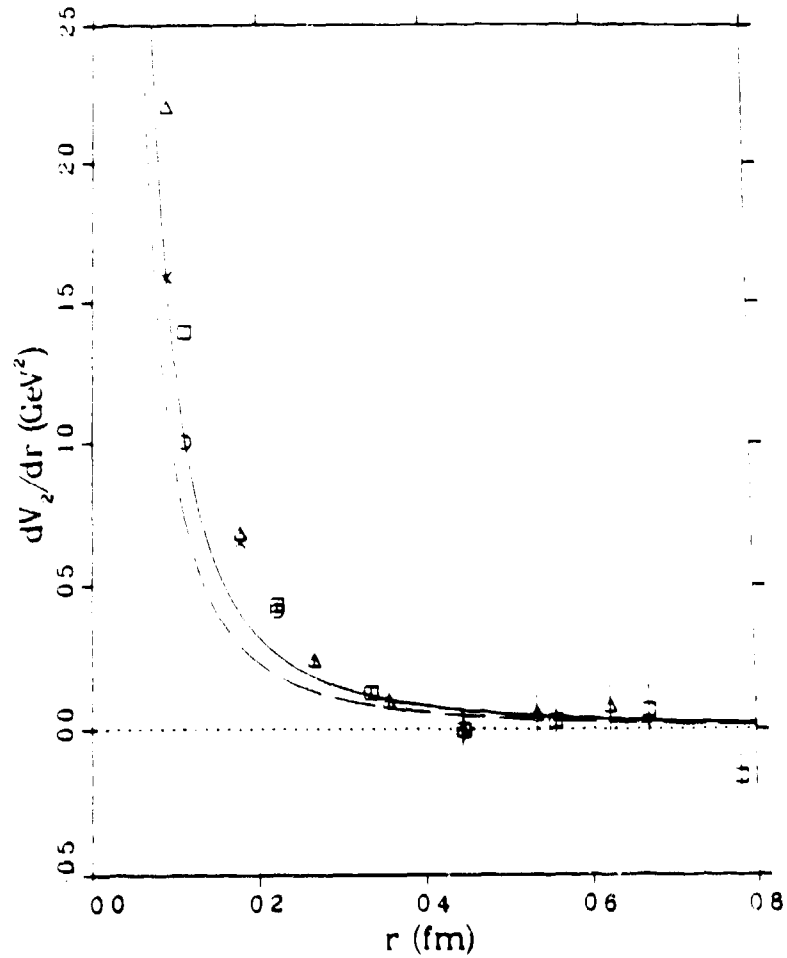


Fig. 9b: Same as Fig. 9a but for dV_2/dr . The addition symbols represent data at $\beta = 6.0$ (circles) and 6.2 (crosses) after a correction for lattice artifacts at small distances. The lines represent the lowest order perturbative behavior, eqn. (1.23), with $\alpha_s = 0.244$ (solid line) and $\alpha_s = 0.175$ (broken line).

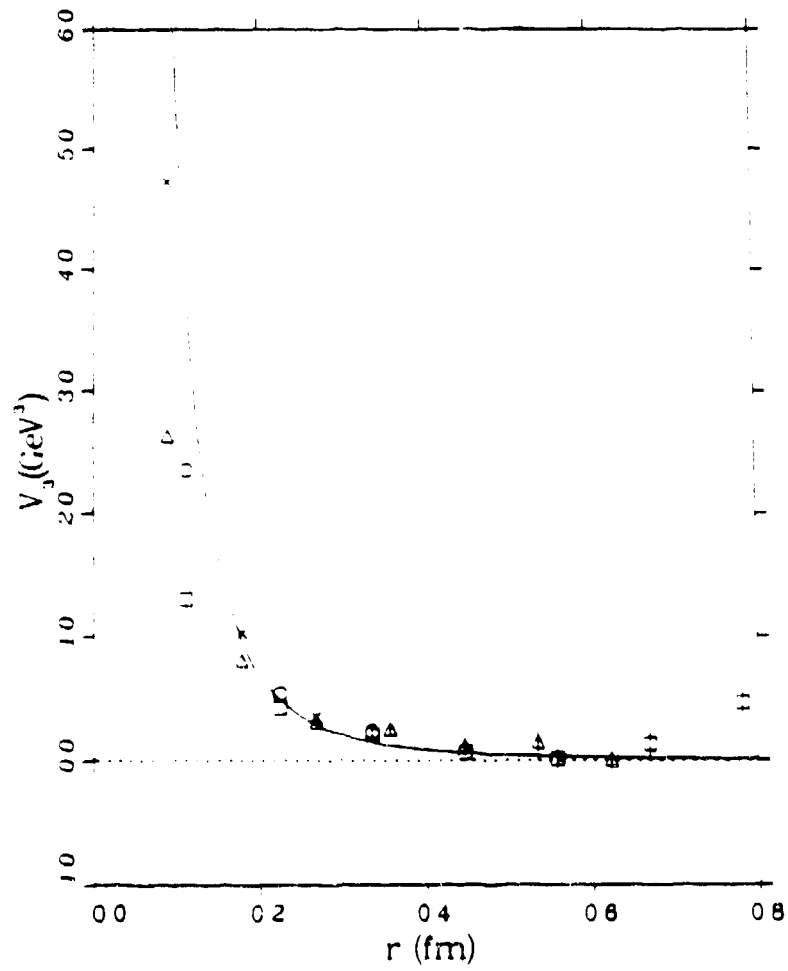


Fig. 9c: Same as Fig. 9b, but for V_3 . The solid line is the lowest order perturbative behavior with $\alpha_s = 0.175$.

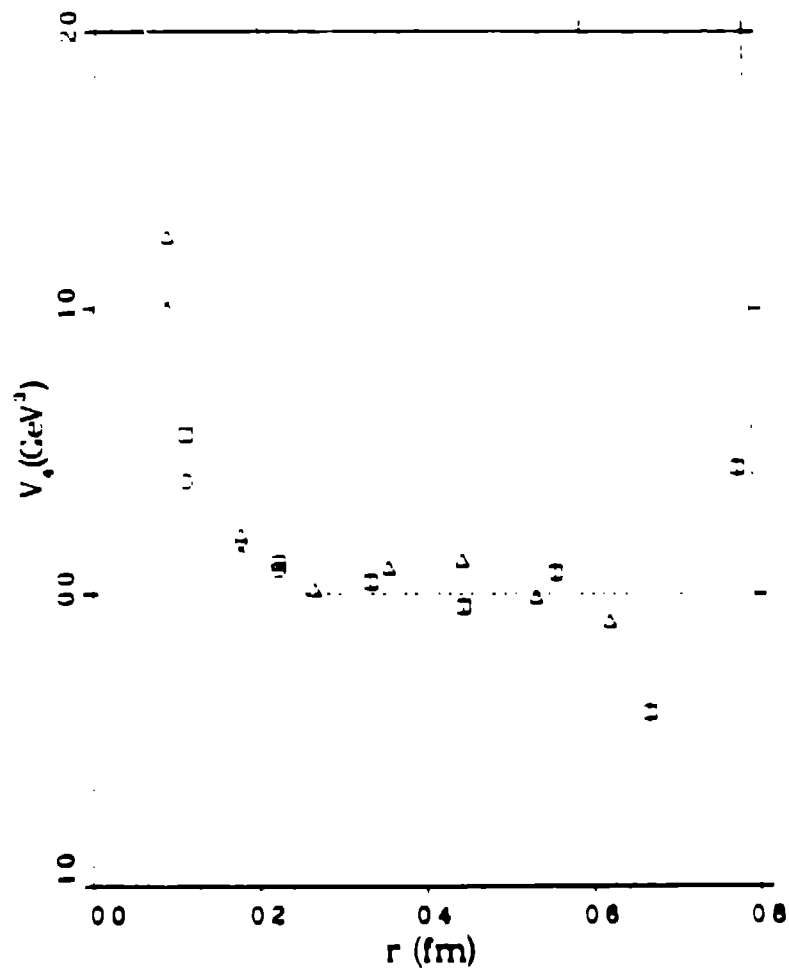


Fig. 9d: Same as Fig. 9b, but for V_4 .

of V_1 is fixed by using Gromes relation for large r

$$\frac{dV_1}{dr} = \frac{dV}{dr} = \sigma$$

where σ is determined from the spin independent potential. The data are converted to physical units using asymptotic scaling.

The data show a clear distinction between the long range term V_1 and the short-range pieces V_2, V_3 , and V_4 . Also evident is the problem at small r due to the discreteness of the lattice. The lattice artifacts give large differences between different definitions of the insertions. The raw lattice data does not explain the observed spin splittings and they provide phenomenological arguments which change things in the right direction. For a discussion of these I refer you to their paper [26]. The data for V_2, V_3 and V_4 agrees qualitatively with the leading order perturbative behavior

$$\begin{aligned} V_2(r) &= -\frac{4}{3} \frac{\alpha_s}{r} \\ V_3(r) &= 4 \frac{\alpha_s}{r^3} \\ V_4(r) &= 2 \vec{\nabla}^2 V_2(r) = -\frac{32\pi}{3} \alpha_s \delta^3(r) \end{aligned}$$

(1.23)

though at r where the lattice artifacts are small, the fits are not very sensitive since the signal for the short range potentials has large errors

Let me describe some computational tricks which were also used in [27]. For each measurement they fixed the lattice to the temporal gauge. Then 1) t parts of the loops do not have to be calculated. 2) They use the DLR variance reduction trick for the spatial links. 3) They average the insertions over t before calculating the expectation values i.e. do the T integral before the Monte Carlo average. This reduces the statistical errors but also hides any T truncation effects that may exist. de Forcrand informs me that these in fact are substantial especially for the long range piece. For V_2 alone they are under control, as shown in figure 10 where the integrand in eqn (1.19) is plotted directly.

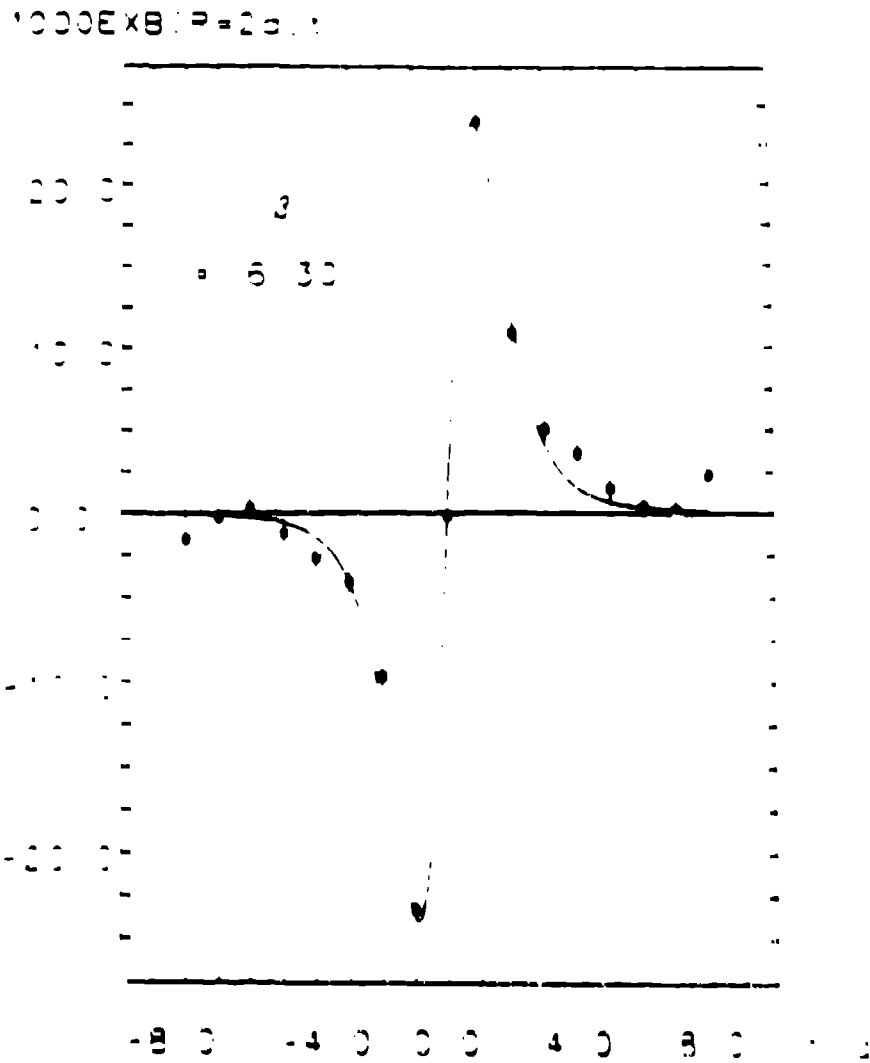


Fig. 10: The integrand $\vec{E} \times \vec{B}$ versus t at $r = 2a$ on a $24^3 \times 48$ lattice at $\beta = 6.3$ [8]. The solid line is the leading order perturbation theory prediction.

The final goal is to be able to compute the spectroscopy of heavy quarks from the lattice derived potential. Over and above statistical and systematic errors, the problems facing the extraction of the spin-dependent potential at the moment are 1) the normalization factors for the various terms and their scaling with β and 2) the need for large loops measured at weaker coupling so that the small r distortions are pushed to small physical r . 3) The small r behavior is expected to be modified by the presence of dynamical quarks and we need to understand it better.

To conclude, I believe that the qualitative prediction that V_1 is long ranged is a major triumph of lattice calculations.

References

- [1] W. Kwong, J.L. Rosner and C. Quigg, Preprint EFI 86-60.
- [2] E. Eichten *et al.* *Phys. Rev. D***17** (1978) 3090; and *Phys. Rev. D***21** (1980) 203.
- [3] J. L. Richardson, *Phys. Lett.* **82B** (1979) 272.
- [4] A. Martin, *Phys. Lett.* **93B** (1980) 338.
- [5] F. Gilman, *Proceedings of the 14th SLAC summer school*, 1986.
- [6] D. Toussaint, Talk at the Brookhaven Meeting, Sept. (1986).
- [7] N. Christ, Private Communications.
- [8] P. De Forcrand, *Proceedings of the Metropolis Conference*, Los Alamos (1985), *J. Stat. Phys.* **43** (1986) 1077; and private communications.
- [9] D. Barkai, K. J. M. Moriarty and C. Rebbi, *Phys. Rev. D***30** (1984) 1292.
- [10] S. W. Otto and J. D. Stack, *Phys. Rev. Lett.* **52** (1984) 2328.
- [11] P. de Forcrand *et al.*, *Phys. Lett.* **160B** (1985) 137.
- [12] M. Lüscher, K. Symanzik and P. Weisz, *Nucl. Phys.* **B173** (1980) 365.
- [13] O. Alvarez, *Phys. Rev. D***24** (1981) 440.
- [14] C. Peterson, Talk given at the DPF meeting, Eugene, Oregon, 1985.
- [15] G. Parisi, R. Petronzio and F. Rapuano, *Phys. Lett.* **128B** (1983) 418.
- [16] K. H. Mütter and K. Schilling, *Phys. Lett.* **117B** (1982) 75.
- [17] E. Seiler, *Proceedings of the 1985 Berkeley Conference on quark Confinement and Liberation*, World Scientific.
- [18] J. Flower and S. Otto, *Phys. Rev. D***34** (1986) 1649.
- [19] M. Peskin, *Proceedings of the 11th SLAC summer school*, 1983.
- [20] C. Michael, and P. E. L. Rakow, *Nucl. Phys.* **B256** (1985) 640.
- [21] M. Campostrini, *Nucl. Phys.* **B256** (1985) 717. He was independently working on these methods using the $U(1)$ model.
- [22] P. de Forcrand and J. Stack, *Phys. Rev. Lett.* **55** (1985) 1254.
- [23] J. L. Rosner, University of Chicago Report No. EFI 85-63 (1985).

- [24] D. Gromes, *Z. Phys.* **C26** (1984) 401.
- [25] C. Michael, *Phys. Rev. Lett.* **56** (1986) 1219.
- [26] M. Campostrini, K. Moriarty and C. Rebbi, BNL preprint 39777 (1987).
- [27] M. Campostrini, K. Moriarty and C. Rebbi, *Phys. Rev. Lett.* **57** (1986) 44.

2) GLUEBALLS

The existence of glueballs are a major untested prediction of QCD. We have not been able to reliably calculate the masses (let alone the mixing with $q\bar{q}$ states), or understand in detail the production and decay mechanisms. What we can do is group theory and determine, if QCD is the correct theory, the quantum numbers of the vast number of glueball states. The predictions for the masses from various models (bag models, flux tube model, sum rules *etc.*) were compiled by Sharpe [1] in 1984 and are summarized in figure 1. There has been no significant improvement in these estimates and even today they are all over the map. This does not help the experimentalists who have to isolate glueball states from the myriad of meson states in the 1 to 2.5 GeV region. Future progress will depend on a combined effort: theorists have to calculate the mass spectrum and understand the production and decay mechanisms, while experimentalists must do very high precision measurements. Clearly, the first goal facing Lattice alchemists is to calculate the spectrum in a world in which the mixing with quark states is turned off.

Experimental Status:

Let me first look at the problem donning the hat of an experimentalist. A good place to look for the lowest mass candidates is certainly in the radiative decays of J/ψ

$$J/\psi \rightarrow \gamma gg \leftrightarrow \gamma X \quad \text{with } X \rightarrow gg.$$

The production of glueballs in hadron collisions is not very well understood. Improved understanding will presumably come with input from the decay modes of glueballs. So for starters let's proceed by elimination. First we tabulate all the states in the 1 - 2.5 GeV region and fill up meson nonets since flavor SU(3) tells us that once one member exists, all exist. If we are lucky, only filled (and well understood) nonets and a single glueball candidate will exist. To be convinced that it is not the first member of the next higher excited nonet, we must check that it has the "right" properties. A reasonable hypothesis is that its

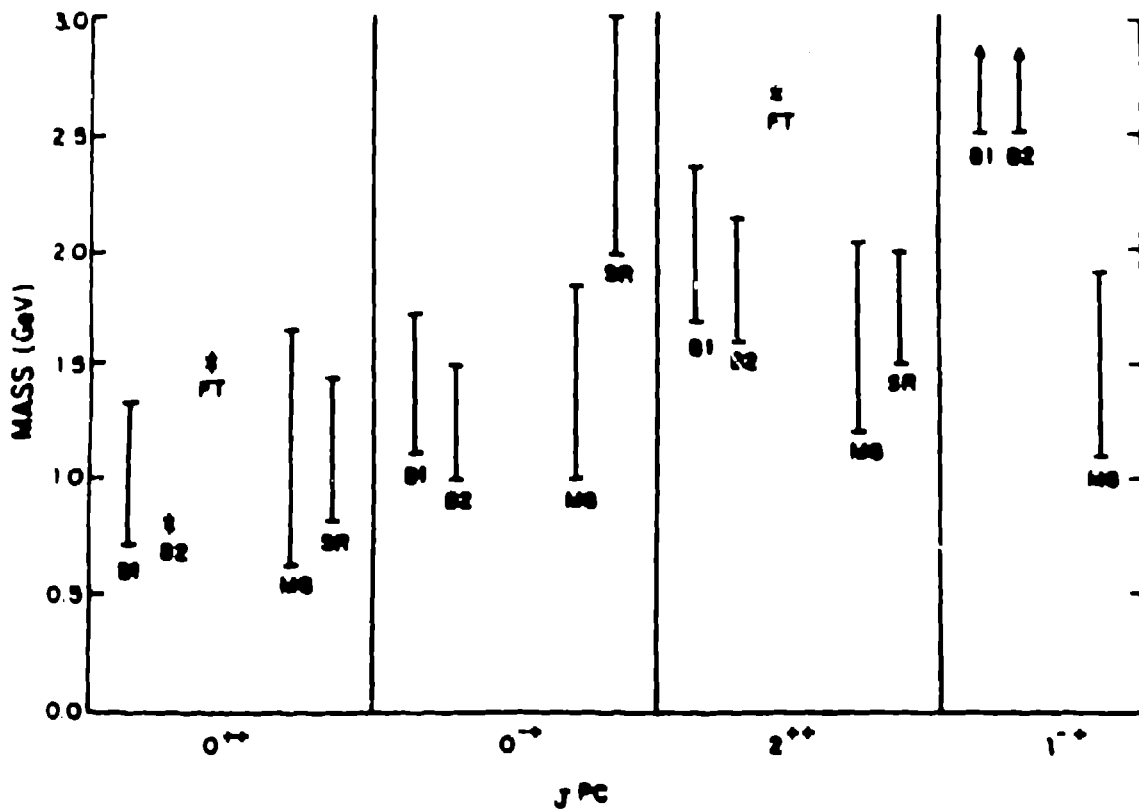


Fig. 1: Glueball mass predictions [1]: $B1$ and $B2$ are bag model estimates; FT is from flux tube; MG is from massive gluon model; and SR is sum rules estimate.

decays should be flavor symmetric since a glueball state should have equal coupling to u, d, s quarks above threshold. In fact, this is violated by one of the favorite candidates; the $f_2(1720)$ has a $\approx 70\%$ branching ratio for decay into $K\bar{K}$. Second, it should not be produced in $\gamma\gamma$ scattering. Flavor singlet mesons, on the other hand, should have a significantly larger branching ratio through $\gamma\gamma$. On the basis of such an analysis we must further convince ourselves that the candidate state is not a $q\bar{q}$ or a more exotic possibility like $q\bar{q}g$ or $q^2\bar{q}^2$. We then sanctify it and start the laborious process of providing proof.

Candidates:

There exist at present two prime glueball candidates below 2 GeV and a possible signal in the s -wave $\pi\pi$ phase shift data for the elu-

2.1) Lattice Calculations of the Glueball Spectrum

The mass of any state in Euclidian lattice calculations is determined from the exponential fall-off of the connected 2-point correlation function. Let O be any interpolating field operator with the correct quantum numbers. Then

$$\Gamma(\tau) \equiv \langle O(\tau)O(0) \rangle - \langle O \rangle^2 = \sum c_\alpha e^{-m_\alpha \tau} \quad (2.1)$$

where the sum is over all states that couple to O . To get the best estimate for the lowest state we need to 1) optimize O to get a large overlap with the wave function by making c_1 large and the rest small, and 2) have the signal extend for large τ to kill any remaining contamination of higher states. I will refer to these as necessary criteria.

The first calculations of the glueball spectrum were made by analyzing the behavior of the 2-point correlation function of the 1×1 plaquette. In this approach, the maximum separation τ that could be measured was ≤ 2 . Estimates of mass from these calculations were dominated by higher excitations. Further, as g is decreased, the overlap of the plaquette operator with the physical glueball state also decreases, and the correlation function at small τ is dominated by spin waves. Thus, even for the 0^{++} state (which has the best signal), this brute force approach did not and will not work.

To incorporate the growing size (in lattice units) of the glueball, Wilson suggested we use the variational method. In this approach, the glueball operator is taken to be

$$O = \sum_{\alpha} c_{\alpha} O_{\alpha} \quad (2.2)$$

where O_{α} are in principle all possible Wilson loops and c_{α} are the variational coefficients to be determined. This method is one way to implement the necessary criterion one. The method works as follows: The c_{α} are determined at time separation $\tau = 1$ by solving a generalized eigenvalue problem; $A\psi = \lambda B\psi$, where A and B are the 2-point

sive 0^{++} . A lot more high statistics data with spin-parity analysis is necessary to establish them.

- [1] The (0^{++}) state at ? MeV: This state is not seen directly. The evidence for and against comes from an analysis of the $I=0$, s-wave $\pi\pi$ phase shift δ_0^0 . By a study of the data below the $K\bar{K}$ threshold, Sharpe, Jaffe and Pennington [2] exclude a glueball unless it is very narrow ($\Gamma \leq 2MeV$) or intrinsically very broad, of mass $\approx 650 MeV$ and appearing very narrow because of mixing with $q^2\bar{q}^2$ through unitarity. Recently, Au, Morgan and Pennington [3] made a coupled channel analysis of the data for δ_0^0 obtained from $pp \rightarrow pp\pi\pi(K\bar{K})$ up to 1.6 GeV. They conclude that there is a glueball candidate state at 991MeV. The analysis uses a highly complex seven pole solution to fit four resonances! So one could be a little doubtful of it. Well, this is the only serious number we have. The corresponding meson nonet is $(K_0^*(1350), a_0(980), f_0(975), f_0(1300))$. A problem for lattice calculations, for which this channel is the most easily measured, is mixing with meson states. There is no argument to exclude a large mixing because of the trace anomaly [4]. Thus any prediction from quenched calculations can be off by say 500 MeV.
- [2] The $\eta(1460)$ or the old $\iota(0^{-+})$: There is evidence for three states in a narrow energy region; both a $0^{-+} \rightarrow a_0\pi$ and a $1^{++} \rightarrow K\bar{K}^*$ meson at ≈ 1420 seen in hadron collisions and a wider $0^{-+} \rightarrow "a_0"\pi$ at 1460 seen in radiative J/ψ decays. This region needs to be sorted out by very high statistics runs.
- [3] The $f_2(1720)$ or the old $\theta(2^{++})$ state: The 2^{++} meson nonet $(K_2^*(1425), a_2(1320), f_2(1270), f_2(1525))$ is complete, well established and reasonably well understood. The $f_2(1720)$ is produced copiously in J/ψ decay. It is at present the best glueball candidate even though a $\approx 70\%$ decay into $K\bar{K}$ violates flavor symmetry. If the 2^{++} state is a relatively pure glueball state then lattice calculations have another prediction. The mass ratio $\frac{m_{2^{++}}}{m_{0^{++}}}$ should specify the location of an unmixed 0^{++} , giving us an estimate of the size of the mixing in the 0^{++} channel.

correlation matrices $\Gamma(1)$ and $\Gamma(0)$ respectively. Then with O defined by these coefficients, the best estimate for the mass is given by

$$m = -\ln \frac{\Gamma(\tau + 1)}{\Gamma(\tau)} \quad (2.3)$$

where $\tau + 1$ is the largest separation at which a statistically significant signal exists. Notwithstanding the fact that this method is mostly used half-heartedly (a single loop with the best signal is chosen rather than solving the generalized eigenvalue problem), it is clear that a few loops are not sufficient and supplementary tricks are needed.

A second embellishment, due to Parisi, replaces non-overlapping links in large planar loops with the mean in a fixed environment *i.e.* $U \rightarrow \bar{U}$ [5]. Using these "DLR variance reduced loops", bought us at best one additional time-slice in the correlation function. Unfortunately, the mass estimate so obtained was not independent of τ and the magnitude of the error was not known.

I would summarize the status of glueball calculations up to 1985 as one of exploring techniques. We had learnt how to construct operators of various spin and parity using the cubic group and the rudiments of such glueball calculations. For hard numbers we had nothing reliable even for the 0^{++} state. For all other states, there was essentially no signal. For details and references I suggest the review by Berg [6].

But what had we learned from these calculations? With 20/20 hindsight, I can say the following:

- [1] The short distance fluctuations in Wilson loops are killing the signal. It is necessary to use renormalized operators. One way to do this is through the Monte Carlo Renormalization Group. This program, first espoused by Wilson, has not been carried through for fear of the computer time required. The DLR variance reduction technique does not work well at small g because in the modified Wilson loops the averaging is too local.
- [2] The glueballs are not local objects, but most likely are spread out over a complete time slice. Thus any attempt at a variational calculation will need too many loops and even given sufficient loops

the calculation will not address the issue that these loops are thin (unrenormalized).

- [3] A source is needed to enhance the signal at large time separations.

I will now briefly describe the ideas proposed and tried to overcome the above problems

2.2) Technical Points

a) Finite Size Scaling

Lattice calculations will always require extrapolation of results calculated on finite lattices to the infinite volume limit. In certain models and under certain assumptions finite size scaling relations can be prescribed. They are not "truths", but should be used as phenomenological guides until verified.

- [1] For the string tension calculated from correlations of Polyakov-Wilson lines, the finite size scaling form suggested by integration of string fluctuation modes is [7],

$$\sigma(L) = \sigma(\infty) - \frac{\pi}{3L^2} + O(L^{-3}). \quad (2.4)$$

where L is the transverse size of the lattice.

- [2] The glueball data can be checked against the finite size scaling form [8]

$$m(L) = m(\infty) \left[1 - \frac{3}{16\pi} \left(\frac{\lambda}{m(\infty)} \right)^2 \frac{1}{m(\infty)L} \exp\left(-\frac{\sqrt{3}}{2} m(\infty)L\right) (1 + O(L^{-1})) \right] \quad (2.5)$$

where $\alpha_{GGG} \equiv \frac{3}{16\pi} \left(\frac{\lambda}{m(\infty)} \right)^2$ is the three scalar glueball coupling constant. This relation is derived under the assumption that finite volume effects come from multigluon interactions and that α_{GGG} is small. As I will show later, the finite size errors in glueball measurements seem to be much too large for eqn. (2.5) to be valid.

Thus, we need very careful runs at one value of the coupling for many L to get a phenomenological understanding of these effects. Otherwise we will have no predictions.

b) Sources for Glueballs

A simple calculation of the mass from a connected 2-point correlation function picks out of the statistical sample those configurations with a glueball in them. These glueballs are created as fluctuations of the QCD vacuum, and so are damped by their Boltzmann factor. Thus the measurements are inefficient. With an external source at time $\tau = 0$, the system near $\tau = 0$ is no longer in the vacuum state. Unlike vacuum fluctuations, the source is strongly coupled to many different states, exciting large number of quanta of each. The time evolution of these states is still given by the unperturbed transfer matrix. Thus, a given excitation with energy E_α will die out as $e^{-E_\alpha \tau}$. Far from the source we then make the standard assumption that only the lowest state of given quantum numbers survives. The mass is then measured from an exponential fit to the decay of the operator *i.e.*

$$\langle O(\tau) \rangle - \langle O \rangle \sim ce^{-m\tau} \quad (2.6)$$

where $\langle O \rangle$ is the vacuum expectation value measured at $\tau \rightarrow \infty$. In figure 2, I show a typical fit [9].

The simplest source for measuring $m_{0^{++}}$ and σ is to set all spatial links at $\tau = 0$ to the identity. The present status of the signal with such a source is that with 50000 sweeps one can follow the signal out to $\tau \approx 9$ at $6/g^2 \approx 6.0$ on a 10^3 spatial size lattice. Thereafter one has the usual bottleneck; the errors fall as $\frac{1}{\sqrt{N}}$, where N is the number of independent configurations. The DLR variance reduction technique is not applicable in the presence of the source, but smeared operators (to be discussed later) should be used. Also, these calculations should be supplemented by the variational method. At present no good source is known for the 2^{++} state.

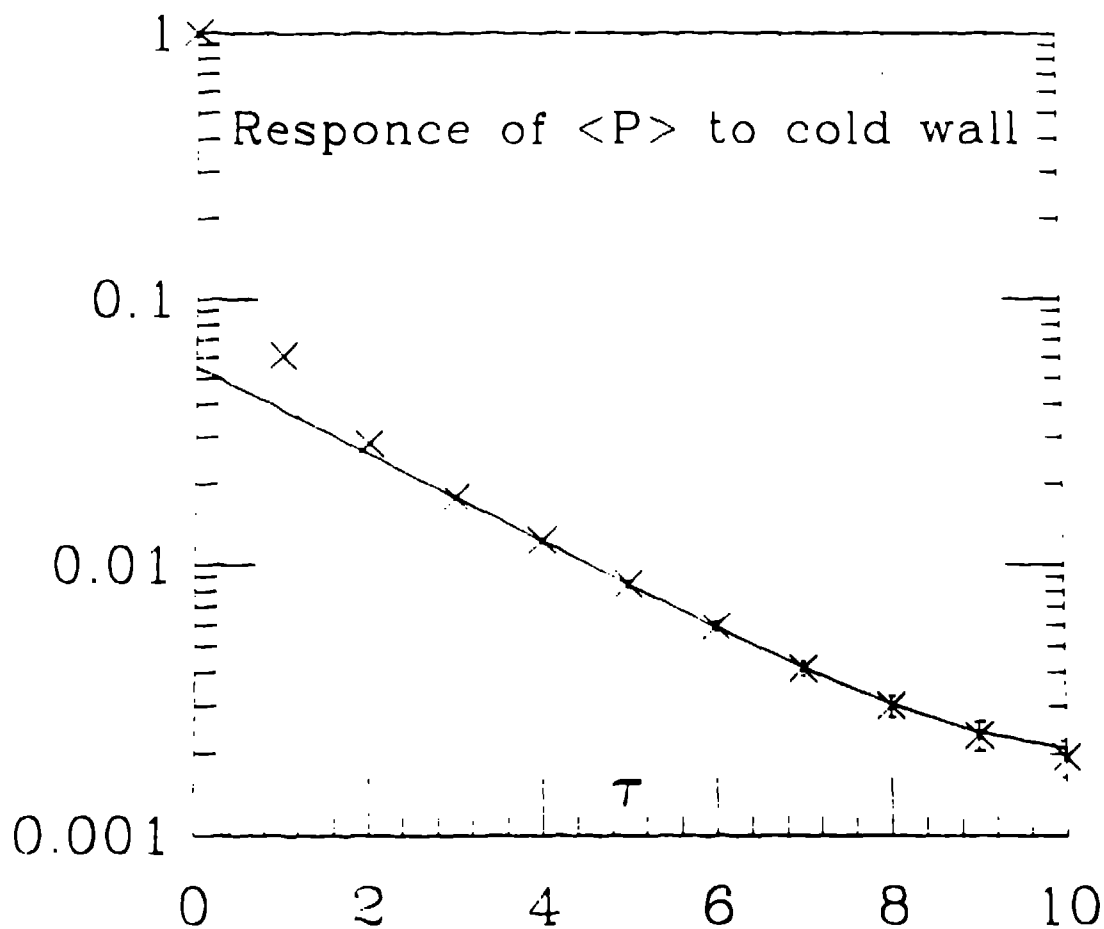


Fig. 2: A typical fit to the response of Polyakov loop operator, $\langle P(r) \rangle$, to a cold wall source with periodic boundary conditions [9]. The exponent at large r , in the exponential fall-off, gives the string tension.

c) Variational method in presence of a source

The standard variational method to estimate the wavefunction Ψ by solving the equation [9]

$$\langle \Theta_i(r) \Theta_j(r+1) \rangle_c \Psi_j = \lambda \langle \Theta_i(r) \Theta_j(r) \rangle_c \Psi_j \quad (2.7)$$

for the lowest eigenvalue can also be used in the presence of a source. The $\Theta_i(r)$ are the various loops (they could be blocked or smeared loops

to be defined later) measured on time slice τ . Eqn. (2.7) follows from the same assumption as in eqn (2.6), i.e. at time slice t the eigenstates of the transfer matrix are simple and ordered and the lowest state dominates the exponential fall off. A check that the solution Ψ is not dominated by the source is that the results be stable at a few successive time slices.

2.3) Large Lattice, High Statistics Results

The story of these calculations changed with the availability of Supercomputers. In this lecture I will focus only on this large lattice data, which is collected in table 1 and figure 3.

de Forcrand *et al.* did the first large scale calculation with a source for the 0^{++} state [10] and the string tension [11]. The source they used was to fix all space-like links at time-slice zero to the identity. The string tension was determined from a measurement of the Polyakov-Wilson line while the glueball mass was determined from the 2×2 Wilson loop. They determined the value for the ratio $\frac{m_{0^{++}}}{\sqrt{\sigma}}$ to be 1.96(7), 2.45(12) and 2.65(18) at the three values of the coupling along the Wilson axis taken to be $6/g^2 = 5.5, 5.7$ and 5.9 . (These ratios are slightly different from those in Table 1 because here I have quoted their infinite volume extrapolations for 0^{++}). These results show scaling violations. It is therefore not possible to deduce the continuum value. Their second result is that calculations on different spatial size lattices are in very good agreement with the presence of the universal Lüscher finite size correction to the string tension, i.e. $\frac{\pi}{3L^2}$. A third (even though negative) result of their calculation is that simple sources for the 2^{++} state don't work as well. Lastly, their calculations suggest that even with the source, the method saturates at $6/g^2 \approx 6.0$ because the number of points remaining are not sufficient to fit to a reliable exponential. This is after the initial time-slices dominated by the transients are discarded.

The improved action calculation [9] was motivated by an understanding of the cause of scaling violations in the calculations of de Forcrand *et al.* and the existence of a MCRG inspired method to avoid

#	K_F	Lattice	$\sigma(L)L$	$\sqrt{\sigma(\infty)}$	$m_G(L)$	$\frac{m_G(L)}{\sqrt{\sigma(\infty)}}$
1	9.2	$6^3 \times 21$	0.76(5)	0.395(25)	0.91(10)	2.3(3)
2	9.9	$6^3 \times 21$	0.32(1)	0.287(12)	0.79(11)	2.8(4)
3	9.9	$9^3 \times 21$	0.63(2)	0.288(10)	0.89(8)	3.1(3)
4	10.5	$9^3 \times 21$	0.38(1)	0.235(14)	0.67(6)	3.0(3)
5	10.5	$12^3 \times 21$	0.57(3)	0.234(28)	0.64(7)	2.8(4)
6	5.5	$6^3 \times 12$	1.86(6)	0.58(1)	1.07(3)	1.84(6)
7	5.7	$6^3 \times 16$	0.63(2)	0.37(1)	0.66(4)	1.8(1)
8	5.7	$8^3 \times 16$	0.94(3)	0.37(1)	0.86(4)	2.3(1)
9	5.9	$8^3 \times 20$	0.33(1)	0.24(1)	0.73(14)	3.0(6)
10	5.9	$10^3 \times 20$	0.52(1)	0.25(1)	0.68(8)	2.7(4)
11	5.9	$12^3 \times 20$	0.65(3)	0.25(1)	0.74(7)	3.0(3)
12	6.0	$10^3 \times 20$	0.41(3)	0.21(1)	-	-
13	5.9	$10^3 \times 32$	0.48(3)	0.24(3)	0.65(3)	2.7(2)
14	5.9	$12^3 \times 32$	0.66(1)	0.25(1)	0.76(4)	3.05(2)
15	5.9	$16^3 \times 32$	0.86(3)	0.24(2)	0.82(5)	3.4(3)
16	6.0	$13^3 \times 18$	-	-	0.65(8)	-
17	6.05	$13^3 \times 18$	-	-	0.66(7)	-
18	6.1	$13^3 \times 18$	-	-	0.64(10)	-

Table 1: Monte Carlo data for the 0^{++} glueball mass and the string tension σ . The first 5 entries are for the improved action, (eqn. (2.8)), calculations [9,21]. Entries 6 to 12 are from de Forcrand et al [10,15], 13 to 15 are from the APE collaboration [20] and 16 to 18 are from DeGrand [18]. All of these correspond to coupling along the Wilson axis.

them. The reason for the scaling violations is a lattice artifact: the lattice theory possesses extraneous critical points in the vicinity of which the universality of the $g \rightarrow 0$ theory is violated. One such known critical point is present in the fundamental-adjoint plane and lies close to the Wilson axis. A naive extrapolation of the specific heat data suggests that its maximum influence along the Wilson axis will be at $6/g^2 \approx 5.5$. At this critical point the 0^{++} glueball mass vanishes. This is based on the specific heat data [12] and a measurement of 0^{++} state, in $SU(2)$, close to the critical point [13]. On the other hand the string tension remains finite [14]. This explanation is consistent with de Forcrand *et al.* data. To avoid this singularity we chose a linear trajectory in a four coupling space consisting of the plaquette in the fundamental, 8 and 6 representations as well as the 1×2 rectangle in the proportion :

$$\frac{K_8}{K_F} = -0.12, \quad \frac{K_6}{K_F} = -0.12, \quad \frac{K_{1 \times 2}}{K_F} = -.04, \quad (2.8)$$

when the traces are normalized to unity. This trajectory is a MCRG estimate of the renormalized trajectory (RT) in this truncated space. Since the RT in principle preserves the mass-ratios of the continuum theory, working along it is a way of avoiding lattice artifacts. The second motivation has to do with using renormalized block operators. There are two ways to do this. One is to generate lattices with any action, block a reasonable number of times and calculate observables on these blocked lattices. This approach has a problem for QCD. The correlation length ξ for most observables (proton, rho, glueballs etc.) on the largest lattices accessible to today's supercomputers are at best a few lattice spacings. Thus any blocking makes $\xi \leq 1$. Since all BST are approximate, there is no guarantee that the flow from a starting action will be attracted to the weak coupling RT for such small ξ . The alternative is to work along the RT. The price one pays is a more complicated action in the update. However, in this case we can simulate in a region where $\xi > 1$ and thus satisfy a basic requirement of lattice calculations. The million dollar question (literally) is how elaborate does the action have to be such that the simple operators with improved actions are equivalent to the renormalized ones obtained by blocking

configurations generated with a simple action. We decided to test the 4-parameter action given in eqn(2.8), and the results are entries 1 to 5 in table 1.

The new result is $\frac{m_{glue}}{\sqrt{\sigma}} = 3.0(3)$. We again confirm the Lüscher term $\frac{\pi}{3L^2}$ but find much smaller finite size corrections for the glueball than de Forcrand *et al.* [10]. To later compare results from improved actions with those with the Wilson action, let me define β_{eff} as the coupling on the Wilson axis which gives the same string tension as a given improved action calculation.

Last October, de Forcrand analyzed data from more extensive calculations at $\beta = 5.9$ on $L = 8, 10, 12$ lattices [15]. His new result is $\frac{m_{glue}}{\sqrt{\sigma}} \approx 3$, in agreement with the improved action calculation. This immediately raises the question, how much better is the improved action? I will discuss this in the conclusions. Second, in his results, the finite size effects for glueballs do not show a monotonic growth with L , so we cannot use Lüscher's result, eqn (2.5). Again, I will have more to say about the finite size effects after discussing how to improve operators.

Designing better operators

I trace through an idea which goes beyond MCRG to reduce the high-frequency noise in operators. The presentation style is evolutionary rather than chronological.

DeGrand [18] presented a calculation with "fat" operators. Rather than the standard blocking with a change of scale, he just uses Swendsen's $b = 2$ transformation to define fat links connecting every alternate site. This operation is performed only on spatial links and glueball operators are made out of these fat links of length 2. Note that in this construction there is no change of scale, as distinct from MCRG ideas. From his calculation, there is evidence that glueball operators are far more extended than those used before. I have shown his results in Table 14 (entries 16 to 18) but I have some minor reservations about the data. The statistical errors are large and the glueball mass shows no variation between $\beta = 6, 6.05$ and 6.1 . Second, the calculations are

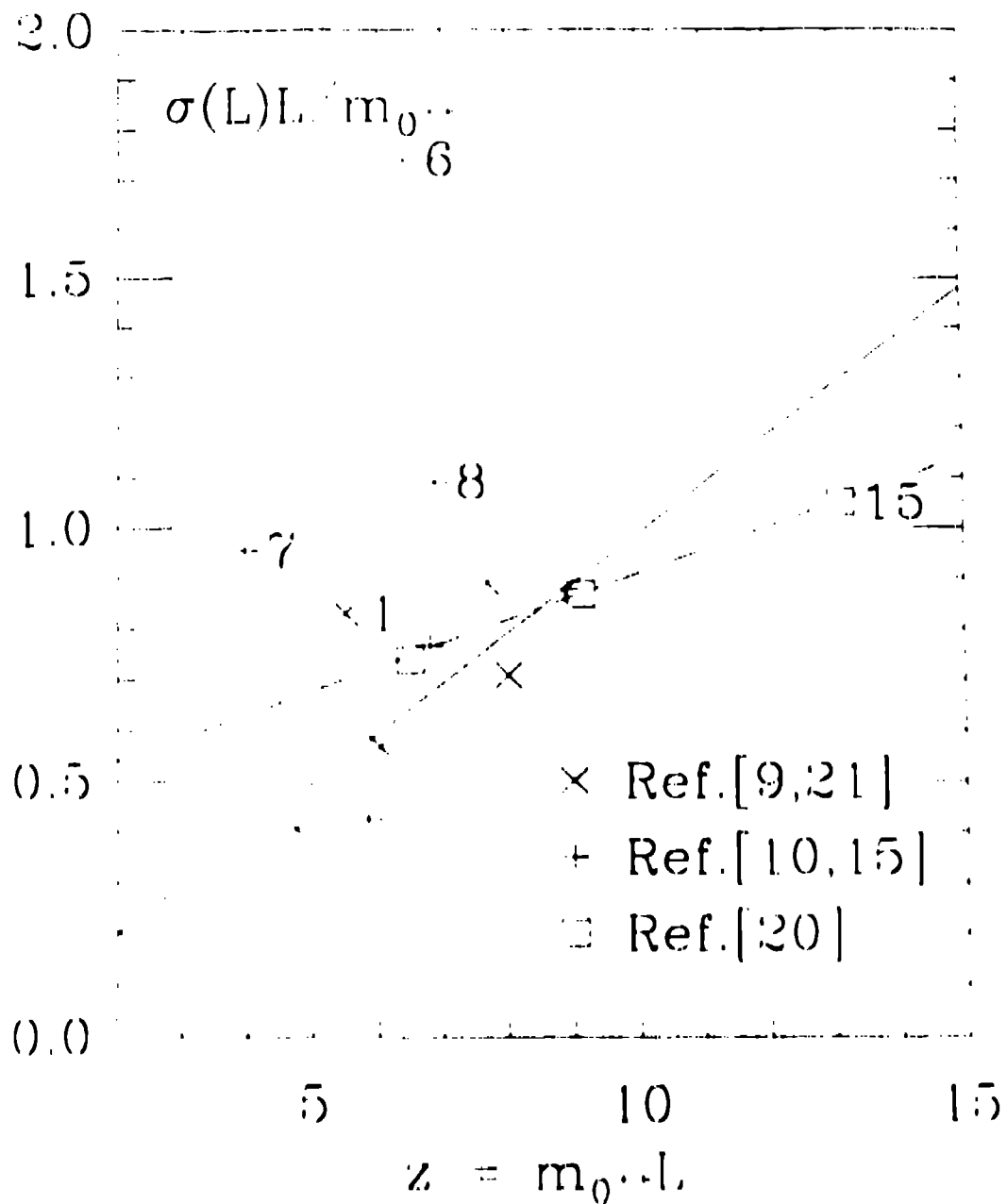


Fig. 3: The van Baal-Koller plot (22), $\sigma(L)L/m_0^{**}$ versus $Z = m_0^{**}L$ showing the high statistics and large lattice results (with sources). The straight lines are two possible infinite volume extrapolations. The difference shows the lack of control over finite volume corrections.

done on one lattice size. Therefore, finite size effects and statistical errors are mixed up. For the present I would conclude that this data provides corroborative support for the previous result $\frac{m_{\sigma^+}}{\sqrt{\sigma}} \approx 3$ once we take σ_∞ measured from elsewhere.

A similar idea of using fat loops has also been proposed by Teper [19]. He uses the same construct as DeGrand, but does not project the averaged link back onto SU(3). This leads to a small gain in CPU time but should be irrelevant for the results provided the extra part does not have larger short distance fluctuations. The more important idea incorporated is to carry through the blocking procedure recursively to produce very fat loops.

The APE collaboration [20] move away from MCRG ideas altogether by their use of "smeared" operators. They replace the field at each link by some average of the field in a neighborhood and study the behavior as the neighborhood is enlarged. In practice, this is done as follows: Each link U on the lattice is replaced by

$$U \longrightarrow U + \epsilon \sum_{\text{spatial}} UUU^\dagger \quad (2.9)$$

where UUU^\dagger is a staple, and ϵ is the smearing coefficient. This process is carried out recursively, so the gauge field on the link represents a smeared average over larger and larger neighborhoods. The sequence of plaquette operators so formed is labeled by the number of the recursive step in defining a link by eqn(2.9). They calculate the glueball mass using just a simple plaquette on each level separately. If we examine the plaquette obtained after a number of smearing steps in terms of original links, it consists of a very large number of thin Wilson loops which form a glob. Thus, the operator is smeared over the physical glueball.

The single parameter ϵ is insufficient to match onto the wavefunction of the glueball. There are two possible extensions: One is to implement a variational calculation with the set of operators taken to be loops of different sizes, measured at different smearing step, and with different ϵ at each level. Another possibility is to first fix to Coulomb

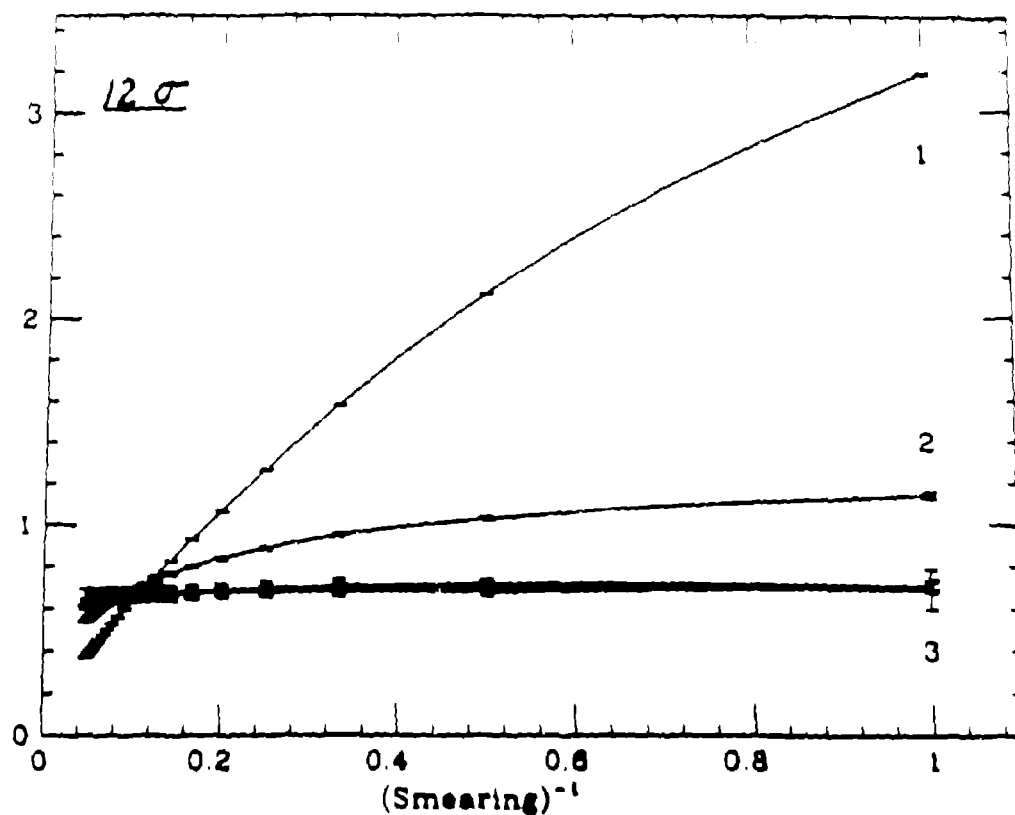


Fig. 4: The effective string tension $\sigma(L)L$ for $L = 12$ as a function of the number of smearing operations [20] and for various r . The best estimate is given by where curves $r = 2$ and 3 intersect.

gauge and then replace each link in a spatial loop by a weighted average over parallel links. The reason for fixing to the Coulomb gauge is that in this "averaging" the link is not gauge invariant i.e. all paths do not start and end at the same point. If the Coulomb gauge fixing is reasonably smooth, then the optimum weighting will provide information about the glueball wavefunction. Again, we would like to play with the size of the loop. Clearly, to even test the usefulness of these enhancement requires more compute power than is currently available. However, they should be kept in mind, especially the notion that glueball operators do not have to have a simple representation in terms of Wilson loops.

The calculation with smeared operators may be further improved by using extended actions. This is based on the following observation:

The average plaquette with the action in eqn. (2.8) at an $\beta_{eff} = 6.0$ is ≈ 0.63 in contrast to 0.594 with the Wilson action. Thus the short distance fluctuations are reduced with such improved actions.

I now return to discussing the results for $\frac{m_{0^{++}}}{\sqrt{\sigma}}$. The source used by the APE collaboration is to set links in only two spatial directions to the identity. In figures 4 and 5, I show their results for σ and 0^{++} . The three curves in figure 4 are for the effective " $\sigma(\tau)$ " with $\tau = 1, 2, 3$. The great hope presented for such calculations (especially glueballs) is that $m(\tau)$ for τ small, agree with the asymptotic mass derived from the standard 1-mass exponential fit to $\tau > 4$ after a sufficient number of smearing operations. They find that this is true at $\tau = 3$ for both the string tension and the glueballs. However, we need some caution here. By themselves, $m(1)$ and $m(2)$ with smeared operators do not lead to a reliable estimate. The estimates $m(3)$ and $m(4)$, for the no smearing case, are by themselves within 10% of the asymptotic result quoted. Also, we [9] had found that the source method supplemented by the variational calculation gives the asymptotic value from $\tau = 3$ at a similar coupling. So, at $6/g^2 = 5.9$ the only new thing the smearing method is really giving us is confidence. We need a test at weaker couplings.

Let me now focus on the finite size effects. For σ they again find reasonable agreement with $\frac{\sigma}{L^2}$. The glueball is a new story. The finite size effects are huge (see Table 1). This is completely consistent with the glueball being a very extended object, but it also makes predictions for infinite volume results difficult because such large effects make Lüscher's derivation incomplete.

In figure 3, I show the global data on the van Baal-Koller plot of $\frac{\sigma(L)L}{m_{0^{++}}}$ versus $z = m_{0^{++}}L$. Some of the points are labeled by the entry number in table 1 and the error bars are suppressed. They are large and can be evaluated from the data in table 1. If scaling holds, then for sufficiently large z , the data should collapse on to a single line with a positive slope λ in the variable z . In that case, $\frac{m_{0^{++}}}{\sqrt{\sigma}}$ is given by $\frac{1}{\sqrt{\lambda}}$. I leave out points 1, 6, 7, 8 since they are at strong coupling and show a deviation from the universal behavior. The preferred fit, so far, is the

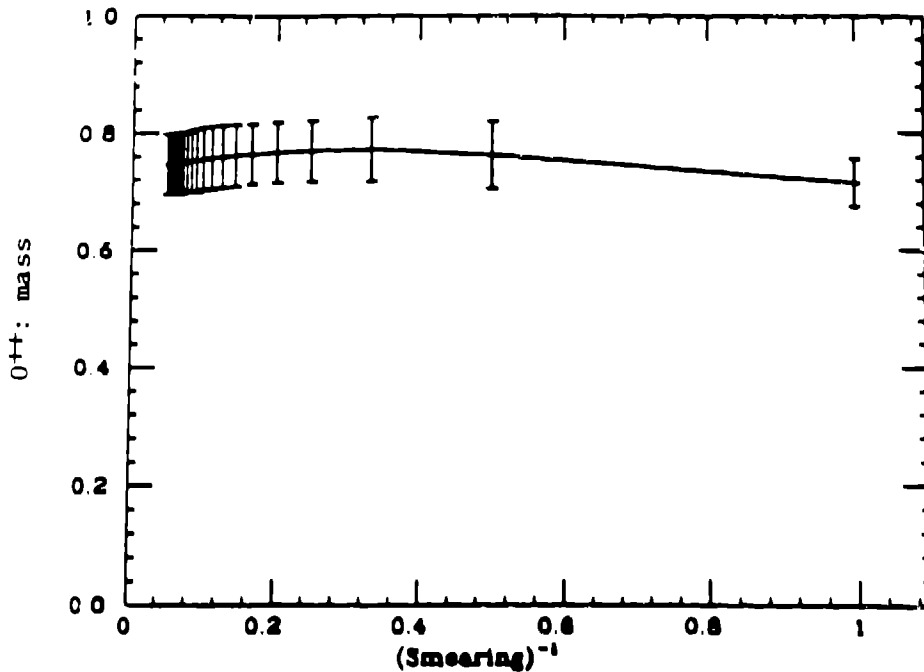


Fig. 5: Estimate of the O^{++} glueball mass obtained from a 1-mass fit with $r_{\min} = 4$ as a function of the number of smearing steps.

solid line which gives $\frac{m_{0^{++}}}{\sqrt{\sigma}} \approx 3.1$ since point 15 has large errors. On the other hand just fitting the data at $6/g^2 = 5.9$, the dotted line, gives $\frac{m_{0^{++}}}{\sqrt{\sigma}} \approx 4.6$! This again highlights the uncertainty in the results due to finite size effects. To summarize, we need more data at $6/g^2 = 5.9$ for various lattices sizes to understand finite size effects.

2.4) The 2^{++} state

Berg, Billoire and Vohwinkel [16] have, over the last two years, devoted considerable effort to taming the 2^{++} state. The basis of their study is a finite volume result derived by Lüscher [8]. The analytic calculation for $SU(3)$ has recently been done [17], and predicts $\frac{m_{2^{++}}}{m_{1^{++}}} \approx 1.2$. This calculation is valid only for small x where x is the dimensionless scaled variable $x = m_{0^{++}} L$. Berg *et al.* advocate the use of x to isolate the finite volume corrections from finite g scaling violations.

If scaling exists, then the finite volume corrections have a simple form and all data should eventually collapse onto a single universal curve.

Berg *et al.* work on $L^3 \times \infty$ lattices and measure the 0^{++} , 2^{++} , masses and σ . To determine the masses of the 0^{++} and the 2^{++} states they measure correlations of Polyakov lines in the adjoint representation without a source. The signal in this channel exists only when $\langle P \rangle$ is large and $6/g^2$ small. Their cumulative estimate is $\frac{m_{0^{++}}}{m_{2^{++}}} = 1 \pm .2$, based on the data shown in figure 6. There has been a lot of controversy over whether, in a small box with $2\sigma(L)L < m$, the states they measure are 0^{++} and 2^{++} or some bound state of color electric excitations. Looking at the errors in the data for $z > 2$ and the lack of an asymptotic value, I think we should wait for calculations in a large box for a reliable number. Meanwhile, what should be taken seriously from their calculations is to question whether the 2^{++} state is really much heavier than 0^{++} .

A question relevant to the above discussion is the connection between the finite box transition at $z \approx 1$ and the Euclidian finite temperature transition at $z \approx 5$ [22]? The most probable scenario is that there exists a single $Z(3)$ symmetry breaking transition that moves from Lüscher's predicted answer in a small volume to $z \approx 5$ as the lattice is changed from $L^3 \times \infty$ to $\infty^3 \times N_t$. An additional possibility is that the $z \approx 5$ transition leaves its signature (maybe as a crossover involving level crossing) on the $L^3 \times \infty$ system at $z \approx 5$. The only relevance of this detail for continuum physics is whether to trust an extrapolation of the small box data, especially for the ratio $\frac{m_{0^{++}}}{m_{2^{++}}}$, from small z . However, if the present trend of large finite size corrections to 0^{++} is not a statistical fluctuation, then there is no reason to expect the 2^{++} or the mass ratio will be better behaved. We therefore need to explore the large z region with dedicated supercomputers like the APE.

For 2^{++} , the signal in the APE calculation exists only up to $r = 4$ and their estimate, $m(3)$, is preliminary because of large statistical and uncontrolled finite size effects. Other than that they feel that $m(3)$ is a reasonable estimate of the asymptotic value because of the smearing

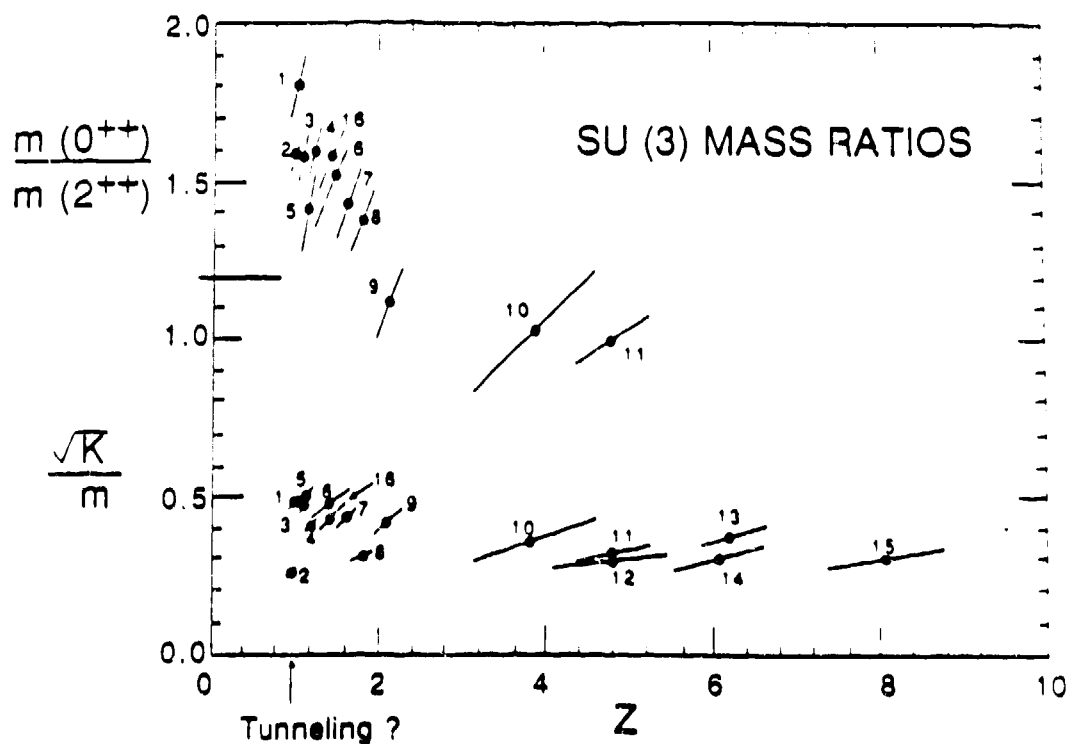


Fig. 6: MC results for SU(3) mass ratios versus z [16]. The straight line at ≈ 1.2 indicates the perturbative result by Weisz and Ziemann [17] for $m(0^{++})/m(2^{++})$. The current status of the large z results for \sqrt{K}/m is given in Fig. 3. For details of Berg et al. data see ref. [16b].

method. Their present conclusion is a light 2^{++} , with $\frac{m_{0^{++}}}{m_{2^{++}}} \approx 1$ within 20% errors.

2.5) Conclusions

In a lot of the following analysis I will probably be guilty of making issues of trends that are statistical fluctuations. So the reader is cautioned in advance.

In all cases for which $2\sigma L \leq m_{0^{++}}$, the statistical errors are large and the fits are comparatively not as good. Thus the physical picture that these string states strongly influence the glueball channels is rea-

sonable. Lesson: Avoid working on small lattices which don't satisfy $2\sigma L > m_{0^{++}}$

The finite-size correction works well for the string tension. However, it should also be pointed out that in many cases the statistical errors are large and the number of different L used are small. So it should not be considered *de facto* yet.

Both de Forcrand and the Rome group have made a finite size analysis on three different lattice sizes. On $L = 10, 12$ their results are in agreement. Neglecting $L = 8$ (for which $2\sigma L < m_{0^{++}}$), one notices a large finite size effect for the 0^{++} glueball. If true, it is too large for Lüscher's formula to be valid. Taking all the results in table 1 into account, let me propose a phenomenological finite size behavior shown in figure 7. In region A , the glueball mass is large due to mixing with the string states and from being squashed into a small box. In region B , the dominant effect is multi-gluon interactions, which if the three glueball coupling is small may be handled by eqn (2.5). The intermediate region has a dip (at least non-monotonic) as all the data seem to show. Thus, unless we understand how to do finite size extrapolations, glueball calculations will require lattices with very large transverse dimensions.

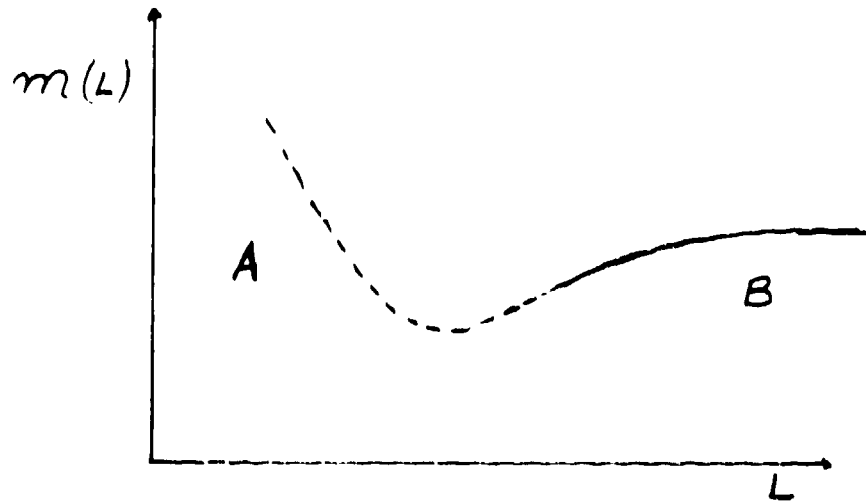


Fig. 7: A heuristic finite size behavior of glueball mass. Region A is dominated by string modes. The infinite volume extrapolation has to be made from region B with a form which is not known yet.

To decide whether the improved action program is working, consider the new point at $K_F = 9.2$ [21], which on the van Baal-Koller plot is marked # 1. It corresponds to $\beta_{eff} \approx 5.67$ based on σ . It should be compared with Wilson axis results at $6/g^2 = 5.7$ (# 7 and 8). I think the data has much too large errors and in light of uncontrolled finite size errors it is not possible to make a confident statement about an improvement.

The evidence is in favor of a light 2^{++} glueball. The objections against the work of Berg *et al.*—extrapolating from small z values for a theory with a first order transition—have to be reexamined in light of the result of the Rome Group. At present the results are still too preliminary to decide details such as which state is lighter and by how much.

Right now the smearing method of the Rome group needs to be explored further. A crucial test is to repeat the calculation with some of the variations mentioned at say $\beta = 6.2$ and check whether it lives up to its promise.

In conclusion, let me say what I would do if I had a year of dedicated X-MP time. I would do a high statistics finite volume study on $L = 14, 18$ and 22 , using the variational method with smeared loops. I would use a source that couples to 0^{++} and 2^{++} (maybe the one the Rome Group used) at effective coupling $6/g^2 = 5.9$ before moving on to 6.2 .

References

- [1] S. Sharpe, *Proceedings of the 6th International Conference*, Vanderbilt University, 1984.
- [2] S. R. Sharpe, R. L. Jaffe and M. R. Pennington, *Phys. Rev.* **D30** (1984) 1013.
- [3] K. L. Au, D. Morgan and M. R. Pennington, *Phys. Lett.* **167B** (1986) 229.
- [4] V. A. Novikov, *et al. Nucl. Phys.* **B191** (1981) 301.
- [5] R. L. Dobrushin, *Theory Prob. Appl.* **13** (1969) 197. ;
O.E. Lanford III and D. Ruelle, *Commun. Math. Phys.* **13** (1969) 194 .
- [6] B. Berg, in *Progress in Gauge Field Theory* (Cargèse, 1983), p105, ed. G. 't Hooft *et al.*, Plenum Press (1984).
- [7] M. Lüscher, *Nucl. Phys.* **B180** [FS2] (1981) 317 ;
R. Pisarski and O. Alvarez, *Phys. Rev.* **D26** (1982) 3735.
- [8] M. Lüscher, in *Progress in Gauge Field Theory*, (Cargèse, 1983), p. 451, ed. G. 't Hooft *et al.*, Plenum Press (1984). ;
M. Lüscher, *Nucl. Phys.* **B219** (1983) 233.
- [9] A. Patel, R. Gupta, G. Guralnik, G. Kilcup and S. Sharpe, *Phys. Rev. Lett.* **57** (1986) 1288.
- [10] P. de Forcrand *et al.*, *Phys. Lett.* **152B** (1985) 107.
- [11] P. de Forcrand *et al.*, *Phys. Lett.* **160B** (1985) 137.
- [12] K.C. Bowler *et al. Nucl. Phys.* **B240** (1984) 213.
- [13] K.-H. Mütter, T. Freimuth and K. Schilling, *Phys. Lett.* **131B** (1983) 415.
- [14] G. Bhanot and R. Dashen, *Phys. Lett.* **113B** (1982) 299.
- [15] P. de Forcrand, Unpublished results.
- [16] B. Berg, A. Billoire and C. Vohwinkel, *Phys. Rev. Lett.* **57** (1986) 400 ;
B. Berg, FSU-SCRI Preprint 86-89 (1986).
- [17] P. Weisz and V. Ziemann, DESY preprint 86-109 (1986).
- [18] T. DeGrand, To appear in *Phys. Rev. D*.
- [19] M. Teper, Oxford preprint 84/86 (1986).

- [20] The APE Collaboration, Rome Preprint ROM2F/87/014.
- [21] R. Gupta, G. Guralnik, G. Kilcup, A. Patel and S. Sharpe, in progress.
- [22] P. Van Baal, *Proceedings of the 1986 BNL Conference on Lattice Gauge Theories*.

3) QCD WITH DYNAMICAL FERMIONS: THE CHIRAL TRANSITION

The partition function for QCD with dynamical fermions in Euclidean space can be written in a number of equivalent forms:

$$Z = \int D\psi D\psi^\dagger DU \exp(S_G + \bar{\psi}(\mathcal{D} + m)\psi) \quad (1a)$$

$$Z = \int DU \det(\mathcal{D} + m) \exp(S_G) \quad (1b)$$

$$Z = \int DUD\varphi D\varphi^\dagger \exp(S_G - \varphi_e^\dagger \frac{1}{-\mathcal{D}^2 + m^2} \varphi_e) \quad (1c)$$

S_G is the gauge action (possibly an improved action). \mathcal{D} is the fermion covariant derivative, and m the quark mass. For staggered fermions, the form (1c) applies in which the scalar psuedofermion (PF) field φ_e lives only on even lattice sites.

Including fermions in the theory makes the action non-local. This non-locality is manifest in the determinant or in the inverse of the Dirac operator. Efficient algorithms to include dynamical fermions in numerical simulations are very important in Condensed Matter Physics, Statistical Mechanics and Lattice Gauge theories. In the last four years, considerable effort has been devoted to algorithm development. The five classes of algorithms that have been explored so far are:

- [1] Pseudo Fermions (PF) [1].
- [2] Exact Algorithm (EA) [2][3][4].
- [3] Molecular Dynamics (MD) [5].
- [4] Langevin (LG) [6].
- [5] Hybrid (HY) [7].

The details of these algorithms have been covered in the lectures by Mike Creutz, John Kogut and M. Fukugita. I will discuss some aspects of the exact algorithm. By and large, I will concentrate on the status of the results for the chiral transition. The status of the hadron spectrum with quenched and dynamical fermions is reviewed by M. Fukugita.

3.1) The Chiral and the Deconfinement Transition

Chiral symmetry plays an important role in modern theories of particle physics. This relies on the observation that the u and d quark masses are very small or equivalently the pion is light. Thus chiral symmetry is regarded as an almost exact symmetry of nature.

Even if the u and d quarks were exactly massless, the zero temperature QCD vacuum would not preserve handedness i.e. the fermion number would not be individually conserved for left handed and right handed particles. This is because in addition to the mass term $\bar{\psi}_L \psi_R + \bar{\psi}_R \psi_L$, $\vec{E} \cdot \vec{B}$ fluctuations (instantons) in the QCD vacuum do not respect handedness. Chiral symmetry is spontaneously broken. The order parameter in this limit is $\langle \bar{\psi} \psi \rangle$. A non-zero value gives the amplitude for a left handed quark to move in a closed loop and end up as right handed.

The chirally symmetric state has higher energy. However, experience with such symmetry broken ground states suggest that at some high enough temperature the symmetry is restored. So, the questions we would like to answer are: Given the physical quark masses and QCD, 1) does the system go into a symmetric state at high temperature, 2) is the nature of the transition discontinuous, continuous or just a cross-over and 3) can we calculate and predict the signatures of this transition.

In addition, our theoretical prejudice is that hadronic matter at high temperature and density undergoes a transition to quark-gluon plasma. This deconfinement transition is important to understand because it will be investigated by the present planned heavy ion experiments if the transition temperature is below a few hundred MeV. Success depends on the nature of the transition and our ability to predict the transition temperature.

The only quantitative tool available at present to address these non-perturbative phenomena is the numerical simulation of Lattice Gauge theory. Since we have a technique (Monte Carlo simulations) that is still in the stage of algorithm development, it is natural to pick a qualitative goal. The one I will focus on is: What is the order of

these two transitions and are these two transitions related?

3.1a) Status of the Pure Gauge Theory

Simulations of pure gauge SU(3) show a strong first order transition at a temperature $T_c \approx \Lambda_{\overline{MS}}$ [8][9]. At this transition the global Z(3) symmetry of the theory is spontaneously broken. This is characterized by a non-zero expectation value of the Polyakov line $\langle L \rangle$ in the high temperature deconfined phase. This non-zero value of the order parameter implies a finite free energy for the quarks. The scaling of the T_c data is discussed in section 4 of my lecture on MCRG. A second order parameter, the chiral condensate $\langle \bar{\chi}\chi \rangle$ measured in the quenched approximation, is also discontinuous at the transition. $\langle \bar{\chi}\chi \rangle$, when extrapolated to $m_q = 0$, changes from a non-zero value at low T to zero in the high T phase.

3.1b) Introducing Dynamical Quarks

Dynamical quarks act as external fields and explicitly break the Z(3) symmetry. $\langle L \rangle$ is still a measure of the quark free energy but it is non-zero for all temperatures due to vacuum polarization. $\langle \bar{\chi}\chi \rangle$ remains a good order parameter to study chiral symmetry. The only theoretical understanding of the realization of chiral symmetry comes from a renormalization group analysis of an effective spin model in $4 - \epsilon$ dimensions [10][11]. The prediction depends on the global flavor group and on whether instantons are important i.e. whether $U(1)$ is broken down to $Z(n_f)$. In case the symmetry is $U(1)$, their analysis suggests that QCD has a fluctuation induced first order chiral symmetry transition for $N_f \geq 2$. For $n_f = 0, 1$, if the transition is second order then it is in same universality class as $O(2n_f)$ vector models. The same is true for $n_f = 2$ if instantons are important i.e. the symmetry is $Z(n_f)$. For $n_f = 0, 1$ there are no predictions, while for $n_f = 3$ the transition should be first order which changes to fluctuation induced first order for $n_f \geq 4$. These predictions are not very firm and there are the usual caveats of the ϵ -expansion. So we should proceed without any strong bias.

For $T < T_c$, one expects $\langle \bar{\chi}\chi \rangle \neq 0$ when extrapolated to $m_q = 0$. For $T > T_c$ the chiral symmetry is restored, consequently $\langle \bar{\chi}\chi \rangle \propto m_q$ for small m_q . This needs to be verified. Also, if, as in the pure gauge theory, there is a discontinuity in $\langle L \rangle$, then we expect to see interesting thermodynamical properties of the quark-gluon plasma [12] created in heavy ion collisions.

The expected phase diagram for QCD is as follows: The confinement transition at $m_q = \infty$ extends to some finite m_q in the $m_q - T$ phase plane, and similarly the chiral transition at $m_q = 0$ extends to some non-zero m_q . The questions to settle are whether the chiral transition with two physical light flavors and heavier s quark is first order, and whether the two transitions are connected.

3.2) Staggered Fermions

Staggered fermions have a remnant continuous chiral symmetry on the lattice. This is sufficient to guarantee that $\langle \bar{\chi}\chi \rangle$ calculated on the lattice does not need any subtractions and that the chiral limit is at $m_q = 0$. For this reason, most of the calculations have been done using staggered fermions. However, for each flavor one puts in by hand, the theory actually has four flavors. Thus the flavor symmetry on the lattice is $4n_f$. This accounts for why, until recently, most results are for 4 flavors.

A technical point: In the continuum, the flavor symmetry at zero temperature is $Z(n_f) \times SU_L(n_f) \times SU_R(n_f)$ which breaks spontaneously to $SU_V(n_f)$. Since the lattice regulator destroys some of the continuum symmetries, the lattice symmetry group is only $U(1)_A \times U(1)_V$ entangled with a complicated mess of discrete symmetries, which we expect breaks spontaneously to $U(1)_V$ plus discrete bits [13]. It is only in the continuum limit that one recovers 4 degenerate flavors. Can this difference in symmetry lead to a spurious result in our calculations considering how sensitive the predictions from the ϵ -expansion are on the flavor symmetry? We don't know and will have to proceed on with a nagging suspicion. On the brighter side, calculations of the quenched hadron spectrum show that for $6/g^2 \geq 6.2$ this

symmetry is restored dynamically to a very good approximation [14]. Another check on this subtlety is to simulate both an effective spin model that has the continuum symmetry and one with the discrete lattice symmetry and to compare the results. We, at present, don't have a spin model with the lattice symmetry and therefore cannot perform the test.

The discussion of the chiral transition should be restricted to small quark masses. This is because for m_q comparable to the cut-off,

$$\langle \bar{\chi}\chi \rangle = \int_0^\Lambda \frac{d^4 k}{k \cdot \gamma + m}$$

is expected to vary simply as $1/m$. The gauge dynamics comes in through $k \cdot \gamma$ and does not contribute in the limit of heavy quarks. Thus, for m_q above some value, the simulation is essentially quenched.

3.3) Results for 4 Staggered Flavors

Prior to the summer of 1986, the status of the chiral transition was not clear. This was primarily due to short data runs at large m_q where the signal is weak. Also, there were doubts about thermalization, or confidence was lacking due to the evolving nature of approximate algorithms with uncontrolled systematic errors. The most detailed calculations were by Kogut *et al.* [15] using the *MD* and hybrid algorithm. Their conclusion was that while the order could not be pinned down, the system showed a very rapid crossover for $m_q = 0.1$ and 0.05 . Similarly, Gavai [16] ruled out evidence for a first order transition. He used the pseudo-fermion algorithm with an acceptance rate of 70%

On the other hand, Fucito and Solomon [17] used perturbation theory to write down a 3 flavor pseudo-fermion algorithm and claimed evidence for a first order transition. Their result suffered from poor statistics, especially since they were using time history of the two states as the probe. They could not rule out the possibility that the signal was due to incomplete thermalization.

Fukugita and Ukawa [18] used the Langevin technique and made hysteresis runs. They found a hysteresis in their runs at $m_q = 0.1$, for

$N_t = 4$, in the interval $6/g^2 = 5.05$ to 5.15 . Their best estimate for a transition coupling was $6/g^2 \approx 5.1$. Their conclusion was that the transition is first order. The chief criticism against their calculations was again that the runs are not long enough for complete thermalization.

3.3a) Present Status: 4×4^3 Lattice

The popular consensus is that the transition for 4 staggered flavors is first order. This was first demonstrated by extensive runs using an exact algorithm on a 4×4^3 lattice [19]. The small volume was dictated to us because we wanted to use an exact algorithm. Only then could we work at any m_q with control over systematic errors and bias. This way one could investigate the chiral limit. Furthermore, the exact algorithm is not limited by the small step size approximation. A 4×4^3 lattice is not as ridiculous as it seems. The system is at finite temperature except that there is no preferred direction i.e. the Boltzmann damping of higher states (definition of temperature) is valid for propagation in all four directions. The effect of a small volume can be a wash out of the transition, but it is much less likely to generate one. The disadvantage of EA is also obvious: We have no quantitative predictions for T_c .

We have used a mixture of two approaches; for a given $6/g^2$ to find a m_q at which the transition occurs or for a given m_q to find the corresponding g_c . The location of the transition is fixed by requiring that at that g the discontinuity in $\langle \bar{\chi}\chi \rangle$ be maximum. To get the value of $\langle \bar{\chi}\chi \rangle$ in the two states, we first make runs away from the transition or take a peek at existing hysteresis data from other calculations. Then we make a crude scan in g till we can observe flip-flops with this discontinuity (or as close to it as possible). In the data you will note that on either side of g_c we observe jumps with much smaller discontinuity.

The next part of the talk is a picture gallery of our data. The attempt is to show how the observables behave near and at the transition. Since all the observables, $\langle \bar{\chi}\chi \rangle$, $\langle L \rangle$, Wilson loops are correlated and show the transition we plot $\langle \bar{\chi}\chi \rangle$ versus Monte Carlo sweep number to demonstrate the transition. In the data the convergence of the conjugate gradient algorithm is specified by the number of iterations,

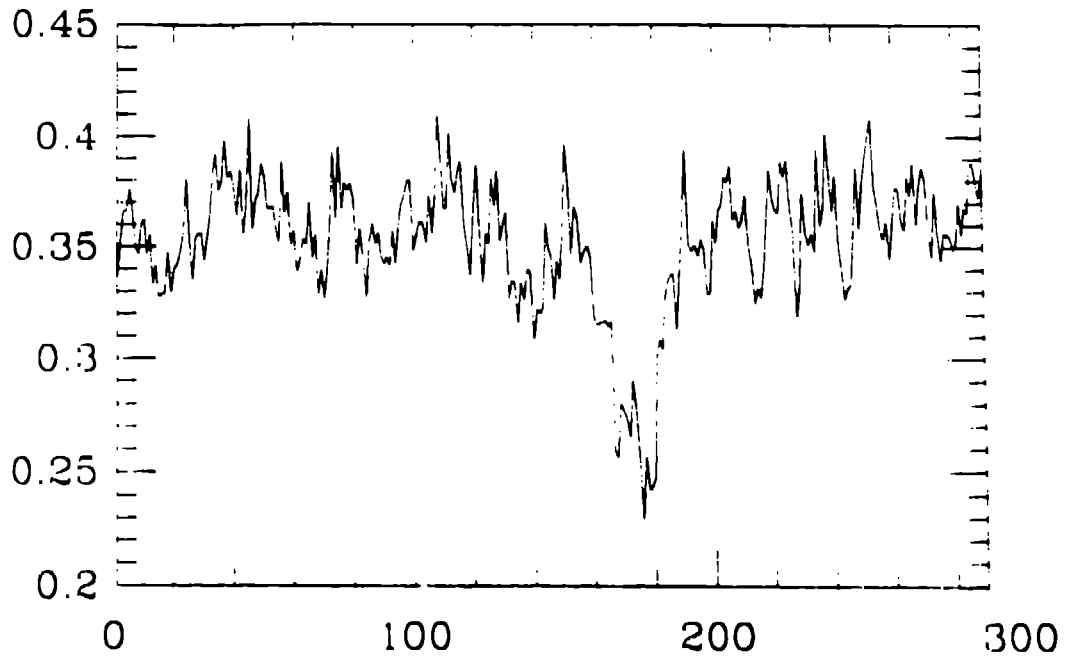


Fig.1: $\langle \bar{\chi}\chi \rangle$ at $m_q=0.025$ $\beta=4.80$ $N_{CG}=60$

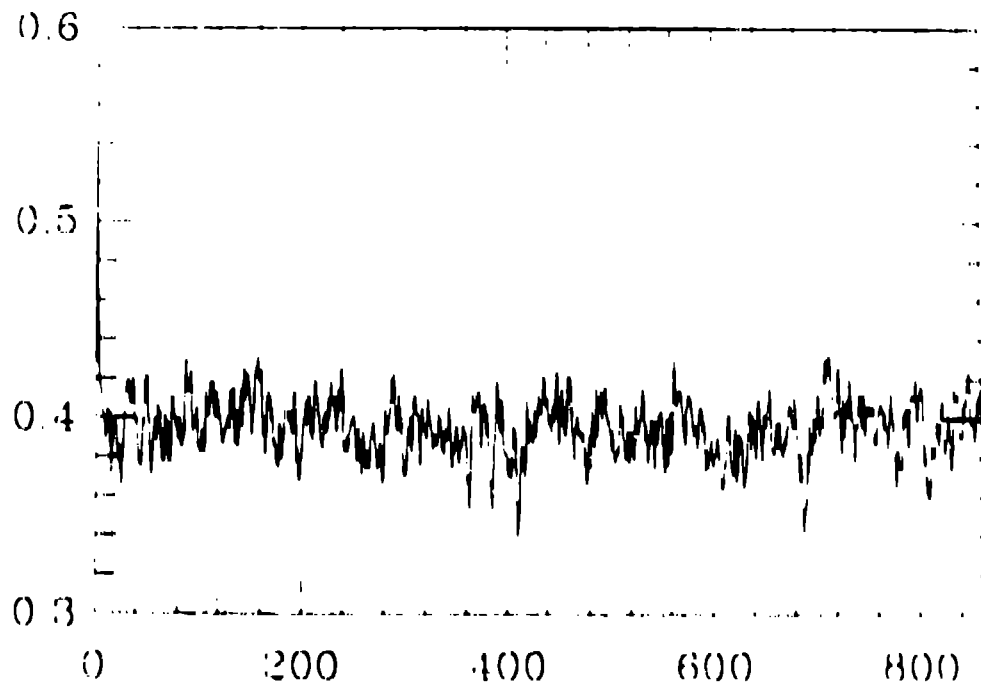


Fig.2: $\langle \bar{\chi}\chi \rangle$ at $m_q=0.1$ $\beta=4.9$ $N_{CG}=60$

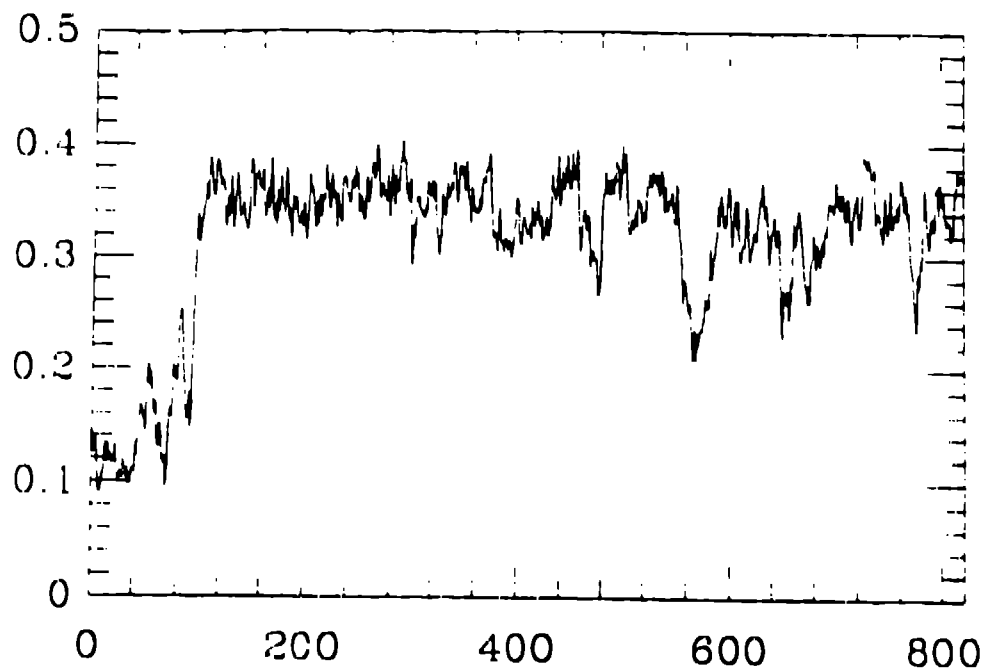


Fig.3: $\langle \bar{\chi\chi} \rangle$ at $m_q=0.05$ $\beta=4.9$ $N_{CG}=60$

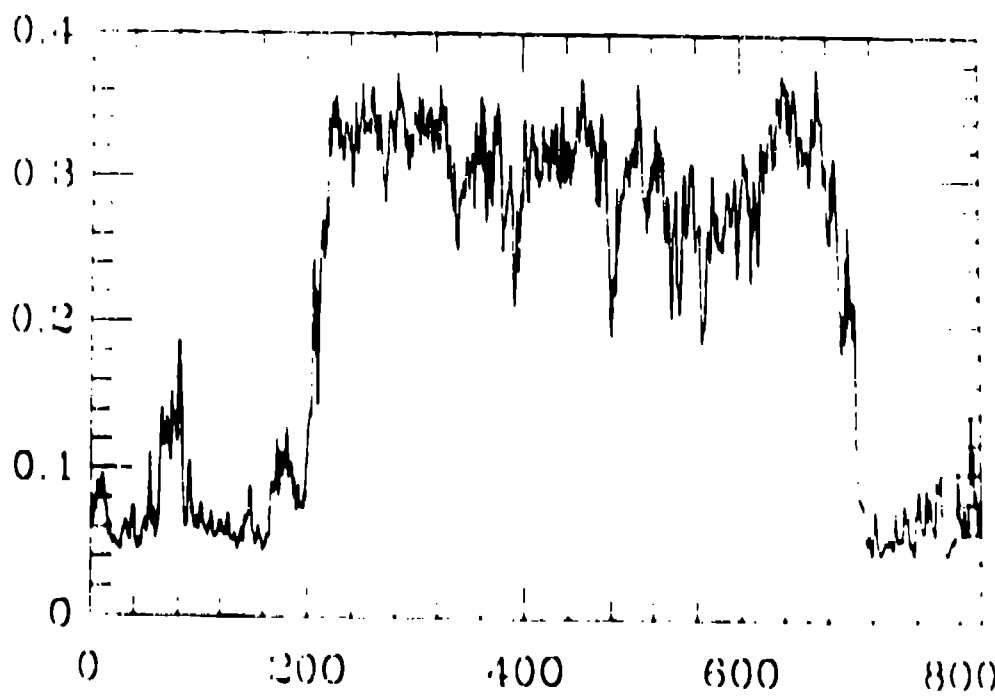


Fig.4a: $\langle \chi\chi \rangle$ at $m_q=0.025$ $\beta=4.9$ $N_{CG}=90$

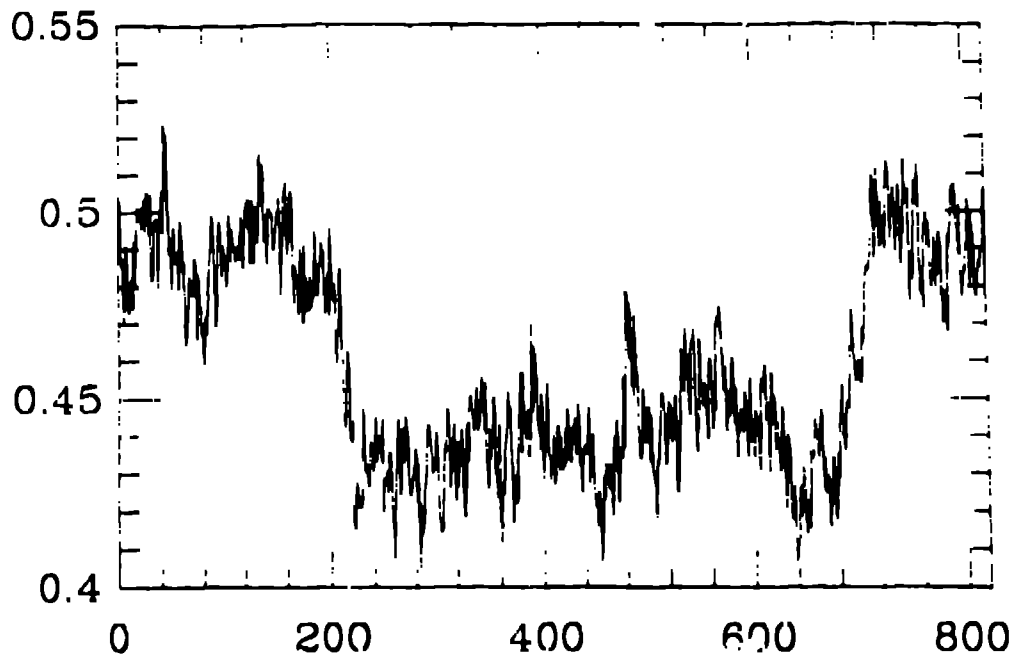


Fig.4b: $\langle \text{plaq} \rangle$ at $m_q=0.025$ $\beta=4.9$ $N_{CG}=90$

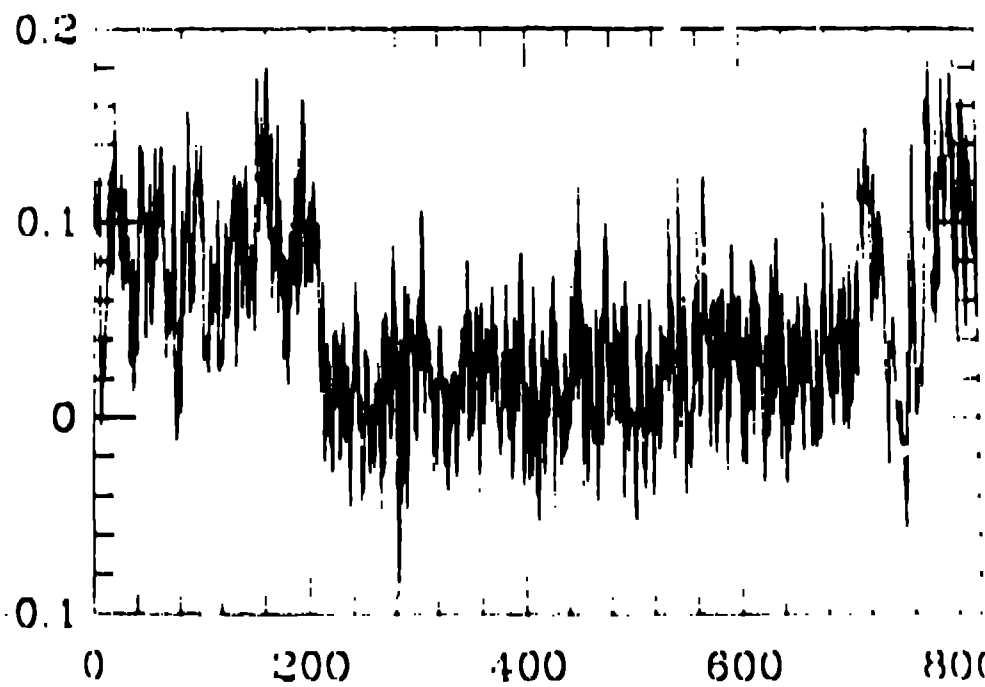


Fig.4c: $\Delta(\text{plaq})$ at $m_q=0.025$ $\beta=4.9$ $N_{CG}=90$

$N_{c\theta}$, as it will be relevant to a later discussion.

- [1] At $6/g^2 = 4.8$, $m_q = 0.025$ and with $N_{c\theta} = 60$ there is a small jump indicating a transition at smaller g (figure 1).
- [2] At $6/g^2 = 4.9$, $m_q = 0.1$, we find only thermal fluctuations with $N_{c\theta} = 60$ (figure 2).
- [3] At for $m_q = 0.05$ (figure 3) we do not see a two state structure, but compared to $m_q = 0.1$ the fluctuations are larger (again indicating a possible transition at smaller g)
- [4] The situation changes at $m_q = 0.025$. The runs with $N_{c\theta} = 90$ are shown in figure 4a. We see metastability and a 2 state behavior characteristic of a first order transition. To protect against inadequate thermalization, we ran long enough to see flip-flop between the states. The discontinuity is the maximum expected (compare with figs. 1 and 6). In Figs. 4b and 4c we also show the data for 1×1 Wilson loop and $\langle L \rangle$ in one of the 4 directions (all 4 directions show similar behavior). There is a clear correlation between all observables. We regard this as evidence that at small m_q , QCD has a first order transition with a discontinuity in $\langle \bar{\chi}\chi \rangle$, $\langle L \rangle$ and in Wilson loops. While the chiral and thermal transitions need not have been related, the data shows that for $T > T_c$, the system is deconfined and chiral symmetry is restored. Having shown the transition, we continue the search for the end point by increasing m_q .
- [5] At $6/g^2 = 4.95$, $m_q = 0.05$ and with $N_{c\theta} = 60$, we again see the transition with the characteristic flip-flop (fig. 5) and the expected discontinuity [20].
- [6] At $6/g^2 = 4.95$ and $m_q = 0.025$ (fig. 6), the transition exists but the system spends more time in the χS phase. Also, $\langle \bar{\chi}\chi \rangle$ in the χSB phase is only ≈ 0.3 . We estimate the transition for $m_q = 0.025$ at $6/g^2 = 4.91(3)$.
- [7] For $m_q = 0.02$ (fig. 7a) and $m_q = 0.015$ (fig. 7b) the system is in the high temperature phase, so the transition has to be for $6/g^2 < 4.95$.
- [8] At $6/g^2 = 5.02$, $m_q = 0.1$ and $N_{c\theta} = 30$ the system is predom-

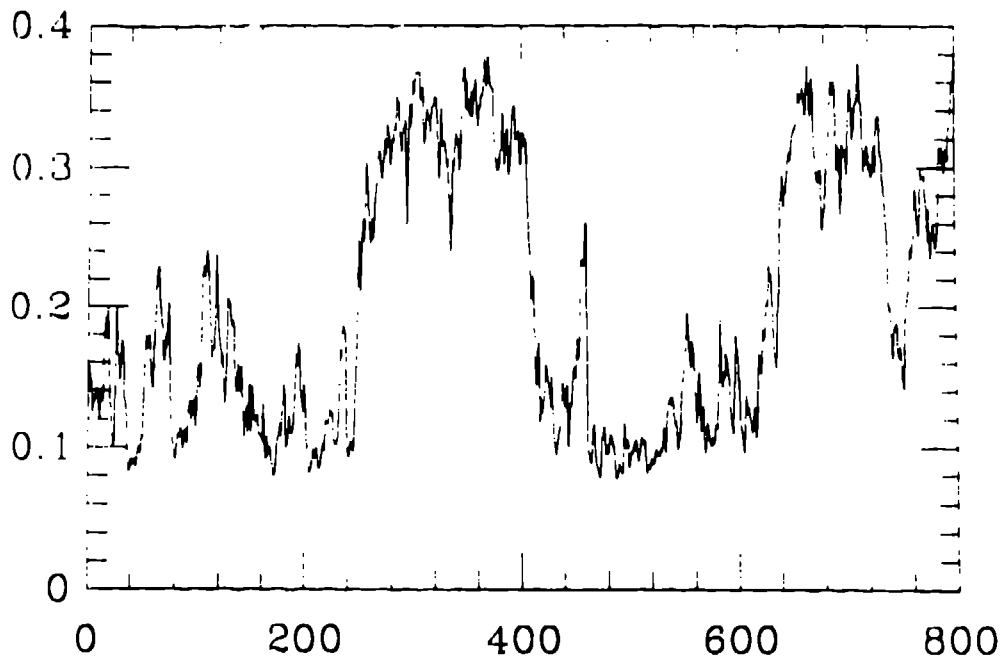


Fig.5: $\langle \bar{\chi}\chi \rangle$ at $m_q=0.05$ $\beta=4.95$ $N_{CG}=60$

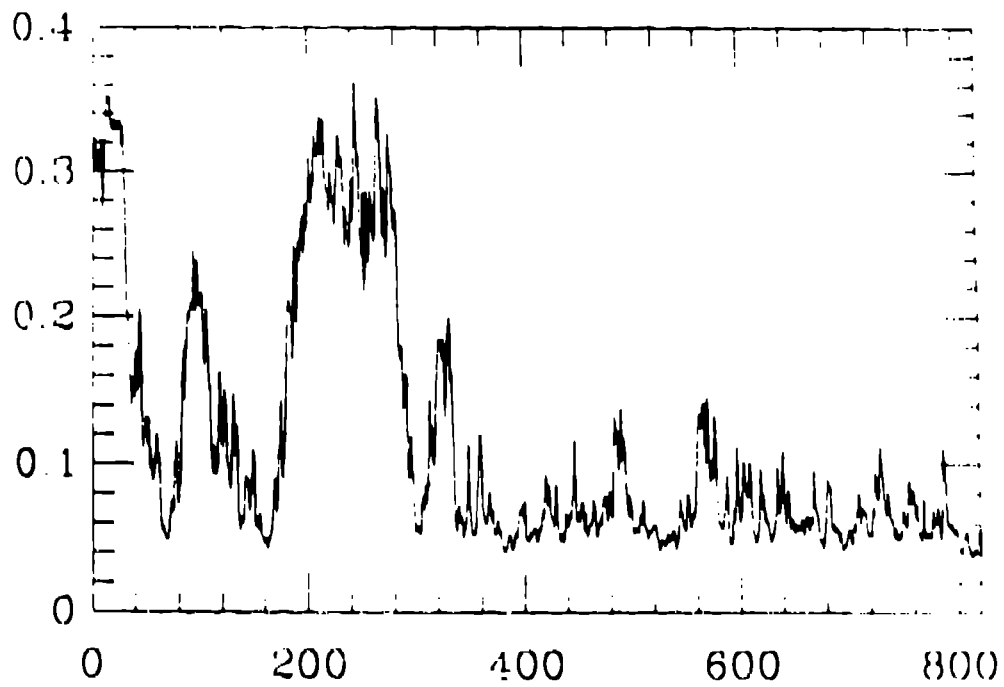


Fig.6: $\langle \bar{\chi}\chi \rangle$ at $m_q=0.025$ $\beta=4.95$ $N_{CG}=60$

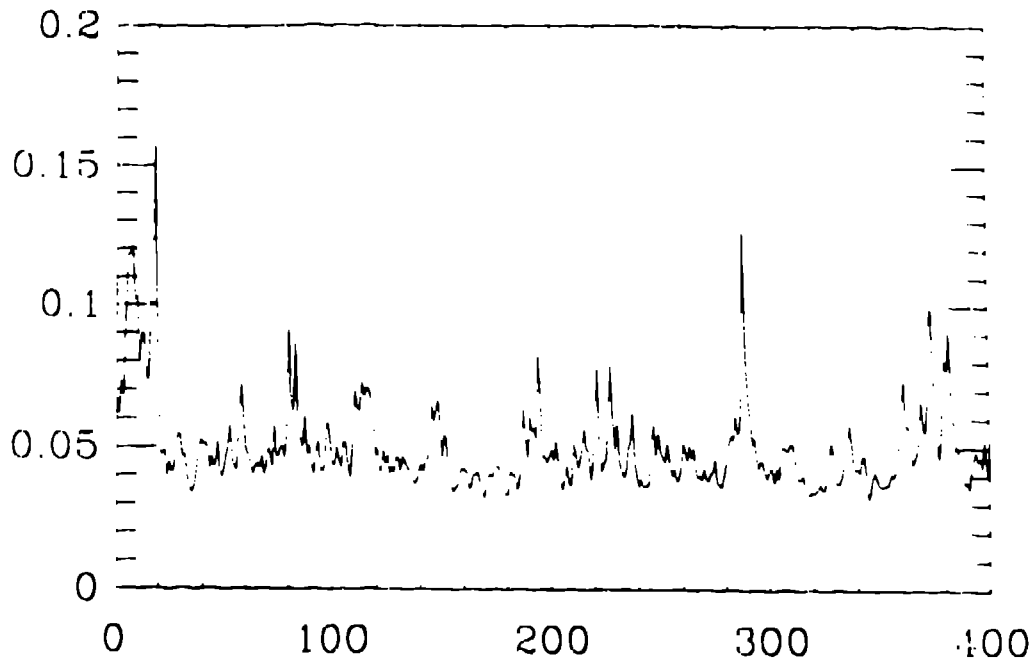


Fig.7a: $\langle \bar{\chi} \chi \rangle$ at $m_q=0.02$ $\beta=4.95$ $N_{CG}=60$

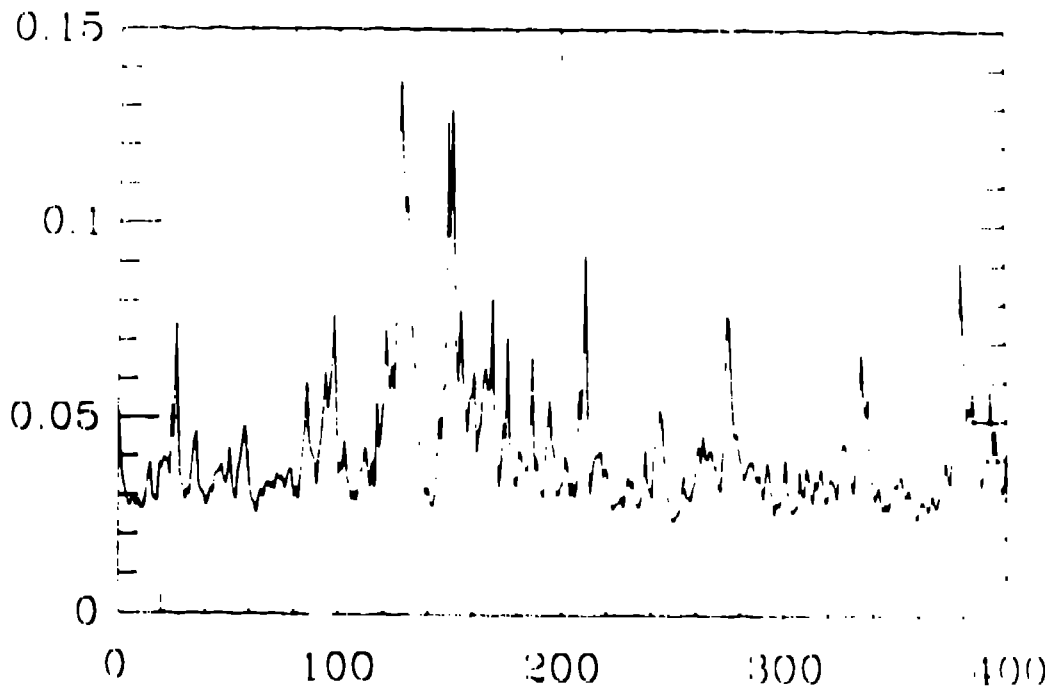


Fig.7b: $\langle \bar{\chi} \chi \rangle$ at $m_q=0.015$ $\beta=4.95$ $N_{CG}=60$

inately confined with hints of an approaching transition in the sharp spike (fig. 8a).

- [9] At $6/g^2 = 5.04$, $m_q = 0.1$ and $N_{cg} = 30$ (figure 8b) the system shows a clear two state structure with the expected discontinuity (see figure 9).
- [10] At $6/g^2 = 5.07$, $m_q = 0.1$ with $N_{cg} = 30$ (figure 8c), the system shows fluctuations but there is no clear signal of metastability. We are, at present, extending this run. At $6/g^2 = 5.1$, $m_q = 0.1$ and $N_{cg} = 30$, we again see flip-flops as shown in figure 8d. However, the discontinuity is small i.e. the value of $\langle \bar{\chi}\chi \rangle$ in the χSB phase is only ≈ 0.3 due to the rounding effect. Thus 5.10 is $> 6/g_c^2$. At $6/g^2 = 5.13$, the system is already in the χS phase (figure 8e). We estimate the transition to be at 5.04(3).

Evidence for a first order chiral transition was found on exploring the small m_q limit. At $6/g^2 = 4.9$ for $m_q = 0.025$, the discontinuity is very large in the order parameter $\langle \bar{\chi}\chi \rangle$ and flip-flops provide clear evidence for a first order transition. If it is a genuine first order transition, the discontinuity should decrease (increase) with m_q increasing (decreasing). We have provided evidence of this at $m_q = 0.05$ and 0.1. Locating the transition at $m_q = 0.1$ has been much harder for a very simple reason. Due to the large finite size rounding, the two states exist over a large range of $6/g^2$. But over most of this range, the discontinuity is small and it is hard to distinguish flip-flops (genuine metastability) from fluctuations. I believe this is a general property of first order transitions -- the width over which one can observe metastability decreases with a decrease in the discontinuity.

Our goal is to confirm whether there really exists a range of $6/g^2$ over which there is no transition. Preliminary evidence shows that even at $m_q = 0.2$ there is metastability. Thus, at present, we support the picture that the transition goes over from a chiral dominated one to the deconfinement transition without a region of analyticity.

To further analyze the transition we study $\langle \bar{\chi}\chi \rangle$ as a function of m_q . The estimates for $\langle \bar{\chi}\chi \rangle$ in the two phases are shown in figure 9. The data has been compiled from the runs given above. In the confined

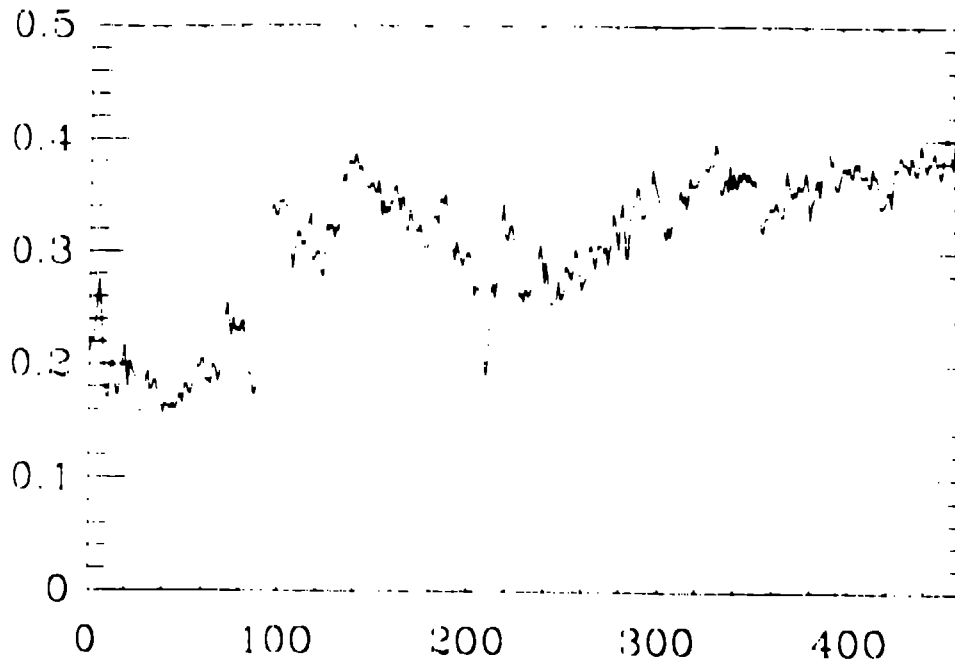


Fig.8a: $\langle \bar{\chi}\chi \rangle$ at $m_q=0.1$ $\beta=5.02$ $N_{CG}=30$

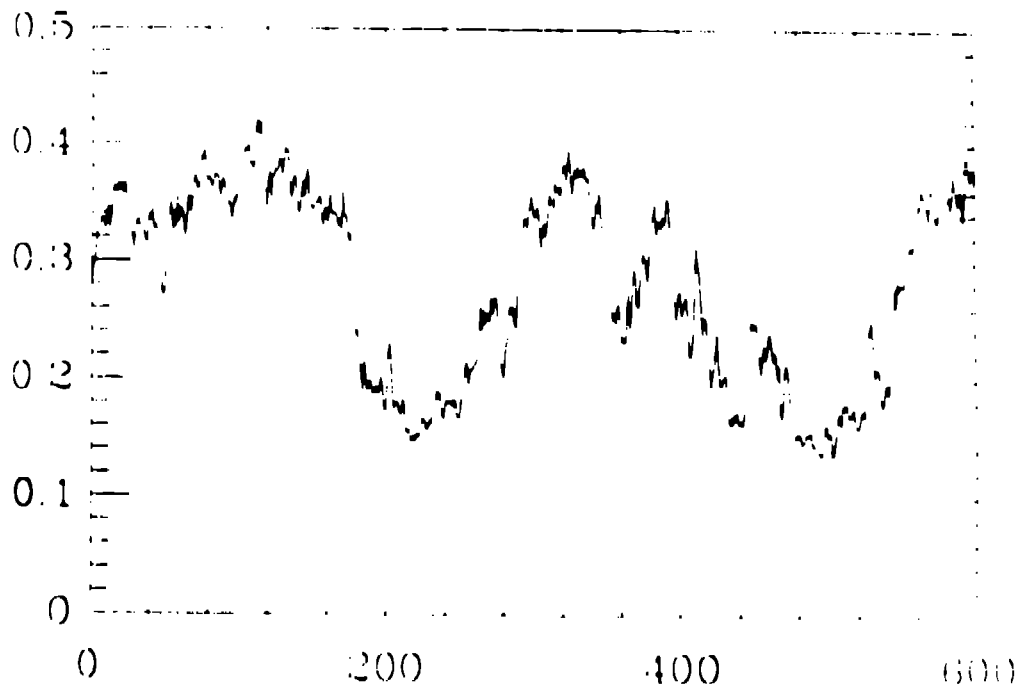


Fig.8b: $\langle \chi\chi \rangle$ at $m_q=0.1$ $\beta=5.04$ $N_{CG}=30$

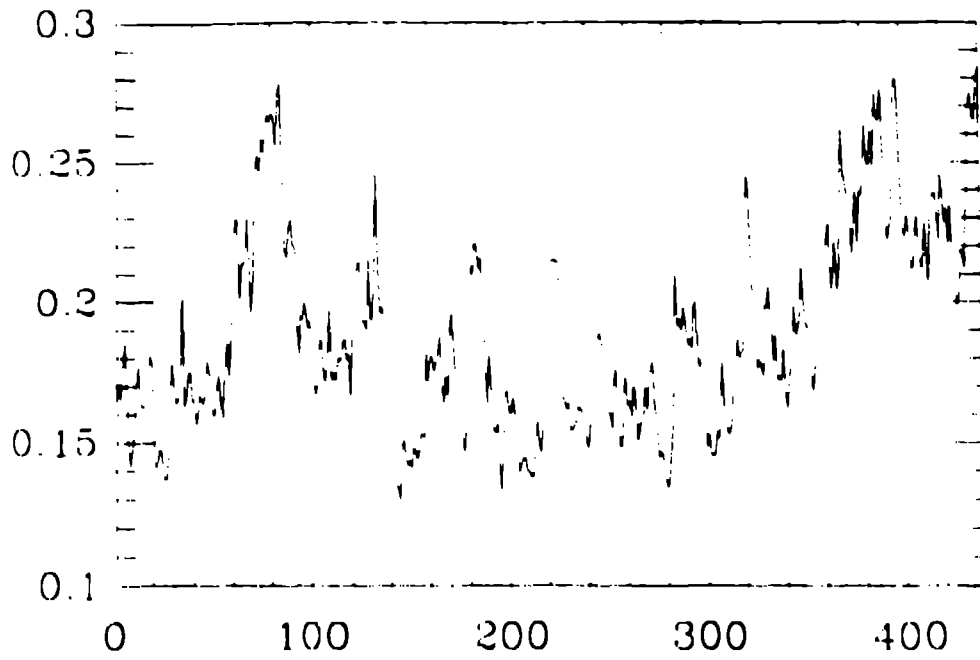


Fig.8c: $\langle \bar{\chi}\chi \rangle$ at $m_q=0.1$ $\beta=5.07$ $N_{CG}=30$

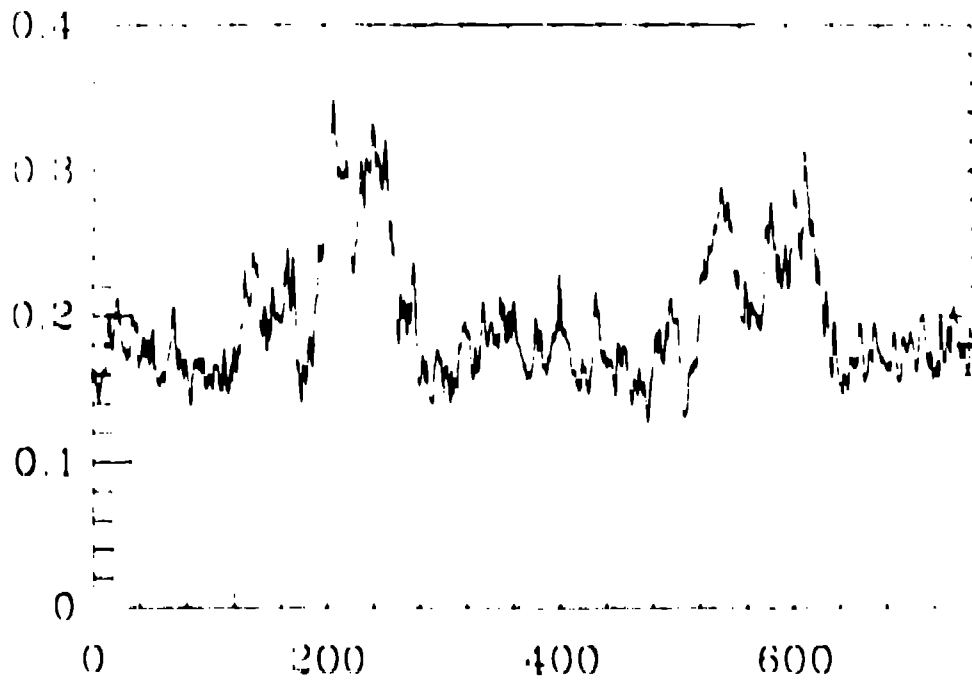


Fig.8d: $\langle \chi\chi \rangle$ at $m_q=0.1$ $\beta=5.10$ $N_{CG}=30$

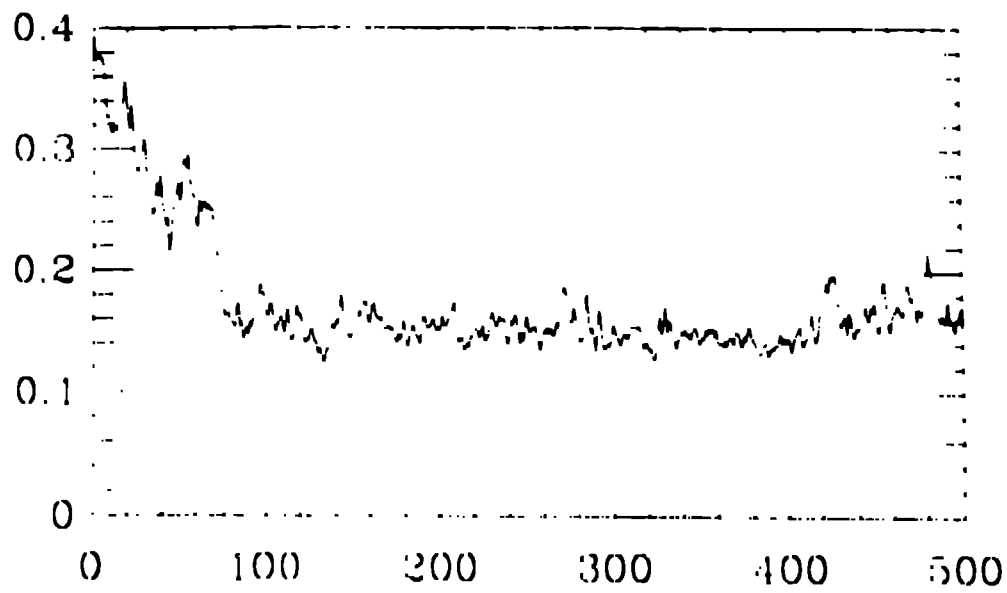


Fig.8e: $\langle \bar{\chi}\chi \rangle$ at $m_q=0.1$ $\beta=5.13$ $N_{CG}=30$

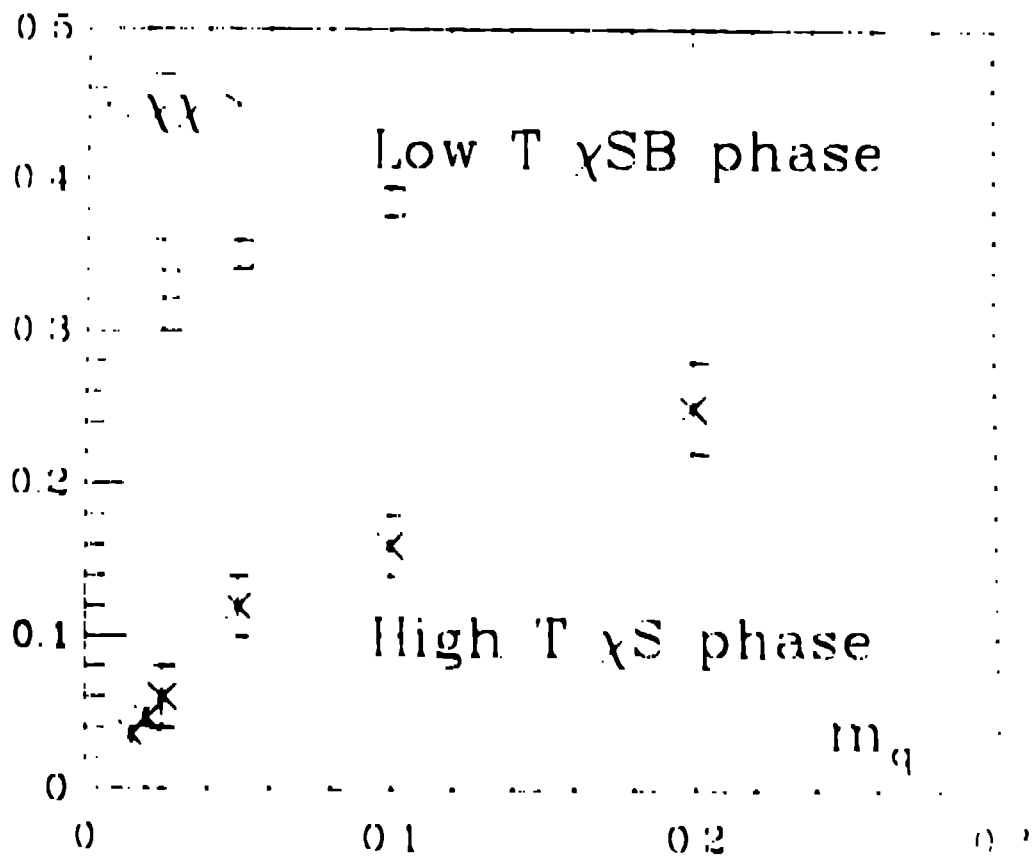


Fig 9 Testing Chiral behavior: $\langle \bar{\chi}\chi \rangle$ versus m_q

phase we estimate $(\langle \bar{\chi} \chi \rangle - 0.3) \propto m_q$. In the deconfined phase the data at small m_q agrees with the expected behavior $\langle \bar{\chi} \chi \rangle \propto m_q$. Thus, with large lattice data we can eventually determine the value of m_q at which the linear chiral behavior breaks down. The observed behavior though significant is not sufficient proof of the order of the transition. A corroboration on lattices with larger N_t and with $N_s \gg N_t$ is necessary.

A technical point about locating the transition: The usual hysteresis run is very useful to locate the region of the transition, it is not a very good method to confirm a first order transition. The best tool we have at the moment is to either show a flip-flop (tunneling on a finite lattice) or use two starting configurations prepared in the two states and show that they coexist as such for runs much longer than thermalization time (barring tunneling which can be distinguished by its abruptness). In figure 10 one such run is shown from [21]. In the second case one needs a good measure of the thermalization time.

3.3b) Comparison of the 4^4 Data with Various Algorithms

The results with the exact algorithm have been reproduced by the hybrid algorithm [21][22] and the Langevin algorithm [23]. These 4^4 results would have been meaningless without the confirmation on the the 4×8^3 lattices [21][22][23]. It turns out that for the actual numbers -- the discontinuity in observables, etc -- there is good agreement between the 4×4^3 and the 4×8^3 lattice data. So, it is meaningful to continue pushing 4^4 calculations to explore the phase transition.

I feel that it is very important to fix the power law, $cV^{1+\alpha+\gamma}$, by which the computation time for producing independent configurations grows for a given small step size algorithms. Here V is the lattice volume, α is the exponent due to step size limited slow movement through phase space, γ is the exponent due to critical slowing down as the coupling g is decreased and c is the prefactor. Both α and γ are a function of g and m_q . I present a crude estimate of the prefactor based on the Monte Carlo time for producing flip-flops in the exact versus step size limited algorithms. Within factors of five, it looks like $r \approx 5$ corresponds to a single sweep of the exact. Since most

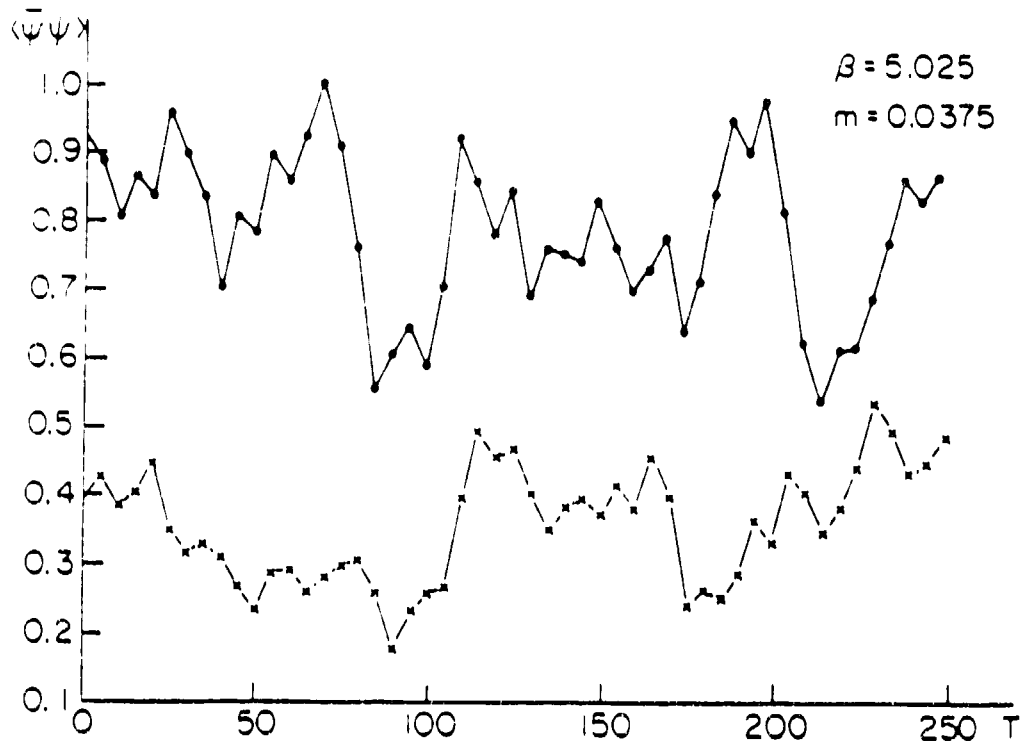


Fig. 10: Time history showing co-existence for a run with the hybrid algorithm on a 4×8^3 lattice with 4 staggered flavors[21].

of these algorithms have been run at $\delta\tau \approx 0.01$ we should keep the large number of sweeps, 500 to 1000, in mind when worrying about statistics in serious calculations of say the hadron spectrum. These estimates depend on the parameters and at weaker coupling and smaller m_q the step size will have to be decreased further [24]. An *a posteriori* justification for our use of the exact algorithm on the 4^4 lattice is that it is no slower than the small step size algorithms once you fold in the decorrelation time. To arrive at this conclusion I have used update times of 0.03, 1 to 2, and 450 seconds for a 4^4 lattice on a Cray X-MP for the pure gauge, Langevin and exact algorithms. The limitation of the exact algorithm used so far is that the lattice volume cannot be made any bigger with the current computer power.

Another feature to study using the 4^4 data is the shift in the critical coupling as a function of ϵ or $\delta\tau$. The present status is shown in

m_q	EA	HY 1	HY 2	LG 1	LG 2
0.025	4.91(3)	4.94(4)	4.96(3)		≈ 5.02
0.05	≈ 4.95		5.05(5)*		
0.1	5.04(3)		5.13(3)	≈ 5.1	

Table 1: The estimates for the transition coupling on $N_t = 4$ lattices and for 4 flavors. The points with * are estimates based on the midpoint of the hysteresis curve. The data is from: Exact - [19][20][25]; Hybrid 1 - [21][26]; Hybrid 2 - [22], Langevin 1 - [18] and Langevin 2 - [23].

table 1. The hybrid simulations are, within statistical errors, in agreement with the exact algorithm at light quark masses. The Langevin algorithm gives a much larger shift than can be explained by the first order correction in ϵ , which is $\approx 0.14\epsilon\beta$. The Brookhaven group is working hard to understand this effect. The discrepancy increases for the HY also at $m_q = 0.1$. It is not clear whether this is just due to systematic errors in fixing the precise location of the transition especially as the rounding gets large or because of something more serious. The various estimates do lie within the width of the hysteresis.

3.3c) Going from $N_t = 4$ to 6

Kovacs *et al.* [26] find evidence for a first order transition at $6/g^2 = 5.125$, $m_q = 0.025$ on a 6×10^3 lattice for 4 flavors. They also find large fluctuations in addition to the metastability. So they propose that the end point of the first order line lies very close to this value of m_q .

Using their data for $N_t = 4$ and 6, they calculate the value of $T_c/\Lambda_{\overline{MS}}$ using asymptotic scaling. The ratio changes from 2.8(2) at $N_t = 4$ to 2.1(1) at $N_t = 6$. This is close to the pure gauge theory result (2.6(1) changes to 2.12(1)), and this behavior is not surprising since gluons are the major contributors. However, we should be cautious in pushing this agreement because we don't know what scaling to use (asymptotic scaling may be violated by as much as a factor of 2 at these g). What is clear is the need to go to larger N_t to get a prediction.

The jump in the gluonic and fermionic energy density at the transition is large. The results from [26] are shown in figure 11a. The errors are large, and there is still some overshooting of the gluonic contribution at the transition. To predict a hard number for the latent heat, we need to further remove finite volume effects. Meanwhile, knowing that a large discontinuity exists is certainly a help to the experimentalists.

In figure 11b, I show the time history of $\langle L \rangle$. A total of 180,000 sweeps were required to show a flip-flop! This should again serve as a warning for the slowness of the algorithm coming from a large prefactor.

3.4) Results for 2 and 3 flavors

Let me for the following ignore the fact that staggered flavor symmetry is broken on the lattice. Then to change the number of staggered flavors in many algorithms is easy. In *MD*, hybrid and Langevin algorithms the fermions are incorporated through a bilinear noise term with a prefactor n_f . This can be adjusted to any value. In the exact algorithm one can take an appropriate power of the ratio of the determinant. A number of groups are using this technique to explore 2 and 3 flavor cases [22][23][25][27].

3.4a) 3 flavors

The result for 3 flavors from the Brookhaven group [23] is evidence of a first order transition at $m_q = 0.025$ at $6/g^2 \approx 5.09$. A lot more data are needed to get an estimate of T_c .

3.4b) 2 flavors

The published results for 2 flavors are controversial. Fukugita *et al.* [27] show a hysteresis cycle but more important a flip-flop signal at $m_q = 0.1$, $6/g^2 = 5.3725$, $\delta r = 0.0025$. The flips are not quick in Monte Carlo time but nevertheless there. In figure 12, I show their results for variance in the $\langle L \rangle$ with $m_q = 0.2$ and 0.1. The large fluctuations (variance in $\langle L \rangle$) at $m_q = 0.2$ compared to 0.1 are indication that the transition at $m = 0.1$ is not the deconfining transition. What

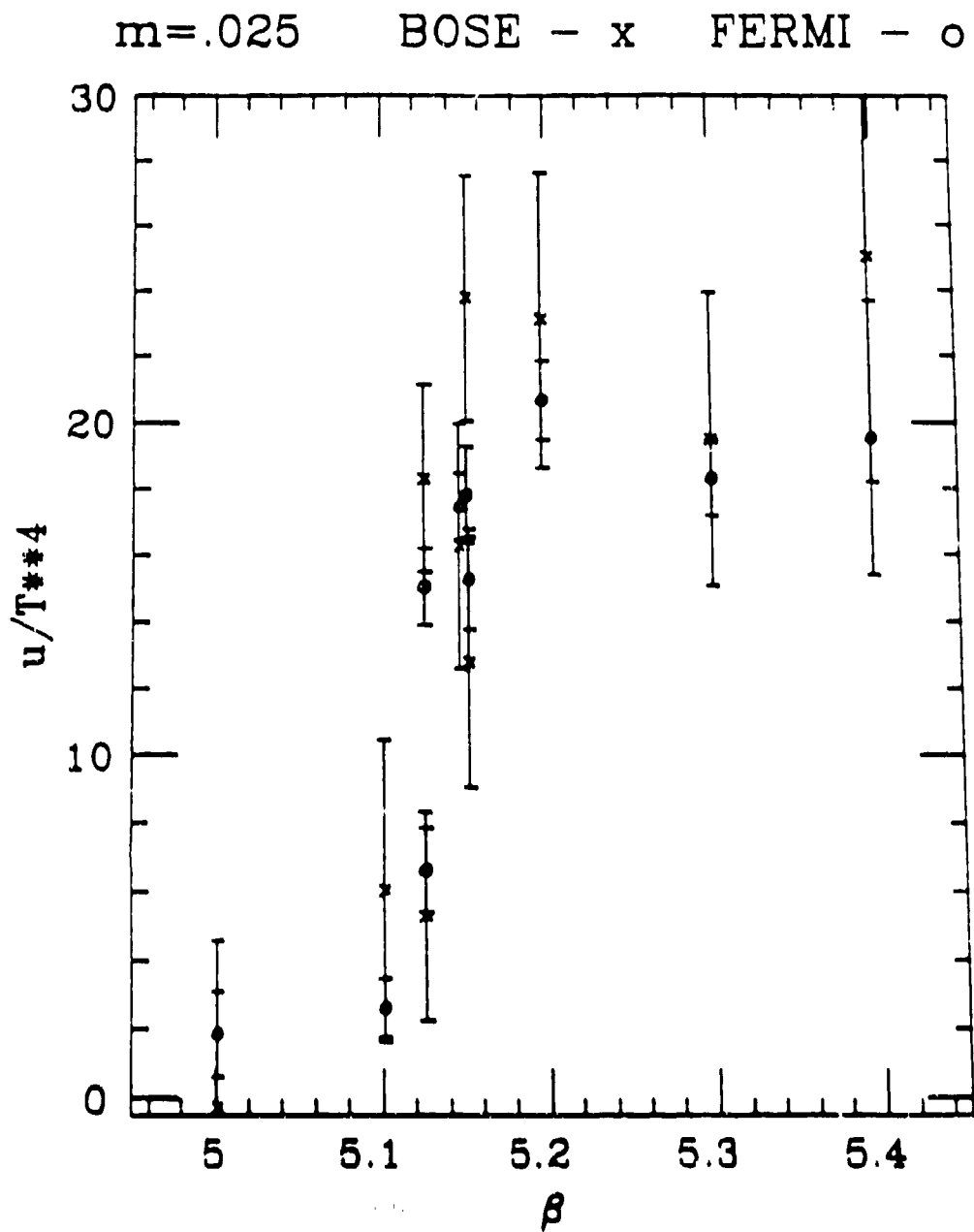


Fig. 11a: The gluonic and fermion energy density u divided by T^4 on a 6×10^3 lattice at $m_q = 0.025$.

$m=0.025 \quad \beta=5.125$

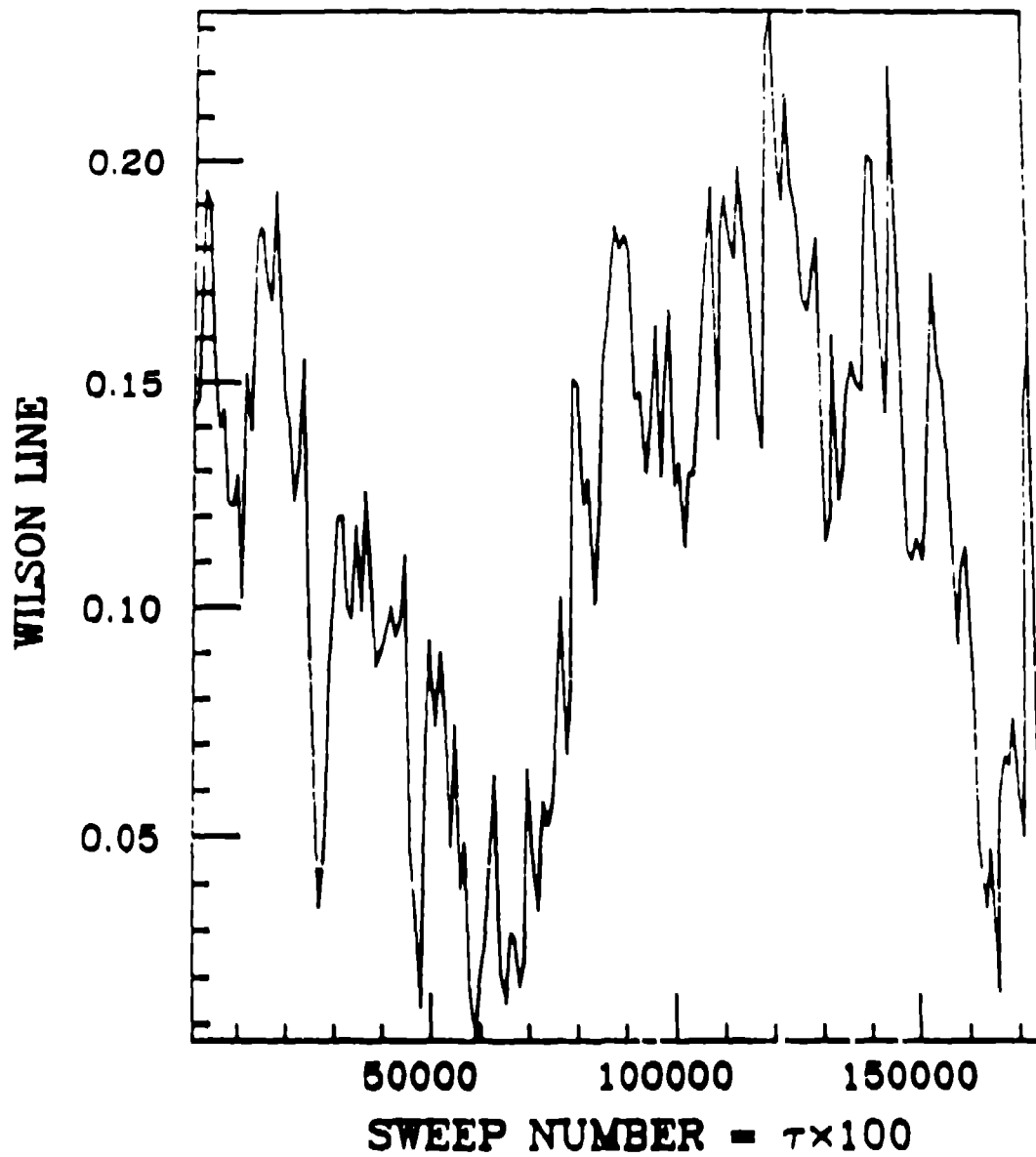


Fig. 11b: The evolution of $\langle L \rangle$ on a 6×10^3 lattice at $m_q = 0.025$ and $6/g^2 = 5.125$ (each point is averaged over 1000 sweeps).

is worrisome in this study is that the system does not spend much time in a given phase. A careful study at $m_q = 0.05$ showing an increase in the discontinuity would be nice for a confirmation.

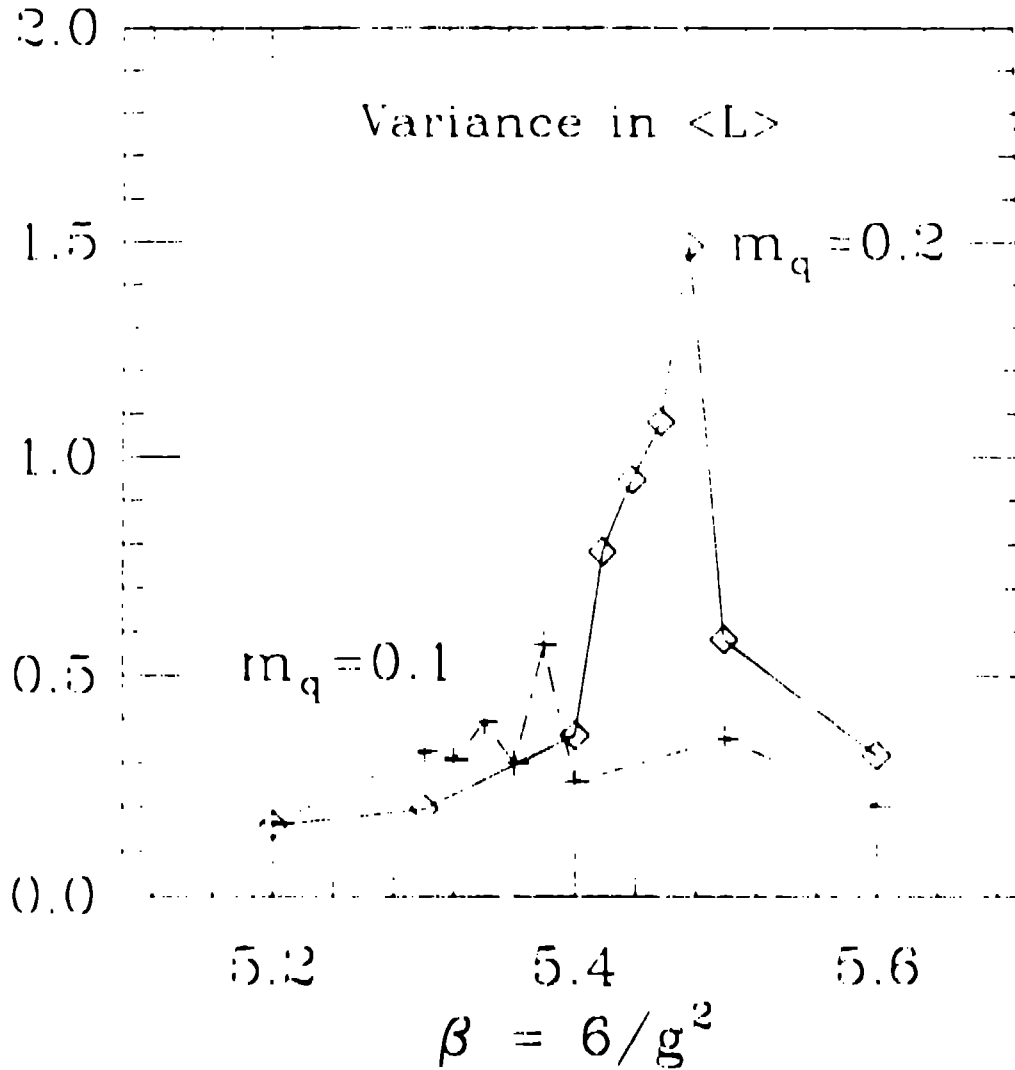


Fig. 12: Variance of the Polyakov line $\langle L \rangle \times 10^3$ for $m_q = 0.2$ and 0.1 on a 4×8^3 lattice and with two staggered flavors [27].

Gavai *et al.* [23] and Gottlieb *et al.* [22] do not find a convincing signal for a 1^{st} order transition at $m_q = 0.025$ and 0.0125 . This is surprising considering the result of Fukugita *et al.*, since we expect the discontinuity to grow with decreasing m_q . In figure 13, the data from

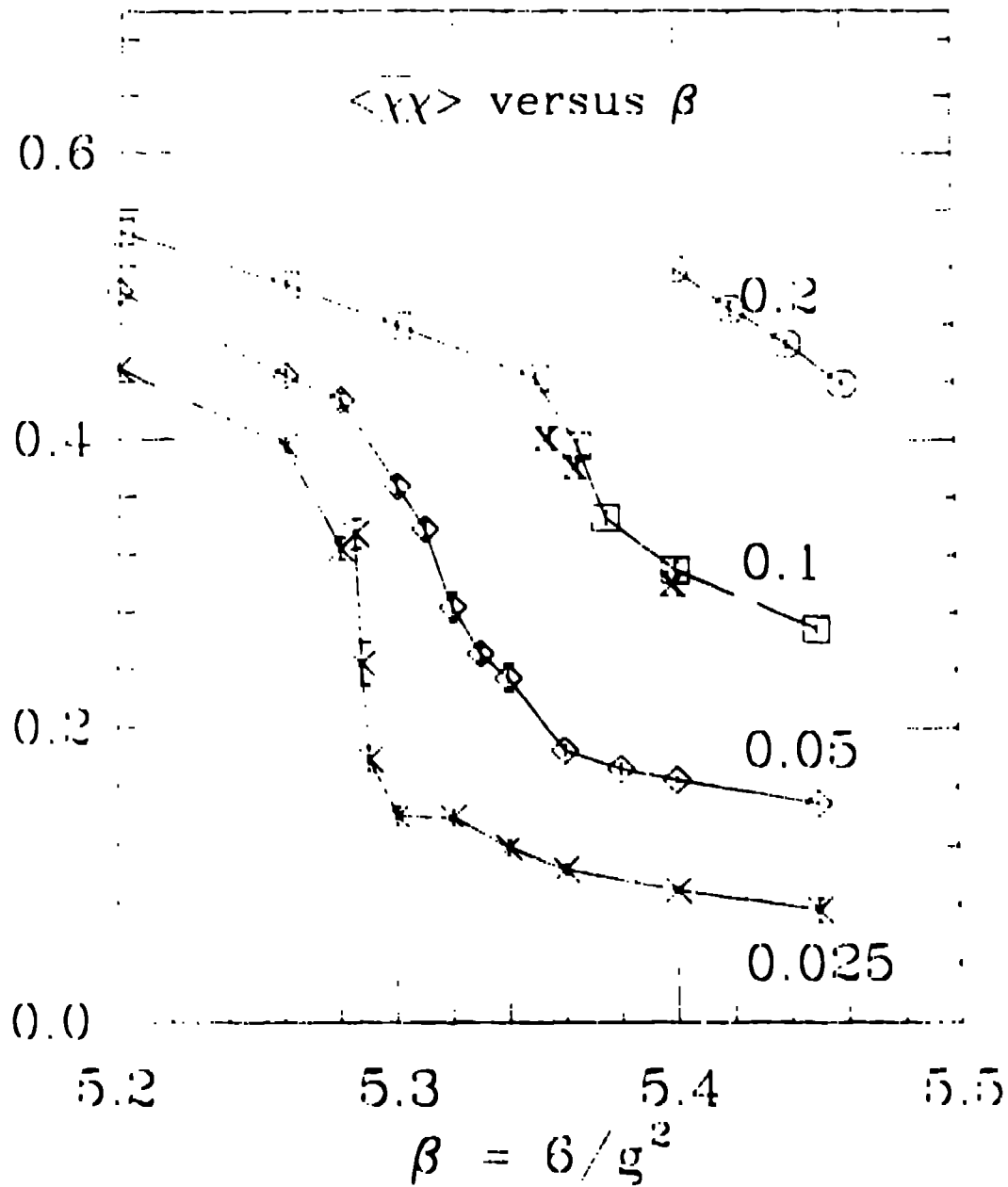


Fig. 13: Two flavor results for $\langle \bar{\chi}\chi \rangle$ on a 4×8^3 lattice for four values of the quark mass, $m_q = 0.2, 0.1, 0.05$ and 0.025 . The points marked X are from 4×10^3 lattices [22].

[22] for $\langle \bar{\chi}\chi \rangle$ is shown. A clear statement from this calculations is that for small quark masses the transition is very rapid.

We have preliminary results at $m_q = 0.02, 6/g^2 = 5.28$ which are shown in figure 14. There is again the characteristic presence of flip-flops. However, the fluctuations in the chirally broken phase are very large. Is this a signature of a fluctuation induced first order transition when approached from the broken phase? We need more data to answer this question.

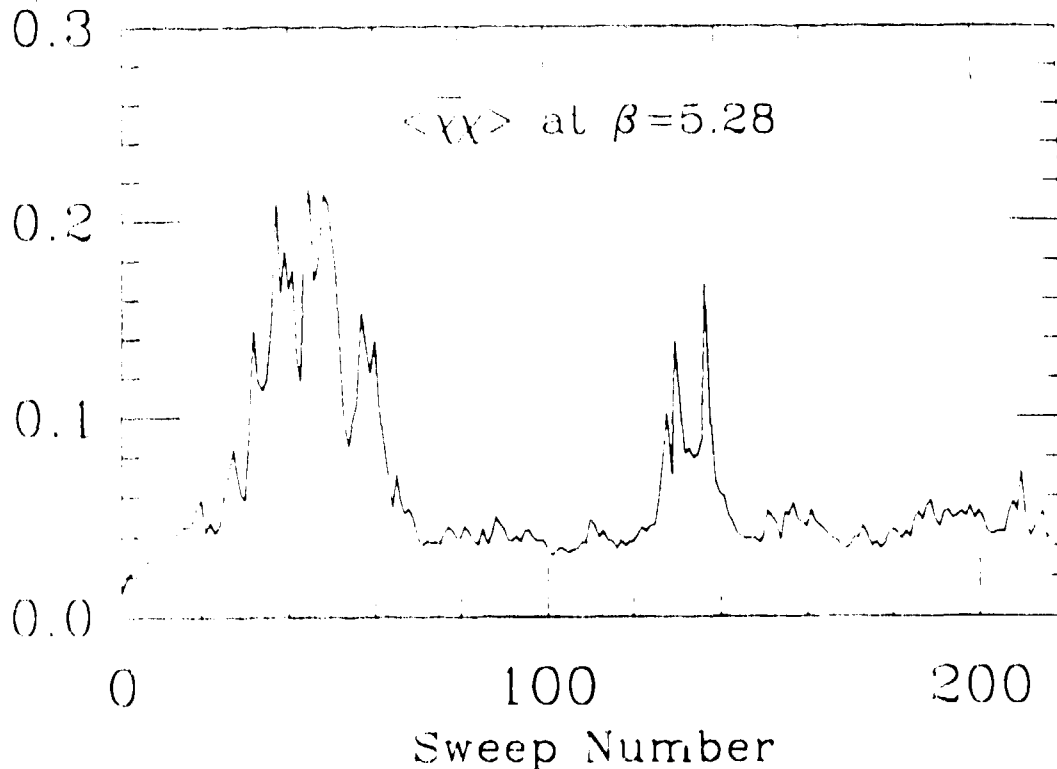


Fig. 14: Evolution of $\langle \bar{\chi}\chi \rangle$ for 2 flavors on a 4×4^3 lattice using the exact algorithm at $m_q = 0.02$ [25].

Figure 15 is from the Brookhaven group. Up to now it shows preliminary evidence of coexistence at $m_q = 0.025, 6/g^2 = 5.32$ on a 4×8^3 lattice. However, Potvin *et al.* would like to finish a longer run so as to rule out slow thermalization.

To conclude, as this evidence accumulates, we shall be able to fix the order of the chiral transition for the case of 2 light flavors and the

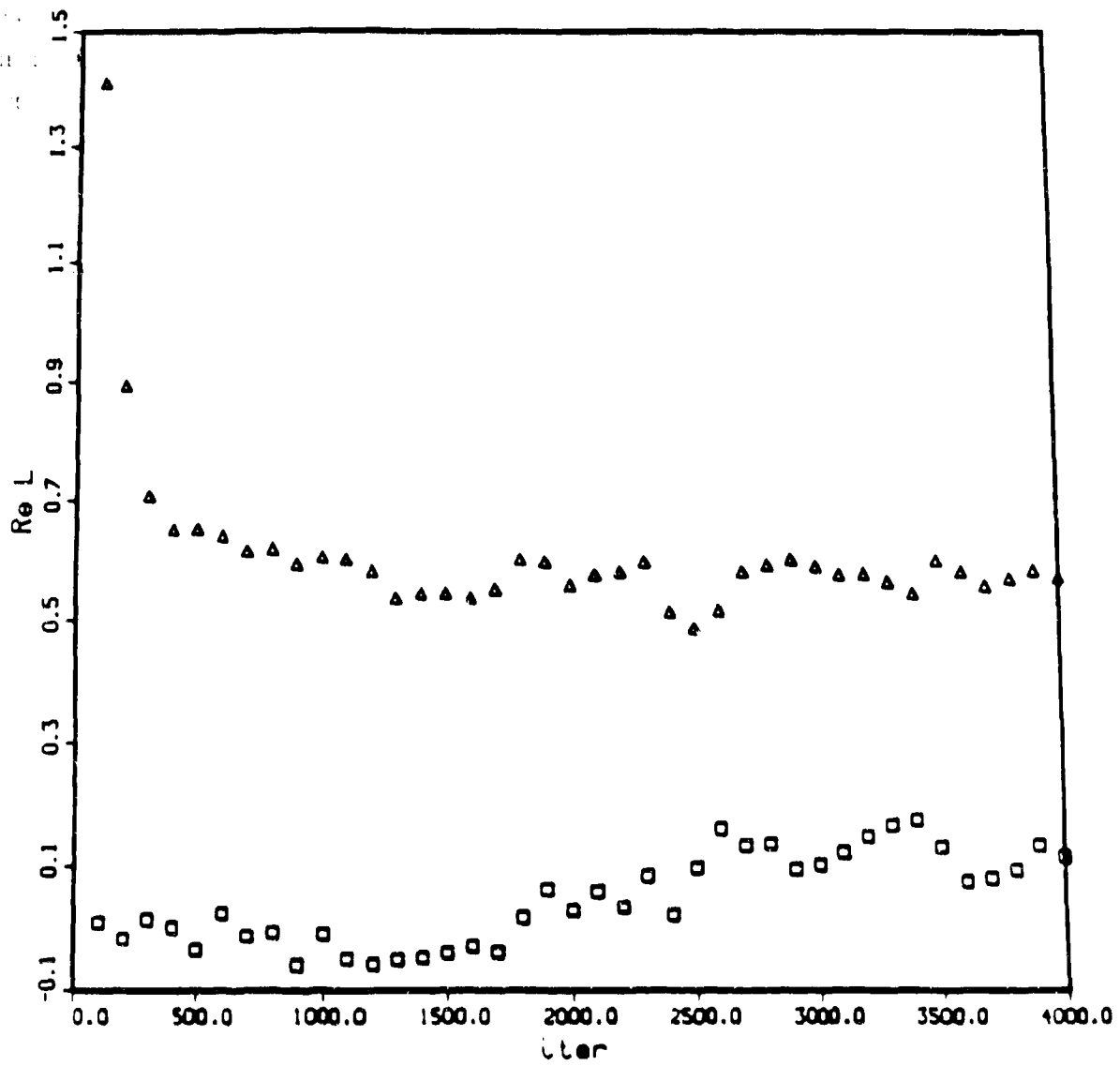


Fig. 15: Coexistence plot at $6/g^2 = 5.32$, $m_q = 0.025$ on a 4×8^3 lattice for 2 flavors using the Langevin algorithm.

strange quark. Looking ahead, we face a much harder challenge. We have to repeat these calculations with non-zero baryon density (non-zero chemical potential). Unfortunately, in this case the determinant is intrinsically a complex number and we don't yet have a way for including it as part of a probability distribution.

3.5) Wilson Fermions

Forcrand *et al.* [28] measure $\langle \bar{\chi}\chi \rangle$ and look for a discontinuity using an exact and an improved ("bush-factorized") PF algorithm. They find a discontinuity for $N_t = 4$ at a larger Wilson quark mass than for the staggered fermions. There are two possibilities: 1) they were assuming the transition for staggered fermions occurs only for $m_q < 0.025$ and 2) due to the explicit chiral symmetry breaking in Wilson fermions, there is no obvious connection between the mass for the two kinds of fermions. In fact, our quenched hadron spectrum calculation at much weaker coupling [14] shows that for constant physics, the bare Wilson mass is a factor of two heavier than the staggered fermion mass.

It would be interesting to push this calculation to see whether near $\kappa_c(g)$ (defined by zero pion mass) Wilson fermions have dynamically regained sufficient chiral symmetry and show the expected continuum chiral properties.

3.6) Systematic Bias in the Exact Algorithm

In the exact algorithm, the ratio of determinants $R \equiv \det(1 + M^{-1}\delta M)$ is calculated at each link update. Since we use staggered fermions (4 flavors), the algorithm requires a calculation of a 6×6 block of M^{-1} . Because M^{-1} is calculated with the conjugate gradient (CG) iterative algorithm to some approximation, even in an exact algorithm there can be a systematic bias. In a Metropolis update, a link can be changed many times without having to recalculate M^{-1} . The fast multi-hit algorithm was first described in detail by Gavaï and Gocksch [4]. Most of the results we obtained are with antiperiodic boundary conditions in all directions. We made some checks with the boundary

conditions switched to periodic in three directions [19]. We update each link with 50 hits and the acceptance is adjusted to $\approx 30\%$. In solving $Ax_{\text{even}} = M^\dagger Mx_{\text{even}} = b$, we define the convergence by $C = \frac{\langle b - Ax | b - Ax \rangle}{\langle x | x \rangle}$, which depends on the number of CG iterations (N_{cg}).

We now present an analysis of the systematic biases in our simulation at $\beta = 4.9$. Our implementation of the CG algorithm tends to underestimate the effects of the fermions, i.e. it tends to give too small a value for $S \equiv |\ln(R)|$. We have studied this by changing a single link and comparing the exact R with that calculated with a variety of CG sweeps. The exact R is obtained by calculating the determinants, before and after changing the link, using gaussian elimination. At $m_q = .1$, $N_{cg} = 60$ suffices to give the exact answer, while, for $N_{cg} = 30$, S is underestimated by a few percent. For $m_q = .025$, the algorithm requires $N_{cg} = 90$ to get S good to a few percent, while for $N_{cg} = 30$ the estimate of S is poor. These estimates remain valid when we make multiple hits on the same link.

To study if there is an accumulation of the bias, we compare the product of the accepted determinant ratios ($A \equiv \ln R_{acc}$) with the exact answer (T). The data for $m_q = .025$, $N_{cg} = 90$ is shown in table 2, together with $\ln(det)$ and $\langle C \rangle$. In the high temperature phase (1-10 and 36-41) one finds $A \leq T$, with only small deviations from equality. On the other hand, the confined phase (11-35) has A significantly less than T , though these are correlated. This phase also shows a marked deterioration in $\langle C \rangle$, suggesting that M has small eigenvalues not present in the high temperature phase. The difference between A and T is large, but it has been accumulated over $\approx 20 \times .3 \times 50 \times 4 \times 4^4$ link changes, and so corresponds to a tiny bias in R for each change.

The disagreement between A and T gets progressively worse with decreasing N_{cg} , but C is consistently a factor of ≈ 20 smaller in the high temperature phase. Conversely, the bias decreases as m_q increases. It is unobservable for $m_q = .1$, $N_{cg} = 60$.

From such an analysis one can determine N_{cg} required to avoid a bias at a given $6/g^2$ and m_q . Some of our best data does not quite meet this requirement, but the presence of the transition for a number

Config. #	Accepted $\ln(\det R)$	True $\ln(\det R)$	$\ln(\det M)$	$\langle C \rangle \times 10^3$
1			110.3	1.3
2	-2.9	-2.9	107.4	1.0
3	-0.5	-0.3	107.0	1.4
4	-40.1	36.6	70.4	0.9
5	29.6	30.9	101.4	3.9
6	5.1	5.1	106.5	0.9
7	-4.5	-4.5	102.0	0.9
8	6.1	6.1	108.1	1.1
9	-24.8	24.3	83.7	3.6
10	4.8	5.5	89.3	2.6
11	-53.4	45.3	43.9	20.
12	-1.1	6.4	50.4	26.
13	-27.8	17.2	33.1	26.
14	8.4	14.8	47.9	26.
15	-11.1	1.6	49.6	26.
16	-8.4	-2.3	47.2	26.
17	7.6	12.2	59.4	26.
18	-27.4	21.2	38.1	25.
19	10.3	24.4	62.6	26.
20	-22.0	18.4	44.1	24.
21	-3.4	1.4	45.6	26.
22	-2.9	4.5	50.1	26.
23	-15.6	-7.0	43.1	26.
24	24.7	29.8	72.9	26.
25	-26.9	20.6	52.2	21.
26	-13.7	-2.1	50.1	26.
27	0.7	9.4	59.5	24.
28	-4.7	-2.2	57.3	24.
29	-5.3	4.7	62.1	23.
30	-12.1	-7.3	54.7	25.
31	-11.3	-3.8	50.9	25.
32	-30.2	19.2	31.6	26.
33	8.6	19.0	50.6	26.
34	-6.2	4.9	55.6	26.
35	5.4	9.8	65.4	23.
36	44.0	44.4	109.8	6.7
37	-3.1	-3.1	106.7	0.9
38	-13.7	13.7	92.9	1.0
39	-9.9	-9.5	83.3	1.5
40	19.8	19.9	103.3	1.7
41	-1.4	-1.9	101.4	3.0

Table 2: Comparison of $\ln(\det R)$ between the accumulated change in the determinant and the true change. Each configuration is separated by 20 sweeps at $\beta = 4.9$, $m_s = 0.025$ and $N_{\tau_0} = 90$. Also given is the determinant on the final configuration and the mean convergence C over 20 sweeps.

of values of N_{cg} makes it very likely that the transition would remain for $N_{cg} = \infty$.

Conclusions

Let me conclude by mentioning what I think is the most promising approach to simulations with dynamical fermions right now. It is to use the algorithm of Scalatter, Scalapino and Sugar [29] in which one uses an approximate update algorithm (say LG or HY with fourier acceleration) to evolve the system through a certain number of link changes and then to make it exact by a Metropolis accept or reject of the whole step. The key point here is to treat the input couplings in the hybrid update as free and to optimize them to get a large acceptance in the Metropolis step. The couplings in the Metropolis step define the final Boltzmann distribution. There are some recent very encouraging results by Duane *et al.* [30] using this approach.

References

- [1] F. Fucito, E. Marinari, G. Parisi and C. Rebbi, *Nucl. Phys.* **B180** (1981) 369.
- [2] D. Weingarten and D. Petcher, *Phys. Lett.* **99B** (1981) 333.
- [3] D. J. Scalapino and R. L. Sugar, *Phys. Rev. Lett.* **46** (1981) 519.
- [4] R. Gvai and A. Gocksch, *Phys. Rev. Lett.* **56** (1986) 2659.
- [5] J. Polonyi and W.H. Wyld, *Phys. Rev. Lett.* **51** (1983) 2257.
- [6] G. Parisi and Wu Yongshi, *Sci. Sin.* **24** (1981) 483. ;
G. G. Batrouni, G. R. Katz, A. S. Kronfeld, G. P. Lepage, B. Svetitsky, and K. G. Wilson, *Phys. Rev.* **D32** (1985) 2736.
- [7] S. Duane, *Nucl. Phys.* **B257** [FS14] (1985) 652. ;
S. Duane and J. Kogut, *Phys. Rev. Lett.* **55** (1985) 2774.
- [8] J. B. Kogut, H. Matsuoka, S. H. Shenker, J. Shigemitsu, D. K. Sinclair, M. Stone and H. W. Wyld, *Phys. Rev. Lett.* **51** (1983) 869.
- [9] S. Gottlieb, A.D. Kennedy, J. Kuti, S. Meyer, B.J. Pendleton, R.L. Sugar and D. Toussaint, *Phys. Rev. Lett.* **55** (1986) 1958 ;
N. Christ, Private Communications.
- [10] R. D. Pisarski and F. Wilczek, *Phys. Rev.* **D29** (1984) 338.
- [11] A. Patkos and A. Margaritis, Bonn Preprint HE-86-12 .
- [12] B. Svetitsky, *Proceedings of the Fifth International Conference on Ultra-Relativistic Nucleus-Nucleus Collisions, Quark Matter, 86* Asilomar ;
M. Matsua, *ibid.*
- [13] G.W. Kilcup and S.R. Sharpe, *Nucl. Phys.* **B283** (1987) 193.
- [14] R. Gupta, G. Guralnik, G. Kilcup, A. Patel, S. Sharpe and T. Warnock, Cornell Preprint 87/75 (May 1987).
- [15] J. B. Kogut and D. K. Sinclair, Urbana Preprint ILL-(TH)-86-46, and references therein.
- [16] R. Gvai, *Nucl. Phys.* **B269** (1986) 530.
- [17] F. Fucito and S. Solomon, *Phys. Rev. Lett.* **55** (1985) 2641.
- [18] M. Fukugita and A. Ukawa, *Phys. Rev. Lett.* **57** (1986) 503.
- [19] R. Gupta, G. Guralnik, G. Kilcup, A. Patel and S. Sharpe, *Phys. Rev. Lett.* **57** (1986) 2621.

- [20] R. Gupta, *Proceedings of the Brookhaven conference on Lattice Gauge Theories*, 1986.
- [21] F. Karsch, J.B. Kogut, D.K. Sinclair and H.W. Wyld, CERN-TH-4636/87.
- [22] S. Gottlieb, W. Liu, D. Toussaint, R.L. Renkin and R. L. Sugar, UCSD Preprint (1987).
- [23] R. V. Gavai, J. Potvin and S. Sanielevici, preprint TIFR/TH/87-2.
- [24] One can take the alternate view that rather than taking the limit $\delta\tau \rightarrow \infty$, one simply regards the physics from small step algorithms as corresponding to different couplings, but in the same universality class.
- [25] R. Gupta, G. Guralnik, G. Kilcup, A. Patel and S. Sharpe, in progress.
- [26] E.V.E Kovacs, D.K. Sinclair and J.B. Kogut, *Phys. Rev. Lett.* **58** (1987) 751.
- [27] M. Fukugita, S. Ohta, Y. Oyanagi and A. Ukawa, *Phys. Rev. Lett.* **58** (1987) 2515.
- [28] P. de Forcrand *et al.*, *Phys. Rev. Lett.* **58** (1987) 2011.
- [29] R. T. Scalettar, D. J. Scalapino and R.L. Sugar, *Phys. Rev.* **B34** (1986) 7911.
- [30] S. Duane, A. D. Kennedy, B. J. Pendleton and D. Roweth, FSU-SCRI-87-27.

4) WEAK INTERACTION MATRIX ELEMENTS ON THE LATTICE

The pseudoscalar octet is, I think, the key to our understanding a significant fraction of modern particle physics. The light pion is a manifestation of a nearly exact chiral symmetry. The kaons are a periscope to the unknown world of CP violation. How well we can explain the large enhancement of $\Delta I = \frac{1}{2}$ amplitude in K decays reflects our ability to calculate strong interaction corrections to any process involving low energy gluons. In all these phenomenon, the Achilles' heel is our inability to calculate the non-leptonic matrix elements at the hadronic scale. Once the machinery to calculate matrix elements (ME) on the lattice is established, the list of problems one can address is large. I will only discuss the $\Delta I = \frac{1}{2}$ rule and $\frac{3}{2}$ in this lecture. By these examples I hope I can convey some of the excitement of the field to you.

In writing this lecture I realized that it would be impossible for me to cover the subject in any detail. Therefore what I will do is to motivate you, make the connection between phenomenology and lattice measurements, mention the important issues and summarize results. For details, I have no option but to direct you to the published literature.

4.1) The $\Delta I = \frac{1}{2}$ Rule

The phenomenology of the $\Delta I = \frac{1}{2}$ rule is very simple. The isospin decomposition of the two pion final state in Kaon decays is

$$\begin{aligned}
 |K^0\rangle &= |I = 2, I_Z = 1\rangle \\
 |K^+ \pi^0\rangle &= \sqrt{\frac{1}{3}} |I = 0, I_Z = 0\rangle - \sqrt{\frac{2}{3}} |I = 2, I_Z = 0\rangle \\
 |K^0 \pi^0\rangle &= \sqrt{\frac{2}{3}} |I = 0, I_Z = 0\rangle + \sqrt{\frac{1}{3}} |I = 2, I_Z = 0\rangle \quad (4.1)
 \end{aligned}$$

From experiments we find

$$\frac{\Gamma(K^+ \rightarrow \pi^+ \pi^0)}{\Gamma(K_s \rightarrow \pi^0 \pi^0)} \approx \frac{1}{670} \quad (4.2)$$

This ratio can be understood if we assume that the weak Hamiltonian is essentially $\Delta I = \frac{1}{2}$. A further corroboration is provided by the ratio

$$\frac{\Gamma(K_s \rightarrow \pi^+ \pi^-)}{\Gamma(K_s \rightarrow \pi^0 \pi^0)} \approx 2.185 \pm 0.10 \quad (4.3)$$

since a value of 2 is obtained from the Clebsch's alone assuming the decay has no $\Delta I = 3/2$ part. Thus these decays provide strong evidence for the $\Delta I = \frac{1}{2}$ rule. The question we would like to answer is where does it come from?

If the electro-weak interactions are described by the spontaneously broken $SU(2) \times U(1)$ Glashow-Weinberg-Salam theory, then we know the fundamental interactions at scale M_W and these do not give a $\Delta I = \frac{1}{2}$ enhancement sufficient to explain the experimental results. The final state in all decays is $|\pi\pi\rangle$, so there is no enhancement from phase space factors. Finally, we don't know of any other selection rule that enhances one over the other. There is only one possible culprit, QCD, that sneaks in to produce the $\Delta I = \frac{1}{2}$ rule. And it does it in an insidious way. The part of the theory we understand (large momentum) is innocent. It is the part that is hidden under the shroud of a large coupling constant that we probe by non-perturbative methods. So we are forced to unravel the mysteries of one black box with another - Monte Carlo calculations.

4.2a) Constructing the 4-fermion Effective Hamiltonian

The full range of momenta involved in these calculations is 0 to M_W . We divide it into two regions; call one \mathcal{L} , for lattice, which ranges from 0 to μ and the other called \mathcal{P} , for perturbation theory, which ranges from μ to M_W . The point μ is taken to be ≥ 2 GeV for two reasons. First, the lattice scale $\frac{1}{a}$ in any serious calculation will be large enough to satisfy this condition and, second, the Wilson coefficients (couplings) at μ can be computed reliably using perturbation theory since the QCD coupling constant throughout \mathcal{P} is small.

Henceforth, I shall label the ME of an operator O_i by M_i and their Wilson coefficients by C_i . The initial and final states for which

the ME are calculated will be clear from the context. $L (R)$ is the projection operator $1 - \gamma_5 (1 + \gamma_5)$.

The weak interaction Hamiltonian density for the charged current in the hadronic sector is [1] :

$$\mathcal{H}_W = \frac{g}{2\sqrt{2}} J_\mu W^\mu + h.c. \quad (4.4)$$

with the W -bosons interacting with the quarks through the current

$$J_\mu = \frac{g_2}{2\sqrt{2}} (\bar{u}, \bar{c}, \bar{t}) \gamma_\mu (1 - \gamma_5) V \begin{pmatrix} d \\ s \\ b \end{pmatrix} \quad (4.5)$$

Here V is the 3×3 Kobayashi-Maskawa (KM) matrix [2] that connects the quark mass eigenstates with the weak eigenstates. It is parameterized in terms of four angles $\theta_1, \theta_2, \theta_3$ and δ

$$V = \begin{pmatrix} c_1 & -s_1 c_3 & -s_1 s_3 \\ s_1 c_2 & c_1 c_2 c_3 - s_2 s_3 e^{i\delta} & c_1 c_2 s_3 + s_2 c_3 e^{i\delta} \\ s_1 s_2 & c_1 s_2 c_3 + c_2 s_3 e^{i\delta} & c_1 s_2 s_3 - c_2 c_3 e^{i\delta} \end{pmatrix} \quad (4.6)$$

where $c_i = \cos\theta_i$ and $s_i = \sin\theta_i$ for $i = 1, 2, 3$.

The lowest order procedure to construct the effective theory at μ consists of the following steps [3] :

- (1) Integrate out the W from the theory. The $\Delta S = 1$ Hamiltonian then consists of the 4-fermion operators, $O_\pm(u)$, $O_\pm(c)$ and $O_\pm(t)$ with say $O_\pm(c)$ defined as

$$O_\pm = \bar{s}_a \gamma_\mu L d_a \bar{c}_b \gamma_\mu L c_b \pm \bar{s}_a \gamma_\mu L c_b \bar{c}_b \gamma_\mu L d_a \quad (4.7)$$

The O_+ transforms as a linear combination of 27 and 8 under $SU(3)_L$ while O_- is pure 8. It is the enhancement of the octet operator we seek since it contributes only to $\Delta I = \frac{1}{2}$. The coefficients ($C_+ = C_-$ valid at M_W) are evaluated by matching \mathcal{H}_{eff} at the boundary. At M_W , the effective 4-fermion theory is

$$\mathcal{H}_{eff} = \frac{G_F}{2\sqrt{2}} [C_u(O_+(u) + O_-(u)) - C_c(O_+(c) + O_-(c)) - C_t(O_+(t) + O_-(t))] \quad (4.8)$$

with

$$C_c = s_1 c_2 (c_1 c_2 c_3 - s_2 s_3 e^{1\delta}) \quad (4.9a)$$

$$C_t = s_1 s_2 (c_1 s_2 c_3 - c_2 s_3 e^{1\delta}) \quad (4.9b)$$

$$C_u = C_c + C_t \quad (4.9c)$$

To scale the coefficients C_q down to m_t one uses the renormalization group (RG) with the 1-loop running coupling constant and the 1-loop anomalous dimensions. Since the operators O_{\pm} are multiplicatively renormalized this is straightforward. On scaling C_- increases with respect to C_+ because of a difference in the anomalous dimensions. This gives some $\Delta I = \frac{1}{2}$ enhancement, (≈ 2), but it is not sufficient to explain the required factor of ≈ 22 .

- (2) Integrate out the top quark from the effective theory at m_t . In tree level matching, one simply sets $C_{\pm}(t)$ to zero and equates $C_{\pm}(u)$ and $C_{\pm}(c)$ below m_t to their value above m_t . More important, integrating out the t quark generates additional 4-fermion operators $O_3 \dots O_8$. These operators arise from mixing with the so called "penguins" diagrams shown in figure 1. Their coefficients start out being zero at m_t and their evolution down to m_b is governed by the 8×8 anomalous dimension matrix calculated by Gilman and Wise [3][4] (with corrections by Buras and Gerard [5]) in the basis $O_1 \dots O_8$ defined as

$$O_1 = \bar{s}_a \gamma_{\mu} (1 - \gamma_5) d_a \bar{u}_b \gamma_{\mu} (1 - \gamma_5) u_b - (u \rightarrow c)$$

$$O_2 = \bar{s}_a \gamma_{\mu} (1 - \gamma_5) d_b \bar{u}_b \gamma_{\mu} (1 - \gamma_5) u_a - (u \rightarrow c)$$

$$O_3 = \bar{s}_a \gamma_{\mu} (1 - \gamma_5) d_a \sum_q \bar{q}_b \gamma_{\mu} (1 - \gamma_5) q_b$$

$$O_4 = \bar{s}_a \gamma_{\mu} (1 - \gamma_5) d_b \sum_q \bar{q}_b \gamma_{\mu} (1 - \gamma_5) q_a$$

$$O_5 = \bar{s}_a \gamma_{\mu} (1 - \gamma_5) d_a \sum_q \bar{q}_b \gamma_{\mu} (1 + \gamma_5) q_t$$

$$O_6 = \bar{s}_a \gamma_{\mu} (1 - \gamma_5) d_b \sum_q \bar{q}_b \gamma_{\mu} (1 + \gamma_5) q_a$$

$$\begin{aligned}
O_7 &= \bar{s}_a \gamma_\mu (1 - \gamma_5) d_a \sum_q e_q \bar{q}_b \gamma_\mu (1 + \gamma_5) q_b \\
O_8 &= \bar{s}_a \gamma_\mu (1 - \gamma_5) d_b \sum_q e_q \bar{q}_b \gamma_\mu (1 + \gamma_5) q_a
\end{aligned} \tag{4.10}$$

where q is summed over u, d, s, c, b quarks; a and b are color indices, and $e_q = 1(-1/2)$ for charge $2/3(-1/3)$ quarks. The operators O_1 and O_2 are linear combinations of O_\pm . These eight operators do not renormalize multiplicatively, and the scaling is easiest done by numerically diagonalizing the anomalous dimension matrix. The final values of C_i and consequently our estimates will depend on what we choose for the unknown top quark mass.

- (3) Repeat step (2) *i.e.* integrate out the b quark and scale down to $\mu > m_c$. Integrating out the b quark changes the anomalous dimension matrix and the running of the coupling constant and the b quark drops out of the sum over q in eqn (4.10), but it generates no new operators.

The eight operators $O_1 \dots O_8$ and their coefficient functions define the effective Weak Hamiltonian \mathcal{H}_{eff} at scale μ .

$$\mathcal{H}_{eff} = \frac{G_F}{2\sqrt{2}} \sum_{i=1}^8 C_i O_i \tag{4.11}$$

where the KM angles and the dependence on α_s and anomalous dimension factors is lumped into the C_i . I have purposely chosen $\mu > m_c$ so that the c quark is not integrated out. This means that we have to explicitly implement GIM cancellation on the lattice by doing all calculations with both c and u quarks propagating in internal loops and doing the $(u - c)$ subtraction. The matrix elements of \mathcal{H}_{eff} are evaluated on the lattice because the region \mathcal{L} is inherently non-perturbative.

Only one LL operator contributes to the $\Delta I = \frac{3}{2}$ amplitude. It is a linear combination of O_1, O_2 and O_3 and transforms as $[27, 1, 3/2]$ under $[SU(3)_L, SU(3)_R, I]$:

$$O_{3/2} = \bar{s}_a \gamma_\mu L d_a [\bar{u}_b \gamma_\mu L u_b - \bar{d}_b \gamma_\mu L d_b] + \bar{s}_a \gamma_\mu L u_a \bar{u}_b \gamma_\mu L d_b \tag{4.12}$$

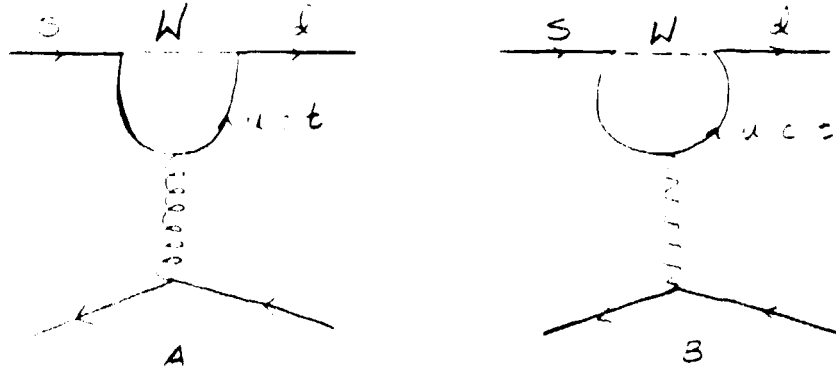


Fig. 1: The diagrams that give rise to a) strong penguins O_5 and O_6 and b) the em penguins O_7 and O_8 . The vector interaction at the lower vertex gives rise to both LL and LR operators.

The operators $O_5 \dots O_6$ (called the strong penguins because a gluon mediates the interaction in the original penguin) are LR in distinction to $O_1 \dots O_4$ and transform as $[8,1,1/2]$. They contribute only to the $\Delta I = \frac{1}{2}$ amplitude. The magnitude of the enhancement depends on the C_i and the ME . The coefficient functions for these operators are large only if we integrate out the charm quark and evolve below 1 GeV. Originally, Shifman et al. [6] proposed that the ME are large due to the LR structure of the penguin operators. They calculated the ME using factorization and vacuum insertion and found that $C_5 M_5 + C_6 M_6$ is large enough to explain a substantial part of the enhancement. That analysis is wrong; they derived a wrong chiral behavior for the matrix elements in the vacuum insertion approximation. The correct chiral behavior of the matrix elements of O_5 and O_6 is the same as for the LL operators i.e. they vanish in the chiral limit as $m_\pi m_K$ [7] [8]. The present status of results from numerical simulations is that these ME are small. Also, it is not kosher to run the C_i down to scales below m_c , for there one has very little confidence in perturbation theory. The real parts of C_5 and C_6 above m_c are small. Thus it seems unlikely that these operators are the cause of the $\Delta I = \frac{1}{2}$ enhancement. So for a choice of scale $\mu > m_c$, the $\Delta I = \frac{1}{2}$ rule has to come from the enhancement of the octet part of the operators $O_1 \dots O_4$ over the 27plet. On the other hand the imaginary part of C_6 is dominant. Thus M_6 will

figure prominently in the analysis of $\frac{\epsilon'}{\epsilon}$.

The em penguins O_7 and O_8 have pieces that transform as $[27,1]$, $[8,1]$ and $[8,8]$ and contribute to both $\Delta I = \frac{3}{2}$ and $\Delta I = \frac{1}{2}$ amplitudes. The real part of their C_i is too small, so these operators are ignored in the analysis of the $\Delta I = \frac{1}{2}$ rule. However, the imaginary part, which contributes to $\frac{\epsilon'}{\epsilon}$, competes favorably with the contribution from the strong penguins. The suppression of their C_i by α_{em} is compensated by the fact that in the chiral limit, the $[8,8]$ part of M_7 and M_8 does not vanish as $m_\pi m_K$, but goes to a constant. Thus, as discussed later, their contribution to $\frac{\epsilon'}{\epsilon}$ may be as large as that from the strong penguins.

All the ME we calculate on the lattice are real. The same ME contribute to both $\Delta I = \frac{1}{2}$ and $\frac{\epsilon'}{\epsilon}$. The coefficients C_i are complex due to the CP violating phase $e^{i\delta}$ in the KM matrix. So when one refers to the real and imaginary parts of the amplitudes, the distinction comes from the C_i . The imaginary part will be proportional to $\sin \delta$.

4.2b) Relating $K \rightarrow \pi\pi$ to $K \rightarrow \pi$:

All the ME we are interested in involve $K \rightarrow \pi\pi$. This requires calculating 4-point functions on the lattice with two particles in the final state. This poses the following problems for lattice calculations at present

- (1) The momentum of the two final state pions. The lowest non-zero momentum on the lattice, $\frac{\pi}{N_a}$, is too large to allow the decay to proceed on mass shell. For off-shell amplitudes, we have to make $3d$ subtractions similar to the ones discussed below. At present these are not under control even for 3-point functions.
- (2) The functional form necessary to fit the data for the 4-point correlators is complicated as can be seen by drawing all the diagrams (for an example see figure 2). Thus to get reliable fits and extract the ME we will need a very large number of configurations.
- (3) We need two calculations of quark propagators with sources at different points as shown in figure 2. This, unlike the first two issues, is not a significant drawback for it only doubles the amount of computer time required.

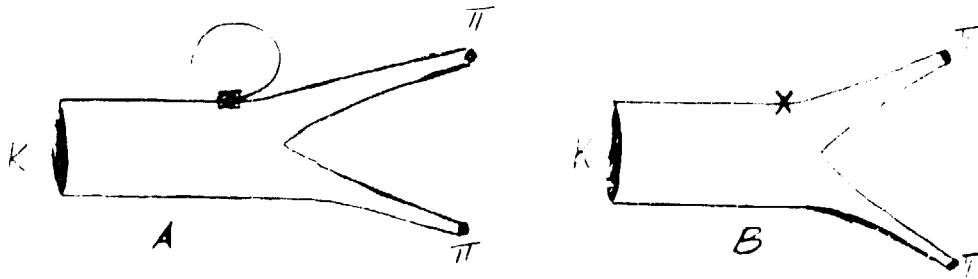


Fig. 2: a) A 4-point diagram and b) its subtraction that contribute to the amplitude $K \rightarrow \pi\pi$ on the lattice.

The present approach is to use chiral perturbation theory (CPT_h) to relate the $K \rightarrow \pi\pi$ amplitude to $K \rightarrow \pi$ and $K \rightarrow vacuum$. This is an additional approximation and for Kaons may not be any better than 50% [9]. Thus, one has to clearly demonstrate the expected chiral behavior in the ME before reliable results can be extracted.

The lowest order CPT_h relates the three matrix elements [10]

$$\langle \pi\pi | \mathcal{H}_{eff} | K \rangle = A \left(\frac{m_K^2 - m_\pi^2}{f_\pi} \gamma + \dots \right) \quad (4.13a)$$

$$\langle \pi | \mathcal{H}_{eff} | K \rangle = A \left(\frac{-m_K^2}{f_\pi} \delta + (p_\pi \cdot p_K) \gamma + \dots \right) \quad (4.13b)$$

$$\langle 0 | \mathcal{H}_{eff} | K \rangle = A \left((m_K^2 - m_\pi^2) \delta + \dots \right) \quad (4.13c)$$

where A is a constant that includes C_i and Z factors. Our goal is to extract the value of γ from the last two off-shell ME which can be calculated on the lattice. However, on the lattice, these operators mix with operators of different chirality (true only for Wilson fermions which explicitly break chiral symmetry) and lower dimension operators. The ME of these lower dimension operators have their own factors of δ and γ analogous to eqn. (4.13). For example $\bar{3}d$ contributes to (4.13b) but not to (4.13c) and vice-versa for $\bar{3}\gamma_5 d$ but with different δ and γ . Thus, one cannot extract the physical ME i.e. γ from eqn (4.13b) and (4.13c) by just using the bare operators of eqn. (4.10). One has to define renormalized operators (which have the correct chiral behavior) by making subtractions. These are discussed next.

4.2c) Subtractions and Contractions

As stated above, we have to include the mixing of operators $O_1 \dots O_8$ with lower dimension operators. There are two such operators relevant to this discussion: The dimension 5 operator $\bar{s}\sigma_{\mu\nu}F^{\mu\nu}d$ and the dimension 3 operator $\bar{s}d$. Both are present in calculations with Wilson fermions, while for staggered fermions, the remnant chiral symmetry guarantees that there is no mixing with $\bar{s}\sigma_{\mu\nu}F^{\mu\nu}d$. There is only one lower dimension operator for staggered fermions [11]:

$$O^{sub} \equiv i\bar{s}\gamma_\mu(1-\gamma_5)(\overleftarrow{\partial}_\mu - \overrightarrow{\partial}_\mu)d = (m_d + m_s)\bar{s}d + (m_d - m_s)\bar{s}\gamma_5d \quad (4.14)$$

which is a total derivative and so absent on-shell. The equality (due to the equation of motion) between the two terms on the right hand side is still valid on the lattice. It is this form that we transcribe on to the lattice [11].

The subtractions necessary to define the physical ME are handled differently by different groups doing the calculations so I will discuss them later with the results.

There are two types of diagrams that arise in the Wick contraction of these operators in the transition $K^+ \rightarrow \pi^+$. The one in which all four Dirac operators are contracted with external quarks are called "figure 8" diagrams, while in the "eye" diagrams two of the operators are contracted to form a closed loop. The $\Delta I = \frac{3}{2}$ transition has only eight contraction for degenerate u and d quarks while the $\Delta I = \frac{1}{2}$ octet operators have both eight and eye contractions. The eye diagrams require subtractions as illustrated for $\bar{s}d$ in figure 3.

In present calculations, the magnitude of the ME of all the eight diagrams is comparable. Thus the $\Delta I = \frac{1}{2}$ rule has to come from a large contribution from the eye diagrams. These diagrams are, at present, hard to calculate because they involve two kinds of subtractions: ($u - c$) to impose the GIM mechanism and the subtractions due to mixing with lower dimension operators. One of the bottlenecks in present lattice calculations is a lack of control in the calculation of these eye diagrams.

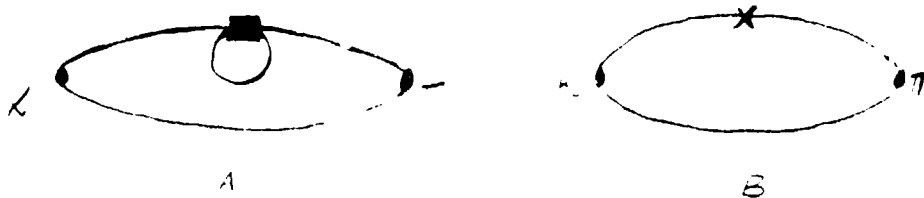


Fig. 3: a) An eye contraction and b) the corresponding subtraction diagram.

4.2d) Vacuum Insertion Approximation (VIA)

A phenomenological method to calculate the ME is the VIA. In this approximation, the 4-fermion operators are factorized into 2 separate bilinears and a complete set of states is inserted in between. Further, the sum over intermediate states is saturated by just the vacuum. With this method one can only calculate those contractions of the eye and *eight* that have 2-color loops. These diagrams breaks into two disjoint parts as shown in figure 4. The 1-color loop terms can be added in by hand by using the continuum approximate relation; $M(\text{1-color loop}) \approx 3 \times M(\text{2-color loop})$ i.e. $M_8 \approx M_6/3$.

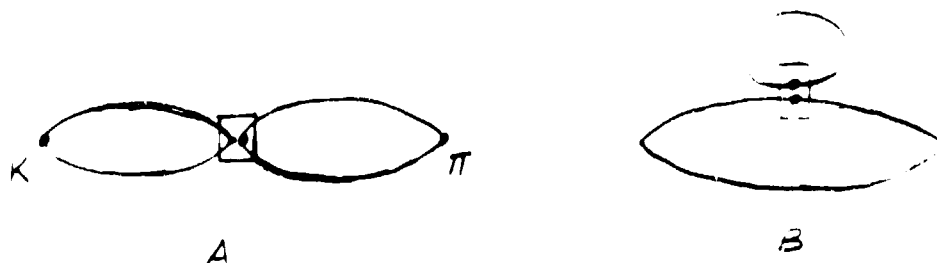


Figure 4: 2-color loop diagrams that contribute to VIA

The utility of VIA is twofold. First, ME_{VIA} can be calculated easily on the lattice and second, they have the same chiral behavior as the physical ME . The second fact states that they have the same factors of m_K and m_π as the ME , so one possible way to reduce lattice

artifacts is to consider the ratio, B , of the two calculated on the lattice *i.e.*

$$M_{\text{lattice}} = M_{\text{cont. VIA}} \frac{M_{\text{lattice}}}{M_{\text{lattice VIA}}} \equiv M_{\text{cont. VIA}} B \quad (4.15)$$

We use this approach to reduce systematic errors and to check for the chiral behavior in both ME . We also hope that the statistical errors in the two measurements are correlated and cancel in the ratio.

4.2e) Connection between the Lattice and Continuum Results

Putting the theory on the lattice does introduce an approximation; the momentum integral is replaced by a discrete sum and the dispersion relation for the propagators is modified from p to $\sin p$. The two approximations can be systematically improved by taking a larger box size Na , since the allowed momenta on the lattice are $\pm \frac{n\pi}{Na}$.

The ME are calculated on the lattice at a given value of the bare charge g . The lattice scale a^{-1} is set by some dimensionful quantity like the ρ mass. Given a^{-1} and the lattice size, we can determine the lattice momenta. Since the lattice dispersion relation differs substantially from the continuum behavior for the gluon and quark propagators at large momenta, we cannot *a priori* define the renormalization point μ to be $\frac{\pi}{a}$. It is customary to choose $\mu = \frac{1}{a}$. This is just an assumption and the definition of μ for a given g is still an open problem.

The anomalous dimension matrix used to scale the coefficients is evaluated with a continuum regularization scheme. The ME are calculated on the lattice. Therefore we have to relate the lattice and the continuum operators at scale μ . These 1-loop Z factors are being calculated in perturbation theory [12] [13].

Given the scale μ in physical units, the evolution of the coefficients proceeds as in the continuum with the experimental values for M_W and the quark masses. The only lattice action dependent quantity is the value of the coupling g at say M_W or equivalently the value of Λ_L . This can be related to say $\Lambda_{\overline{MS}}$ by 1-loop perturbation theory and then fixed by taking the value of $\Lambda_{\overline{MS}}$ from experiments. The

evolution of the coefficients has strong dependence on the value of Λ . For lattice actions with small Λ_L (like the Wilson action) the evolution is small. The corresponding matrix elements (and the Z factors) have to be larger than in the continuum to give a scheme independent result.

4.3) RESULTS

I will discuss the results for the $\Delta I = \frac{1}{2}$ and $\Delta I = \frac{3}{2}$ amplitudes from the three groups separately.

4.3a) UCLA group:

Their goal has been to first verify whether the ME show the correct chiral behavior for Wilson fermions [14]. To check this they look at the simplest operators, the $LL \Delta S = 2$ operators arising in $K^0 \bar{K}^0$ mixing and the $\Delta I = \frac{3}{2}$ one. Their results show a deviation from the expected chiral behavior $m_\pi m_K$ as shown in figure 5. Both amplitudes cross zero for $500 < m_\pi < 700$ MeV and change sign. The issue of whether this is due to finite size effects and a large coupling g has not been resolved. Given that CPT is central to the lattice calculation, we need to understand this feature.

The other results for the LL matrix elements are 1) they agree with VIA at large quark masses, 2) the ME show reasonable scaling behavior between $\beta = 5.7$ and 6.1 , 3) the magnitude of the $\Delta I = \frac{3}{2}$ amplitude is comparable to the $\Delta I = \frac{1}{2}$ one, so eye diagrams are essential to explain the enhancement and 4) the finite size effects are significant at small m_q and a large statistical sample is needed to get a clean signal.

To calculate the eye diagrams they implement the GIM cancellation on the lattice. The $\mathfrak{J}d$ operator then has the form

$$\frac{\delta_3}{a^2} (m_c - m_u) \mathfrak{J}d . \quad (4.16)$$

which is quadratically divergent ($1/a^2$ versus $1/a^3$) due to GIM. They calculate the leading term for δ_3 using perturbation theory. Similarly, they also calculate the coefficient of the dimension 5 operator

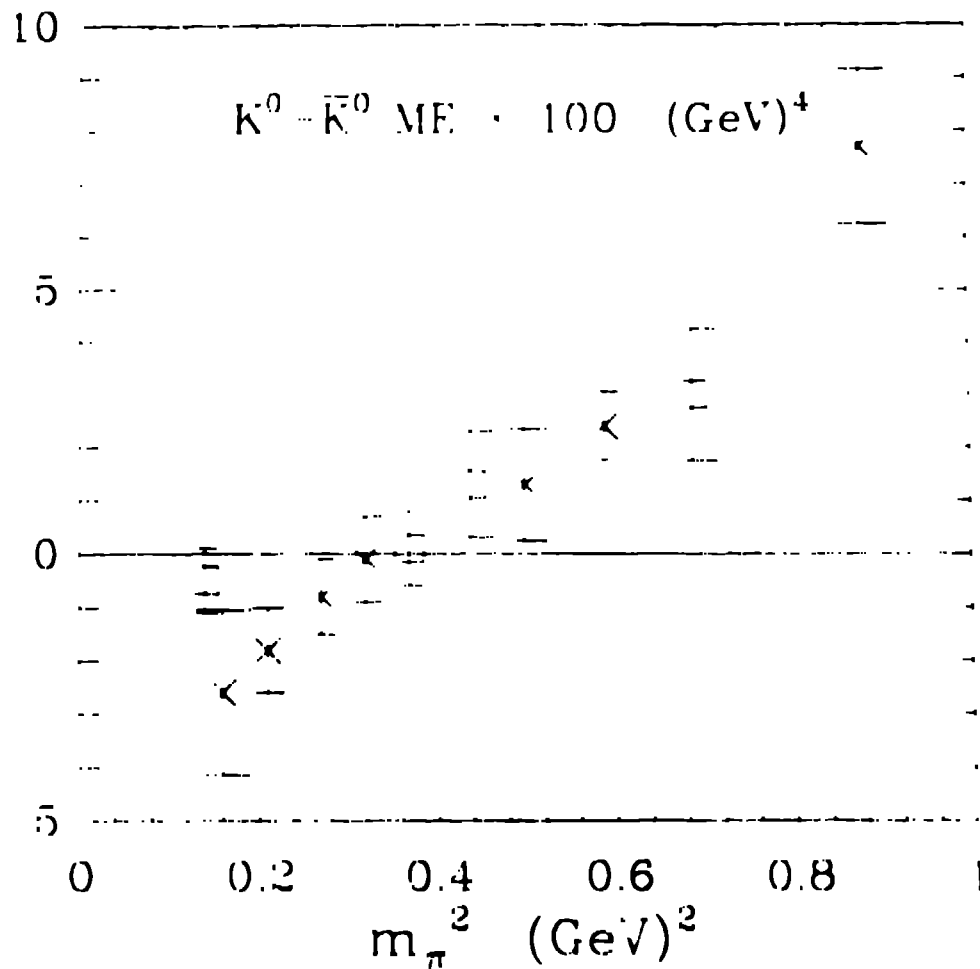


Fig. 5: The $K^0\bar{K}^0$ matrix element, λ_{LL} , as a function of the kaon mass-squared. The crosses are the results at $\beta = 5.7$ on a $10^3 \times 20$ lattice with 18 configurations while squares are from $\beta = 6.1$ on a $12^3 \times 33$ lattice with 18 configurations [14].

$\mathcal{J}\sigma_{\mu\nu}F^{\mu\nu}d$ in perturbation theory. The hope is that there exists a range of couplings over which this perturbative estimate is valid and also in this interval the lattice results scale so that one is extracting continuum physics. The preliminary results for $\Delta I = \frac{1}{2}$ show that a lot more work is necessary before one has control over the 3 separate

subtractions, so conclusions are lacking. The encouraging feature is that the magnitude of these ME is large and there is room to explain the $\Delta I = \frac{1}{2}$ rule.

4.3b) CERN Group:

The CERN group [15] test for the chiral behavior of *eight* by using the same operators as the UCLA group. The two groups differ in how they fit the data to extract the ME . Martinelli *et al.* sum over the time position of the operator keeping the location of the π and K fixed at some large separation τ , which on their lattices is 10. They assume that the π and K correlators are dominated by a single particle for all positions of the source. Since tests are not made for different separations τ , this process cannot reveal whether the separation between the mesons is large enough. Indeed there is preliminary evidence from the UCLA group that it is not. Martinelli *et al.* do not show any check for such systematic errors and their paper does not give enough information for me to judge fairly. The result, however, is in good agreement with the chiral behavior as shown in figure 6. This is in direct contradiction with the results of the UCLA group, so both groups are working hard to resolve the discrepancy.

The scheme proposed by Maiani *et al.* [16] to calculate the subtracted eye diagrams is as follows: Consider the two ME for a generic operator O (here the subscript refers to the dimension of the operator)

$$\langle \pi | O_8 + \delta_6 O_6 + \delta_5 O_5 | K \rangle = \delta_2 + \gamma_2 p \cdot k \quad \dots \quad (4.17a)$$

$$\langle \pi | \bar{3}d | K \rangle = \delta_6 + \gamma_6 p \cdot k \quad \dots \quad (4.17b)$$

where $\delta_6 O_6$ are the dimension 6 operators of different spin-parity which are induced by the chiral symmetry breaking Wilson term and O_5 is the dimension 5 operator given above. They calculate both δ_5 and δ_6 in perturbation theory. The physical ME is then given by

$$\lim_{m_\pi, m_K \rightarrow 0} Z_L \left(\gamma_2 - \delta_2 \frac{\gamma_6}{\delta_6} \right) \quad (4.18)$$

where the factor Z_L relates the lattice and continuum operators. So, they use one extra ME to do one non-perturbative subtraction. The

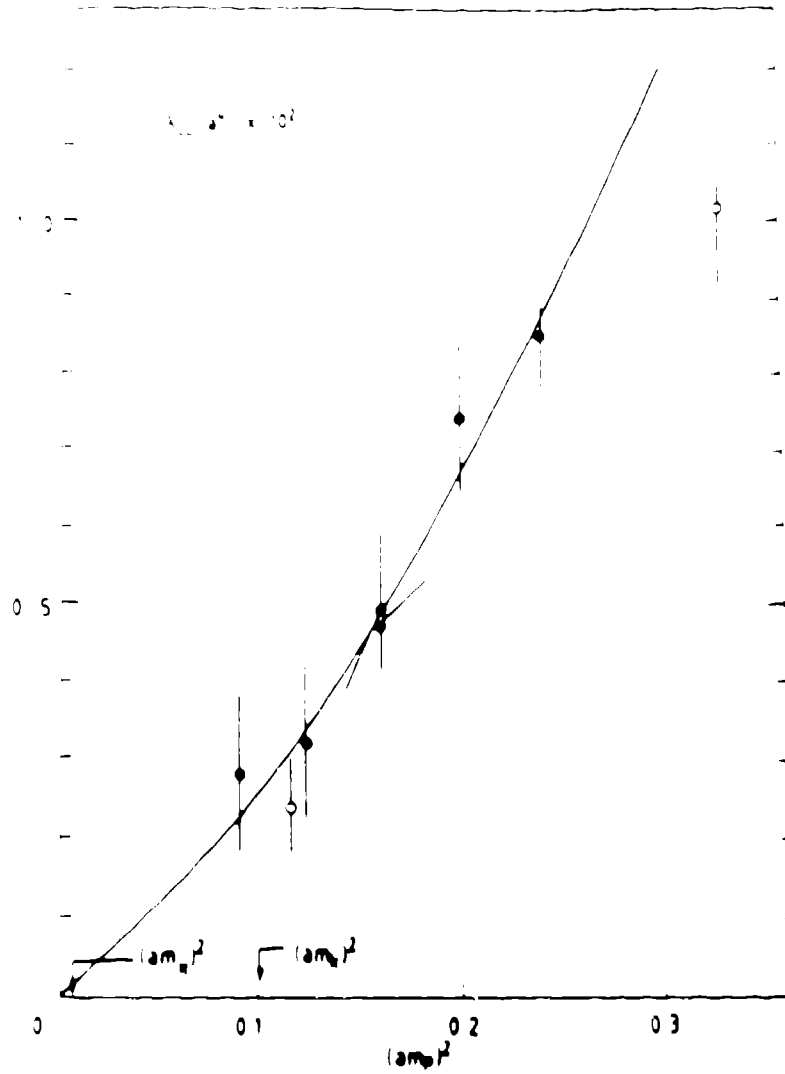


Fig. 6: The $K^0 \overline{K^0}$ matrix element, λ_{LL} , as a function of the kaon mass-squared. The curve shown is the fit; $\lambda_{LL} = (0.05(2) \text{ GeV}^2) m_p^2 + 0.07(5) m_p^4$ [15]. The results are on a $10^3 \times 20$ lattice at $\beta = 6.0$ and with 15 configurations.

above subtraction is in practice done at finite quark mass, so one needs very good data to cancel all terms on the right hand side and get just the correct chiral behavior. We have to wait for the first results to see how well it works.

The present limitation to measuring $\frac{c_1}{\tau}$ using Wilson fermions is

the operator $\bar{s}\sigma_{\mu\nu}F^{\mu\nu}d$. With the GIM mechanism this is

$$O_5 = \left(\frac{C_t}{C_u}m_t + \frac{C_c}{C_u}m_c - m_u\right)\bar{s}\sigma_{\mu\nu}F^{\mu\nu}d \quad (4.19)$$

with the C defined in eqn. (4.9). The multiplication by GIM mass term makes it a dimension 6 operator. However, in the calculation of $\frac{\epsilon'}{\epsilon}$, there is no GIM cancellation after integrating the t quark so the operator has a linear divergence. Thus to determine its coefficient one has to calculate more ME than shown in eqn (4.17), and then do the subtraction. Alternately, we need to measure $K \rightarrow \pi\pi$ directly.

4.3c) Los Alamos Group (Staggered Fermions):

The machinery necessary to calculate the ME with staggered fermions is spelt out in detail in refs. [11][17]. Here I shall just state the main ideas and results. To transcribe \mathcal{H}_{eff} on to the lattice required more work because of the mixing of spin and flavor degrees of freedom. Since these 16 degrees of freedom are spread out over a hypercube, the quark bilinears in the operators can be split by up to 4 links that span the hypercube. Our first calculation indicates that the noise introduced by these extra gauge links in the correlators is not significant compared with the noise intrinsic to staggered fermions.

Calculations with SF automatically involve 4 staggered flavors. These flavors are degenerate in the continuum limit and our recent calculation of the hadron spectrum shows that the symmetry is dynamically restored to a good approximation at $\beta \approx 6.2$ [18]. Thus we assume that these flavors can be accounted for by an overall factor of four.

There is only one lower dimension operator

$$O^{su\bar{b}} = (m_d + m_s)\bar{s}d + (m_d - m_s)\bar{s}\gamma_5d \quad (4.20)$$

that mixes with the dimension 6 operators. The physical operator can be defined as $O - \alpha O^{su\bar{b}}$ with the unknown parameter α determined non-perturbatively by requiring [11]

$$\langle 0|O - \alpha O^{su\bar{b}}|K\rangle = 0 \quad (4.21)$$

for each operator O in eqn. (4.10). The test that this subtraction procedure works is that the ME of the subtracted operators show the correct chiral behavior. This is verified for the penguin eye diagrams for which we have a stable signal. For the LL eye contractions we don't yet have a clean signal to draw any conclusions.

Some of the *eight* contractions for the LL operators do not show the correct chiral behavior. The reason is not yet understood.

We believe there are large "wrap around" contributions due to (anti-) periodic boundary conditions that afflict our correlators (see example in figure 7). These have to be isolated from the signal in all calculations which have (anti-) periodic boundary conditions in any of the four directions.

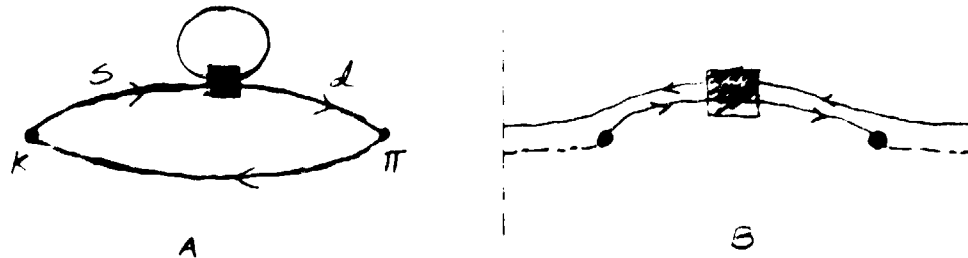


Fig. 7: An eye diagram and its corresponding "wrap-around" contribution.

In most cases, where we can extract a signal, the lattice VIA works very well. As shown in the discussion of $\frac{c'}{c}$, M_0 is smaller than its VIA value. This implies that penguins are irrelevant to explain the large $\Delta I = \frac{1}{2}$ enhancement since VIA does not. There is always the possibility that the behavior we are seeing is just an artifact of large m_q and that things will change when simulations are done with physical u and d quarks. A test of this will have to wait for some time.

To summarize, the technical machinery necessary to calculate ME with staggered fermions is set up but the statistical signal is not under control. The penguins are too small to explain the $\Delta I = \frac{1}{2}$ rule, but their signal is good enough to make a preliminary statement about $\frac{c'}{c}$.

4.4) ϵ'/ϵ : CP Violation in K Decays

The parameter ϵ measures the amount of CP violation in $K^0\bar{K}^0$ mixing:

$$|K_L\rangle = \frac{1}{N} [(1 + \epsilon)|K^0\rangle + (1 - \epsilon)|\bar{K}^0\rangle] \quad (4.22a)$$

$$|K_S\rangle = \frac{1}{N} [(1 + \epsilon)|K^0\rangle - (1 - \epsilon)|\bar{K}^0\rangle] \quad (4.22b)$$

where N is the normalization. The standard KM model, predicts a second independent CP violating parameter, ϵ' [19]. This arises in the decay of neutral kaons. The simplest characterization of it is if we choose a basis in which the $\Delta I = \frac{1}{2}$ decay amplitude A_0 is real; then ϵ' is non-zero if the $\Delta I = \frac{3}{2}$ amplitude has an imaginary part.

Let me briefly introduce the notation. Consider the two amplitudes

$$\begin{aligned} \langle \pi\pi(I=0) | \mathcal{H}_W | K^0 \rangle &= A_0 e^{i\delta_0} \\ \langle \pi\pi(I=2) | \mathcal{H}_W | K^0 \rangle &= A_2 e^{i\delta_2} \end{aligned} \quad (4.23)$$

and the corresponding ones for \bar{K}^0 . Here δ_0 and δ_2 are the $\pi\pi$ phase shifts for isospin 0 and 2 respectively and the exponential factor incorporates the final state interaction of the two pions. In the lattice basis both A_0 and A_2 are complex. The two CP violating parameters measured in experiments are

$$\begin{aligned} \eta_{+-} &= \frac{\langle \pi^+\pi^- | \mathcal{H}_W | K_L \rangle}{\langle \pi^+\pi^- | \mathcal{H}_W | K_S \rangle} \\ \eta_{00} &= \frac{\langle \pi^0\pi^0 | \mathcal{H}_W | K_L \rangle}{\langle \pi^0\pi^0 | \mathcal{H}_W | K_S \rangle} \end{aligned} \quad (4.24)$$

Now using eqns. (4.1,4.23,4.24), one can express η_{+-} and η_{00} in terms of ϵ and ϵ' as

$$\begin{aligned} \eta_{+-} &\approx \epsilon + \epsilon' \\ \eta_{00} &\approx \epsilon - 2\epsilon' \end{aligned} \quad (4.26)$$

with ϵ' defined as

$$\epsilon' = \frac{i}{\sqrt{2}A_0} e^{i(\delta_2 - \delta_0)} \left\{ \frac{ImA_2}{ReA_0} - \omega \frac{ImA_0}{ReA_0} \right\} \quad (4.27)$$

where

$$\omega \equiv \frac{\text{Re}A_2}{\text{Re}A_0} \approx \frac{1}{22} \quad (4.28)$$

is obtained from $\Delta I = \frac{1}{2}$ enhancement. At present we also use the experimental value for ϵ

$$\epsilon = 2.27 \times 10^{-3} e^{i\pi/4} \quad (4.29)$$

and calculate only ϵ' on the lattice. Later we hope to measure ϵ and ω from the lattice.

At $\mu \approx 2$ GeV, $\text{Im} \mathcal{H}_{eff}$ is dominated by the 3 operators O_6, O_7 and O_8 ,

$$\text{Im} \mathcal{H}_{eff} \approx \frac{G_F}{2\sqrt{2}} (s_1 s_2 s_3 c_2 s_5) \sum_{i=6}^8 \tilde{C}_i O_i \quad (4.30)$$

where the KM angles have been isolated to define \tilde{C} from C .

In lattice calculations, A_0 is not real. In fact the dominant contribution to eqn. (4.27), with \mathcal{H}_{eff} defined in eqn. (4.30), comes from $\text{Im}A_0$ since only *em* penguins contribute to both $\text{Im}A_0$ and $\text{Im}A_2$. Using the experimental value for ϵ and writing all *ME* as ratios to their VIA value, one gets the master formula [20] [21] [22]

$$\left| \frac{\epsilon'}{\epsilon} \right| = 3 \times 10^{-3} \left| \frac{s_1 s_2 s_3 c_2 s_5}{2 \times 10^{-4}} \right| \left| \frac{\tilde{C}_6}{0.1} \right| \left(\frac{125 \text{MeV}}{m_s} \right)^2 \frac{B_6 (1 + \Omega_{emp} - \Omega_\eta - \Omega_{\eta'})}{B_6} \quad (4.31)$$

where

$$\Omega_{emp} = 0.23 \left(\frac{\tilde{C}_7 B_7 + 3\tilde{C}_8}{3\alpha_{em} \tilde{C}_6} \right) \frac{B_8}{B_6} \quad (4.32)$$

and the B are defined in eqn. (4.15). The *ME* are calculated using the physical operators defined by eqn. (4.21). The factor, α_{em} , has been taken out of \tilde{C}_7 and \tilde{C}_8 . The factor $\Omega_\eta + \Omega_{\eta'}$ is due to isospin breaking and its present estimate is ≈ 0.27 [5] to 0.4 [21]. It is the B_i alone that we calculate on the lattice.

In the lattice calculation with staggered fermions [22][23], we have $1/a \equiv \mu = 1.7 \text{GeV}$. Using $m_b = 4.5 \text{GeV}$, the coefficients are: $\tilde{C}_6 =$

0.08 – 0.09 (0.12 – 0.15), $\tilde{C}_7/\alpha_{em} = 0.15 – 0.22$ (0.11 – 0.18) and $\tilde{C}_8/\alpha_{em} = 0.01 – 0.02$ (0.01 – 0.03) with the ranges corresponding to $m_t = 30$ to 70 GeV , $\Lambda = 0.1$ or (0.3) GeV . We assume that $\Lambda_L = \Lambda_{\overline{MS}}$ for the improved action used.

The calculation was done with 2 values of the quark mass; one a little heavier than the s quark and the other a factor of 8 lighter. With this data, GIM subtraction cannot be done on the lattice. One can regard it as one of two approximations: 1) The c quark mass is equal to the lattice scale. $1/a$, and we take \mathcal{M}_{eff} just below threshold with c integrated out or 2) the contribution of c graphs is small. In fact the second point is demanded by consistency if one assumes the first.

The 4-link part of the operators (fermion bilinear in \mathcal{M}_{eff} split by 4 links) are left out. They were either too noisy to fit or for eight contractions were not calculated due to an oversight. Indications are that for our m_q , these are small and to first approximation can be neglected.

The ME of eight contractions do not fall as $m_* m_K$ for either the physical operators or their VIA . We don't have a good explanation and for the moment assume that the estimates for the ratios, B , are reasonable. The “penguin” contractions do show the chiral behavior at heavy masses (heavy-heavy and heavy-light combination of quark propagators), but the signal is too poor at the small mass to confirm it. These results are summarized in figures 8a and 8b [24].

Given all the uncertainties mentioned above (and some more), we can only point at trends observed in the data; 1) the strong penguins are suppressed with respect to their VIA value. This decreases the estimate for $\frac{\epsilon'}{\epsilon}$. 2) The electromagnetic penguins are enhanced wrt to VIA and they increases $\frac{\epsilon'}{\epsilon}$. 3) The magnitude of the em penguin contribution maybe comparable to M_6 .

Putting in numbers for the ratios B , the final estimate for $\frac{\epsilon'}{\epsilon}$ is still $(1 - 2) \times 10^{-3}$ (0.6 to 0.7 of the VIA value) compared to the present experimental value of $0.0035 \pm 0.003 \pm 0.002$ [25]. Our goal is to push the accuracy of the lattice calculation of ME below the combined uncertainty in the coefficient functions due to $\Lambda_{\overline{MS}}$, m_t and the KM

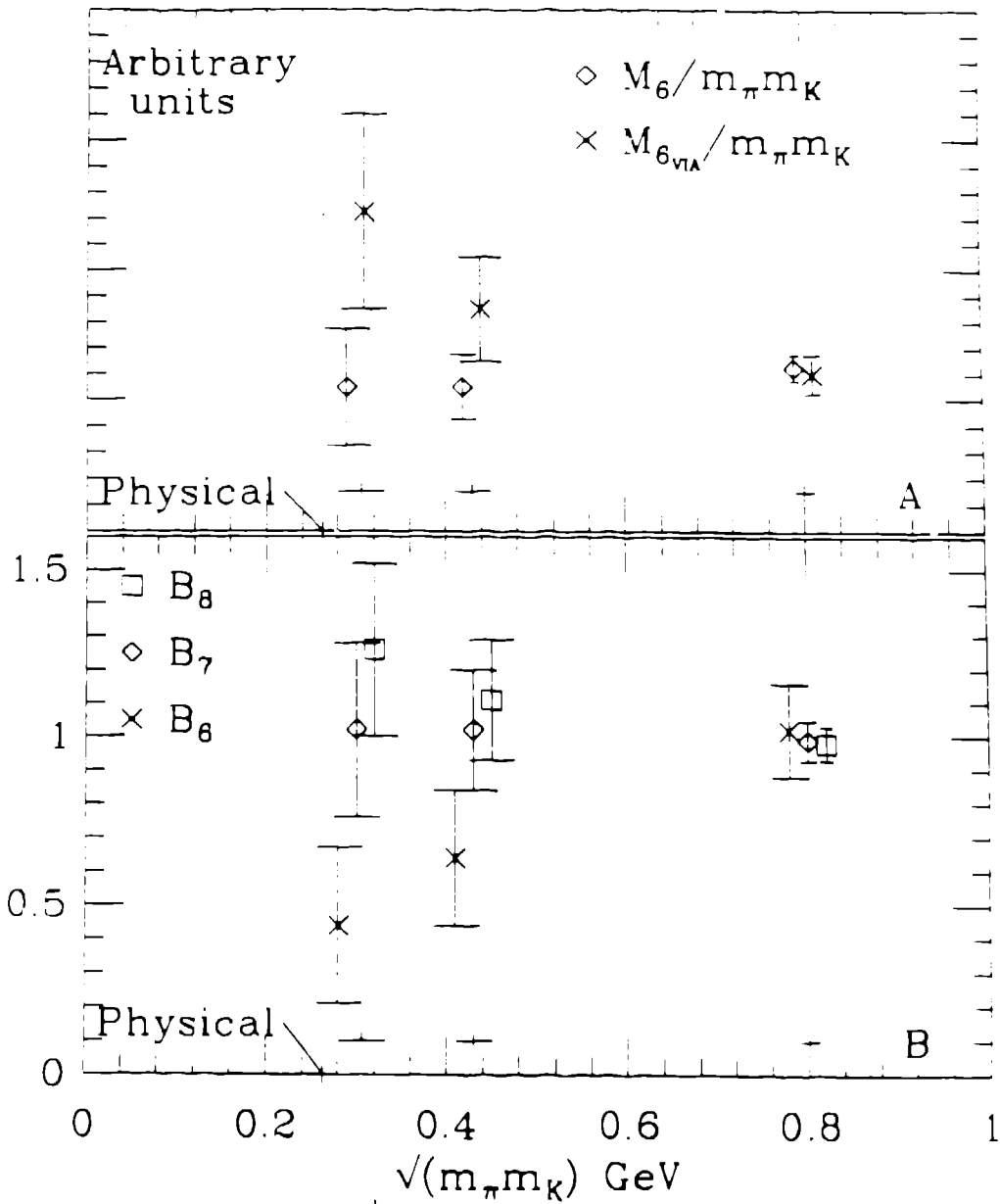


Fig. 8: Results for ME with staggered fermions on a $12^3 \times 32$ lattice with an improved action (25 configurations). The horizontal bars show the statistical error in the lattice determination of $\sqrt{m_\pi m_K}$. The data is shifted for clarity. a) Testing the chiral behavior of M_6 and its VIA. Note the unphysical increase in VIA estimate with decrease in m_q . b) Results for the B parameters defined in eqn. (4.15).

angles. We hope to realize this in the next generation calculation.

Conclusions

The subject material necessary to understand how to calculate ME from the lattice is extensive. The above discussion should convince you that not all the issues are fully resolved. We have come a long way from the first lattice calculations [26] [27] [28] , however the status of numerical studies is still preliminary. Yet, the prospects of solving some of the fundamental problems is sufficient lure for a sustained effort. I hope that a similar review few years from now will have some definite results.

References

- [1] H. Georgi, *Weak Interactions and Modern Particle Physics*, Benjamin (1984). This book provides a comprehensive introduction to the modern theory of weak interactions.
- [2] M. Kobayashi and T. Maskawa, *Prog. Theor. Phys.* **49** (1973) 652.
- [3] F. Gilman and M.B. Wise, *Phys. Rev.* **D20** (1979) 2372.
- [4] F. Gilman and M. B. Wise, *Phys. Rev.* **D27**(1983)1128.
- [5] A. Buras and Gerard, MPI-PAE/Pth 7/87, Jan 1987.
- [6] M. A. Shifman, A. I. Vainshtein and V. I. Zakharov, *Nucl. Phys.* **B120** (1977) 316.
- [7] R. S. Chivukula, J. Flynn and H. Georgi, *Phys. Lett.* **171B** (1986) 453.
- [8] W. A. Bardeen, A. J. Buras and J. Gerard, MPI-PAE/Pth 45/86.
- [9] J. Bijnens, H. Sonoda and M. Wise, *Phys. Rev. Lett.* **53** (1984) 2367.
- [10] C. Bernard, T. Draper, A. Soni, D. Politzer and M. Wise, *Phys. Rev.* **D32** (1985) 2343.
- [11] S. Sharpe, A. Patel, R. Gupta, G. Guralnik and G. Kilcup, *Nucl. Phys.* **B286** (1987) 253.
- [12] G. Martinelli, *Phys. Lett.* **141B** (1984) 395.
- [13] C. Bernard, A. Soni and T. Draper, UCLA/87/TEP/18.
- [14] C. Bernard, T. Draper, G. Hockney and A. Soni, *Talk at the BNL lattice meeting 1986*, UCLA/86/TEP/48.
- [15] L. Maiani and G. Martinelli, *Phys. Lett.* **181B** (1986) 344.
- [16] L. Maiani, G. Martinelli, G.C Rossi and M. Testa, *Phys. Lett.* **176B** (1986) 445; and CERN-TH.4517/86.
- [17] G. Kilcup and S. Sharpe, *Nucl. Phys.* **B283** (1987) 493.
- [18] R. Gupta, G. Guralnik, G. Kilcup, A. Patel, S. Sharpe and T. Warnock, Cornell Preprint CLNS-87/79 (May 1987).
- [19] For a review of the predictions of the KM model see L. Wolfenstein, *Ann. Rev. Nucl. Part. Sci.* **36** (1986) 137.
- [20] J. Bijnens and M. Wise, *Phys. Lett.* **137B** (1984) 245.
- [21] J. F. Donoghue, E. Golowich, B. Holstein and J. Trampetic, *Phys. Rev. Lett.* **179** (1986) 361.

- [22] S. Sharpe, R. Gupta, G. Guralnik, G. Kilcup and A. Patel, SLAC-PUB-4236, March 1987.
- [23] S. Sharpe, SLAC-PUB-4296, May 1987.
- [24] S. Sharpe, *Proceedings of the XXII Moriond Conference*, 1987; SLAC-PUB-4316.
- [25] B. Winstein, *Proceedings of the APS-DPF meeting*, Salt Lake City (1987).
- [26] R. Brower, M.B. Gavela, R. Gupta and G. Maturana, *Phys. Rev. Lett.* **53** (1984) 1318.
- [27] N. Cabibo, G. Martinelli and R. Petronzio, *Nucl. Phys.* **B244** (1984) 381.
- [28] C. Bernard, T. Draper, G. Hockney, A. M. Rushton and A. Soni, *Phys. Rev. Lett.* **55** (1985) 2770.

MONTE CARLO RENORMALIZATION GROUP

The development of Monte Carlo Renormalization group method (*MCRG*) was essentially complete in 1979 with the work of Wilson [1], Swendsen [2] and Shenker and Tobochnik [3]. Prior to this Ma [4] and Kadanoff [5] had provided key ingredients. The method is therefore relatively new, and furthermore its application to field theories has been carried out only since 1982. In this short period there has been considerable activity and I shall review the methodology and summarize the status with emphasis on 4-dimensional gauge theories. There already exists extensive literature on *MCRG* and I direct the reader to it [1][3][6] [7] for details and for a wider exposure. Similarly, the reviews [8] [9] are a good starting point for background on Lattice Gauge Theories and on spin systems. The topics I shall cover are

- 1) Introduction to *MCRG* and its methodology.
- 2) Renormalization Group Transformations for $d = 4$ lattice gauge theories.
- 3) $U(1)$ Lattice Gauge Theory.
- 4) β -function and scaling for $SU(3)$ Lattice Gauge Theory.
- 5) Improved Actions and Methods to calculate them.
- 6) Improved Monte Carlo Renormalization Group.
- 7) Renormalization Group inspired Multigrid update.
- 8) Measuring auto-correlations with block operators.
- 9) Effective Field Theories.

The main results in QCD from *MCRG* are 1) the determination of the β -function and the consequent prediction for the value of the coupling at which asymptotic scaling sets in and 2) an estimate of the improved gauge action [10]. These results are not spectacular in the sense of confirming that QCD is the correct theory of strong interactions, however they have led to a deeper understanding of the lattice theory and provided a quantitative estimate of the approach to the continuum limit. I shall attempt to show that this method is as yet in its infancy and should be used to tackle a number of problems.

1) INTRODUCTION TO *MCRG*

Renormalization Group [11] [12] [13] is a general framework for studying systems near their critical point where singularities in thermodynamic functions arise from coherence at all length scales. This phenomenon occurs in Statistical Mechanics near and on the critical surface (defined by a divergent correlation length) and in the strong interactions of quarks and gluons. The *MCRG* method was developed to handle this problem of infinitely many coupled degrees of freedom so that sensible results can be obtained from finite computers. There are two central ideas behind *MCRG*: One is to average over these infinitely many degrees of freedom in discrete steps preserving only those which are relevant for the description of the physical quantities of interest. The interaction between these averaged (block) fields is described by an infinite set of couplings that get renormalized at each step. In QCD this discrete reduction is carried out until the correlation length is small enough so that the system can be simulated on a lattice with control over finite size effects. The second idea is that singularities in the coupling constant space are much softer even though the correlation length diverges on the critical surface. In section 6.1, I show that some of elements of the linearized transformation matrix diverge. But this happens only in the limit of infinite range couplings. Thus these elements should not be important if the fixed point is short ranged.

The *MCRG* methods discussed here have a fundamental assumption that there exists a fixed point of the transformation and that this is short ranged. Thus, even though an infinite number of couplings are generated under renormalization, we shall assume that only a few short range ones are sufficient to simulate the system at a given scale and preserve the long distance physics. Present results suggest that the fixed point for QCD is short ranged.

1.1) Standard Monte Carlo:

Consider a magnetic system consisting of spins $\{s\}$ on the sites of a d - dimensional lattice L described by a Hamiltonian H with all

possible couplings $\{K_\alpha\}$. All thermodynamic quantities can be found from a detailed knowledge of the partition function

$$Z = \sum e^{-H} = \sum e^{K_\alpha S_\alpha} \quad (1.1)$$

where S_α are the interactions. In Monte Carlo, configurations of spins on the original lattice are generated by the Metropolis [14], heat bath [15], molecular dynamics alias Microcanonical [16] or the Langevin [17] [18] algorithm with a Boltzmann distribution $e^{-H} \equiv e^{K_\alpha S_\alpha}$. All thermodynamic quantities are given as simple averages of correlation functions over these "importance sampled" configurations. The accuracy of the calculations depend on the size of the statistical sample and the lattice size L used. Both these quantities depend on the largest correlation length ξ in the system. Near the critical temperature, T_c , associated with second order phase transitions, the correlation length and thermodynamic quantities like the specific heat diverge as functions of $(T - T_c)$ with universal critical exponents that have been calculated for many systems either analytically or by Monte-Carlo using finite size scaling [19] or by the *MCRG* method. Because ξ diverges at T_c , long runs are needed to counter the critical slowing down and the lattice size has to be maintained at a few times ξ . The problem of critical slowing down is addressed by analyzing update algorithms (Metropolis vs. heat bath vs. Microcanonical vs. Langevin with acceleration techniques like multi-grid [20], fourier acceleration [21] etc). The optimum method is, of course, model dependent and has to take care of metastability (local versus global minima) and global excitations like vortices, instantons etc that are not efficiently handled by local changes. This last feature has not received adequate attention. To control the second problem in standard Monte Carlo, effects of a finite lattice especially as $\xi \rightarrow \infty$, finite size scaling [19] has been used with success. In this review I shall concentrate on *MCRG*. First I shall describe how universality and scaling are explained by the renormalization group.

The renormalization group transformation (*RGT*) is an operator R defined on the space of coupling constants, $\{K_\alpha\}$. In practice the *RGT* is a prescription to average spins over a region of size b , the scale

factor of the *RGT*, to produce the block spin which interacts with an effective theory $H^1 = R(H)$. The two theories H and H^1 describe the same long distance physics but the correlation length in lattice units $\xi \rightarrow \xi/b$. If this *RGT* has a fixed point H^* such that $H^* = R(H^*)$, then clearly the theory is scale invariant at that point and ξ is either 0 or ∞ . An example of a trivial fixed point with $\xi = 0$ is $T = \infty$. The interesting case is $\xi = \infty$, close to which the theory is governed by a single scale ξ . I will discuss this assumption of hyperscaling, i.e. a single scale controlling all physics, later. If this fixed point is unstable in 1 direction only (this direction is called the Renormalized Trajectory (*RT*)), then non-critical H close to H^* will flow away from H^* along trajectories that asymptotically converge to the *RT*. Thus the long distance physics of all the trajectories that converge is identical and is controlled by the *RT*. Similarly, points ϵ away from H^* on the $\infty - 1$ dimension hypersurface on which $\xi = \infty$ (the critical surface) will converge to H^* . The fact that the fixed point with its associated *RT* control the behavior of all H in the neighborhood of H^* is universality.

Next, consider a non-critical H that approaches H^* along the *RT*. Thermodynamic quantities depend on a single variable i.e. the distance along the *RT*. This is scaling. Corrections to scaling occur when H does not lie on the *RT*. These are governed by the irrelevant eigenvalues of the *RGT* which give the rate of flow along the critical surface towards H^* and, for H not on the *RT*, the rate of convergence towards it. The relevant eigenvalue gives the rate of flow away from the fixed point along the unstable direction (*RT*) and is related to the critical exponent ν . This terse exposé ends with a word of caution; all these statements have validity "close" to H^* .

1.2) Standard MCRG Method

In the *MCRG* method, configurations are generated with the Boltzmann factor $e^{K \cdot S}$ as in standard Monte Carlo. The *RGT*, $P(s^1, s)$, is a prescription for averaging variables over a cell of dimension b . The blocked variables $\{s^1\}$ are defined on the sites of a sublattice L^1 with lattice spacing b times that of L . They interact with a priori undetermined couplings $\{K_{ij}^1\}$, and the configurations are distributed

according to the Boltzmann factor e^{-H^1} i.e.

$$e^{-H^1(s^1)} = \sum P(s^1, s) e^{-H(s)} \quad (1.2)$$

All expectation values, with respect to the Hamiltonian H^1 , can be calculated as simple averages on the blocked configurations. The blocking is done n times to produce a sequence of configurations distributed according to the Hamiltonians H^n . They all describe the same long distance physics but on increasingly coarse lattices. The fixed point H^* , the *RT* and the sequence of theories, H^n , generated from a given starting H depend on the *RGT*.

The *RGT* should satisfy the Kadanoff constraint

$$\sum_{s^1} P(s^1, s) = 1 \quad (1.3)$$

independent of the state $\{s\}$. This guarantees that the two theories H and H^1 have the same partition function. The *RGT* should also incorporate the model's symmetry properties; a notable example is the choice of the block cell in the anti-ferromagnetic Ising model. Usually, there exists considerable freedom in the choice of the *RGT*. In fact many different *RGT* can be used to analyze a given model. In such cases a comparison of the universal properties should be made and the *RGT* dependent quantities isolated. I defer discussion on how to evaluate the efficiency of a *RGT* to section 2.5.

1.3) Methods to Calculate the Critical Exponents:

There are three methods to calculate the critical exponents from expectation values calculated as simple averages over configurations. In both there is an implicit assumption that the sequence H^n stays close to H^* . The more popular method is due to Swendsen [2][7] in which the critical exponents are calculated from the eigenvalues of the linearized transformation matrix $T_{\alpha\beta}^n$ which is defined as

$$T_{\alpha\beta}^n = \frac{\partial K_{\alpha}^n}{\partial K_{\beta}^{n-1}} = \frac{\partial K_{\alpha}^n}{\partial \langle S_{\alpha}^n \rangle} \frac{\partial \langle S_{\alpha}^n \rangle}{\partial K_{\beta}^{n-1}} \quad (1.4)$$

Each of the two terms on the right is a connected 2-point correlation matrix

$$U_{\sigma\beta}^n \equiv \frac{\partial \langle S_\sigma^n \rangle}{\partial K_\beta^{n-1}} = \langle S_\sigma^n S_\beta^{n-1} \rangle - \langle S_\sigma^n \rangle \langle S_\beta^{n-1} \rangle. \quad (1.5)$$

and

$$D_{\sigma\beta}^n \equiv \frac{\partial \langle S_\sigma^n \rangle}{\partial K_\beta^n} = \langle S_\sigma^n S_\beta^n \rangle - \langle S_\sigma^n \rangle \langle S_\beta^n \rangle. \quad (1.6)$$

Here $\langle S_\sigma^n \rangle$ are the expectation values on the n^{th} renormalized lattice and K_σ^n are the corresponding couplings. The relevant exponent ν is found from the leading eigenvalue λ_t of $T_{\sigma\beta}^n$ as

$$\nu = \frac{\ln b}{\ln \lambda_t} \quad (1.7)$$

where b is the scale factor of the *RGT*. The magnetic exponent is given by replacing λ_t by λ_h in Eqn.(1.7) where λ_h is the largest eigenvalue of T constructed from odd interactions. I have restricted the discussion to the special case of one relevant eigenvalue. In general, systems can have multi-critical points with more than one relevant interaction. Next, the eigenvalues which are smaller than one (called irrelevant) yield exponents that control corrections to scaling. An eigenvalue of exactly one is called marginal. Lastly, there is an additional class of eigenvalues, the redundant eigenvalues, that are not physical. Their value depends on the *RGT*, so one way to isolate them is to repeat the calculation with a different *RGT*. I shall return to these in section 2.5.

The accuracy of the calculation of exponents improves when they are evaluated close to the fixed point. This can be achieved by starting from a critical point and blocking the lattice a sufficient number of times i.e. H^n for large n . In this case the convergence is limited by the starting lattice size and how close the starting H^c is to H^* . This method can be improved if the renormalized couplings $\{K^n\}$ are determined starting from a known critical Hamiltonian. We assume that the couplings fall off exponentially with the range, so that H^c can be approximated by a small number of short range couplings. For calculations in models for which the critical coupling is not known exactly,

when using a truncated H^n the system will flow away from H^* under blocking. This flow away from H^* can be avoided by first putting H back on the critical surface by Wilson's 2-lattice method described in section 1.4. In sections 5 and 6, I describe a few methods to calculate the renormalized couplings.

A second possible improvement is to tune the RGT so that the convergence to H^* from a starting H^c takes fewer blocking steps. This is discussed in section 2.5

The practical limitation to the calculation of the exponents is that the two matrices U and D can only be determined in a truncated subspace. Further, in order to set up T , the matrix D has to be inverted. Thus the determination of exponents has two types of truncation errors: The truncated T differs from the true T due to the inversion of a truncated D and because we diagonalize a truncated T . These errors will be analyzed in detail in section 6.

The second method to calculate the leading relevant exponent is due to Wilson [6]. Consider once again the 2-point connected correlation function (the derivative of an expectation value) $\langle S_\alpha^i S_\beta^j \rangle_c$ with $j > i$. Expand S_α^i in term of the eigenoperators O_α^i of the RGT . Close to H^* the level dependence in O_α^i (equivalently in the expansion coefficients $c_{\alpha,\beta}^i$) can be neglected. Then to the leading order

$$\langle S_\alpha^i S_\beta^j \rangle_c \sim \lambda_t^{j-i} c_{\alpha,t} \langle O_t S_\beta^j \rangle \quad (1.8)$$

where λ_t is the leading relevant eigenvalue and corrections are suppressed by $(\frac{\lambda}{\lambda_t})^{j-i}$. Thus for each α and β , the ratio $\frac{\langle S_\alpha^i S_\beta^j \rangle}{\langle S_\alpha^{i+1} S_\beta^j \rangle}$ gives an estimate for the leading eigenvalue λ_t . This method works even when the starting coupling is not exactly critical. The accuracy of the method improves if $j-i$ is large (since non-leading terms are suppressed geometrically) and if used close to the fixed point.

I have compared the results for the two methods in the $d = 2$ Ising model [22] using a 64^2 lattice and blocking 3 times starting from a 44 term Hamiltonian H^2 . For $i = 1$ and $j = 2, 3, 4$, $\lambda_t = 2.00(3), 2.01(2)$ and $2.01(1)$, while $\lambda_h = 3.658(5), 3.660(5)$ and $3.663(5)$. Swendsen's method gave $1.998(2), 1.993(3), 1.990(3)$ and

3.666(1), 3.662(2), 3.66. (2) respectively and thus seems slightly better. However, the trends leave room for Wilson's method becoming better for large j . So, further tests in other models need to be made.

The third method – Wilson's 2-lattice method – is described in section 4 around eqn (4.3).

The calculation of ν from the leading eigenvalue does not assume hyperscaling. The relation between ν and the specific heat index α i.e. $\alpha = 2 - \nu d$ does. A known cause of hyperscaling violations are dangerous irrelevant operators [19]. In the presence of these, universal scaling functions have a power-law singularity $\frac{1}{(u|\varphi|)^\mu}$ in the limit $u \rightarrow 0$ where u is a dangerous irrelevant scaling field and φ is the corresponding scaling exponent. In the renormalization group approach is preserved but the hyperscaling law is modified to $\alpha = 2 - \nu d + \mu|\varphi|$. However, to predict α we need μ , the power with which the scaling function diverges. It is not known how to calculate this with *MCRG*. A side remark: in applying finite size scaling analysis to this case (with an enhanced definition of the scaling functions for the specific heat data), we need to specify u to study the divergence in the limit $u \rightarrow 0$. But scaling fields are a function of the *RGT*. So a *MCRG* calculation is necessary to identify it. Thus at present it is an open problem.

On the critical surface the 2-point correlation functions (like in Eq. (1.5) and (1.6)) diverge in the thermodynamic limit. However, their ratio is the rate of change of couplings and these are well behaved provided one considers only short ranged correlation functions as will be shown later. The reason that *MCRG* is assumed to have better control over finite size effects is that if H^* is short ranged then a truncated $T_{\alpha\beta}^n$ is sufficient to determine the leading eigenvalue. Also, the finite size contributions to the elements $T_{\alpha\beta}^n$ fall off like the couplings i.e. exponentially. Thus reliable estimates may be obtained from small lattices.

QCD: At the tree level, the coupling g in QCD does not renormalize and the fixed point is at $g_{bare} = 0$. At 1-loop the leading operator has eigenvalue equal to one, is relevant and the fixed point changes from simple gaussian to being asymptotically free and non-trivial. A

special feature of asymptotic freedom is that even though the leading eigenvalue is one there is a flow away from the fixed point at a constant rate. At 2-loop, this operator becomes truly relevant *i.e.* with eigenvalue > 1 . Perturbation theory also tells us that leading scaling violations are $\sim 1/k^2$, so the second eigenvalue should be $\sim 1/b^2$ for a *RGT* with scale factor b . Present studies [23] show that the leading eigenvalue is close to 1 and the second near $1/b^2$. However, the statistics are poor and the calculation was done at large g_{bare} . Thus reliable quantitative results are lacking.

1.4) Wilson's 2-lattice Method to Find a Critical Point:

The critical temperature is not known analytically for most models. Also, couplings calculated after blocking may not be critical due to truncation and statistical errors. The following method can be used to put H on to the critical surface.

Consider *MCRG* simulations L and S with the same starting couplings K_α^0 but on lattice sizes $L = b^n$ and $S = b^{n-1}$. If K_α^0 is critical and after a few blockings the 2 theories are close to H^* , then all correlation functions attain their fixed point values. For non-critical starting H , expand about H^* in the linear approximation

$$\begin{aligned} \langle L_\alpha^m \rangle - \langle S_\alpha^{m-1} \rangle &= \frac{\partial}{\partial K_\beta^0} \{ \langle L_\alpha^m \rangle - \langle S_\alpha^{m-1} \rangle \} \Delta K_\beta^0 \\ &= \{ \langle L_\alpha^m L_\beta^0 \rangle_c - \langle S_\alpha^{m-1} S_\beta^0 \rangle_c \} \Delta K_\beta^0 \end{aligned} \quad (1.9)$$

to determine ΔK_α^0 . To reduce finite size effects the compared expectation values are calculated on the same size lattices. The critical coupling is given by

$$K_\alpha^c = K_\alpha^0 - \Delta K_\alpha^0 \quad (1.10)$$

and this estimate should be improved iteratively.

2: RENORMALIZATION GROUP TRANSFORMATIONS IN 4-DIMENSIONS

It has been mentioned before that there is no unique *RGT* for a given model. There are at present four different transformations that have been proposed for 4-dimensional lattice gauge theories. In each of them the block link variable is constructed from a sum of paths $\Sigma \equiv \sum \text{paths}$. This sum of $SU(N)$ matrices is not an element of $SU(N)$, and the new block link matrix is selected with the distribution

$$P(U_b) = e^{p \text{Tr} U_b \Sigma} \quad (2.1)$$

where p is a free parameter to be optimized. The advantage of taking the sum is that such a *RGT* preserves gauge invariance. The 4 *RGT* are (in chronological order)

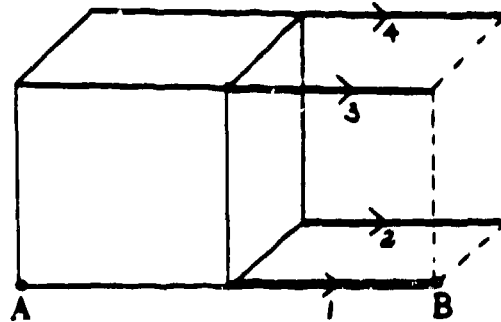


Fig. 1: Wilson's $b = 2$ transformation. Four of the eight links that connect two hypercubes are shown. The lattice is locally transformed into the Landau gauge since the ends of the links are not tied.

2.1) $b = 2$ by Wilson [1]: The geometry of the transformation is shown in Fig. 1. The block cell has 2^4 sites of which any one can be defined to be the block site. There are 8 links between two block sites in any given direction of which 4 are shown in the 3-dimensional projection. In this method the gauge has to be fixed on the 15 sites that are

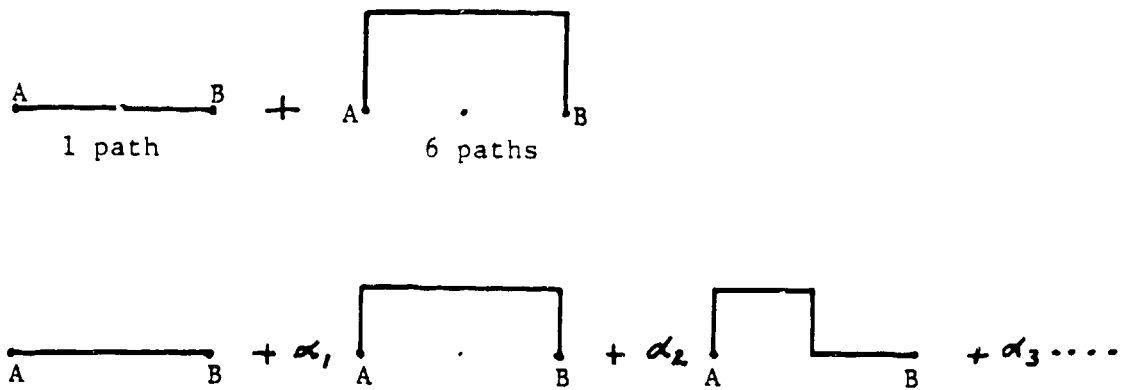
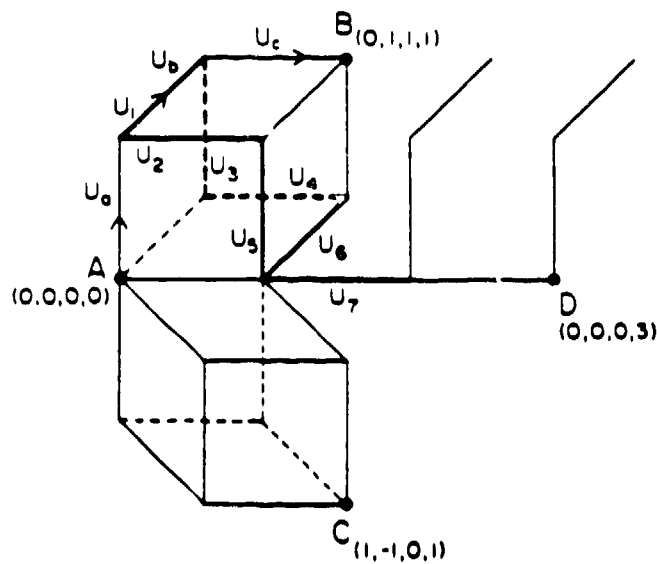


Fig. 2: Swendsen's $b = 2$ transformation. a) The original transformation that connects sites A and B by the average of the straight 2 link path and the six staples. b) The generalized transformation which includes paths of arbitrary size with corresponding strength parameters α_i that have to be determined by optimization.



4-DIMENSIONAL HYPERCUBIC LATTICE

Fig. 3: The geometry of the $b = \sqrt{3}$ transformation. The 4 block links originating from each block site are the body diagonals of the four 3-cubes. The six paths used in the construction of the block link between $(0,0,0,0)$ and $(0,1,1,1)$ are shown. Path U_7 is ignored.

not the block site. This local gauge fixing is done to take into account the fact that the ends of the 8 links are at different sites. The ansatz Wilson used was to transform the hypercube locally into the Landau gauge. The process of fixing the gauge is slow and a disadvantage of the method. The gauge fixing can be avoided by extending the 8 links into 8 paths that run between the block sites and include those links. This modified construction violates cubic rotational invariance because of the particular choice of the ordering of the paths within the cell. In either form only $\frac{32}{49}$ degrees of freedom are used in this approximate averaging at each level. Since Wilson's preliminary investigation, this method has not been used because the next two methods are simpler.

2.2) $b = 2$ by Swendsen [24] : The transformation in its initial form is shown in Fig. 2a. The more general version is shown in Fig. 2b where the parameters α_i have to be determined. In this construction all paths start and end at the block sites. Thus no gauge fixing is necessary and arbitrarily complex paths can be included. However calculations show that an optimization of the parameters has to be done to improve the convergence. I shall discuss this tuning later.

2.3) $b = \sqrt{3}$ by Cordery, Gupta and Novotny [25] : This transformation is specific to gauge theories in 4-dimensions and is based on the fact that the body diagonals of the 4 positive 3-cubes out of a site are orthogonal and of length $\sqrt{3}$. The geometry is shown in Fig. 3 and under one *RGT* the new lattice is still hypercubic but rotated with respect to the old basis. Also, the box boundary becomes jagged. This can be undone by a second application of the *RGT* with different basis vectors. So the original box geometry is recovered after every scale change by a factor of 3. The construction of the paths requires no gauge fixing, all paths are of equal length (no free parameters to be tuned) and $\frac{24}{28}$ degrees of freedom are used at each step. Further, the block cell consists of the block site and its 8 nearest neighbors. This provides an easy and natural way to include complex matter fields and block them simultaneously. This makes it the transformation of choice to study the $SU(2) \times U(1)_Y$ theory. It is also better suited to the

termion block diagonalization process of Mütter and Schilling [26] as is explained in section 5.10. In practice, for both $SU(2)$ and $SU(3)$, this RGT has consistently shown good convergence at strong and at weak coupling. It is therefore recommended.

2.4) $b = \sqrt{2}$ by Callaway and Petronzio [27] : The construction of paths shown in Fig 4a is based on a planer structure *i.e.* $x - y$ and $z - t$ planes are treated separately at all blocking steps. No gauge fixing is required but only 2 paths are used in the averaging *i.e.* in Eq. (2.1). This drawback of using only 2 planar paths can be improved by including nonplanar paths as shown in Fig. 4b. Because this RGT has the advantage that $b = \sqrt{2}$ is the smallest scale factor possible, a serious test should be made.

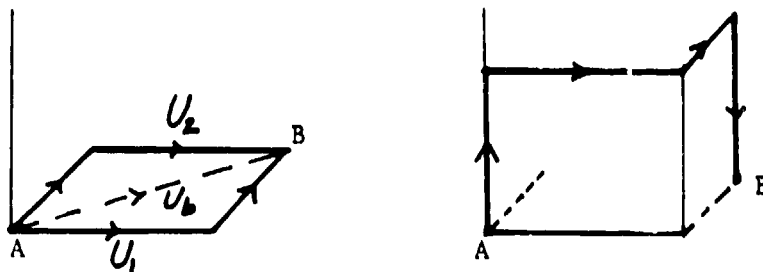


Fig. 4: The geometry of the $b = \sqrt{2}$ transformation. a) The two paths in the original proposal. b) Additional 4-links paths to make the transformation non-planar.

2.5) Optimization of the RGT : In addition to the freedom of the choice of the RGT , there are the free parameters p and α_i introduced above. Hasenfratz *et al.* [28] have shown that the convergence of the original $b = 2$ Swendsen transformation is improved if p is tuned. I will give a qualitative description of how this works. Consider a set of RGT that are a function of the continuous parameter p *i.e.* R_p . Starting from a given point H , the blocked theories generated are described by $H^1(p)$. They all have the same long distance behavior as can be checked by measuring expectation values of large Wilson loops. In fact

there is an effective Wilson action H_{eff} which will have the same long distance behavior for one observable. The short distance behavior of $H^1(p)$ will be different and for some values of p , the $\langle plaq \rangle_p$ will be larger than the $\langle plaq \rangle_w$ corresponding to H_{eff} . I have checked that this is the case for the original Swendsen transformation when $p = \infty$ and $g^2 < 1$. Lowering p reduces the blocked $\langle plaq \rangle_p$, making it agree better with H_{eff} . Thus, the tuning makes the short and long distance behavior correspond better to the same approximate H_{eff} . This leads to improved matching (using small loops) in the 2-lattice method to calculate the β -function. Hasenfratz *et al.* [28] estimate p using perturbation theory and by Monte Carlo using the criterion of early matching of block expectation values in Wilson's two lattice method. They found that the best value at $\frac{6}{g^2} = 6.0$ given by Monte Carlo (~ 35) does not agree with the value found using perturbation theory (~ 15). So as of now this optimization is still by trial. Also, p_{opt} depends on the coupling g . This implies that the RT cannot be pulled close to the Wilson axis globally by this optimization. So the usefulness of such optimization is limited to the β -function calculation. The parameters α_i can similarly be optimized using the same improvement criterion.

Gupta and Patel [23] used $p = \infty$ in the $\sqrt{3}$ RGT . This is equivalent to choosing the matrix U such that $Tr U \sum$ is maximized (the δ -function construction). They find that even with this choice the small block Wilson loops are more disordered than for an H_{eff} determined using large loops. Thus $p = \infty$ is optimal by the above criterion. The $\sqrt{3}$ RGT has shown good convergence properties and provided reliable results with $p = \infty$.

The freedom to choose the RGT and further tune the parameters α_i and p leads to the question: What are the criteria by which to decide what is the best RGT ? I will first address the question -- what is the effect of changing the RGT on the fixed point and on the RT ? Postulate [29] [30] : Changing the RGT moves the fixed point on the critical surface but only along redundant directions. A simple argument is as follows: Consider two different RGT , R_1 and R_2 , and their associated fixed points H_1^* and H_2^* . There are no non-analytic corrections to

scaling at either fixed points and the associated RT . If these two points are distinct, then H_2^* flows to H_1^* under R_1 . Consequently there are no scaling violations along the flow. This is by definition a redundant direction. This implies that the associated RT differ by redundant operators.

The presence of redundant operators does not effect the physics, but it can obscure results. The redundant eigenvalues are not physical, depend on the RGT , and can be relevant or irrelevant. If a relevant redundant operator is present then the flows will not converge to the H^* or to the RT . Thus it is desirable to pick a RGT for which the redundant eigenvalues are small [31]. Similarly, the coefficients of the leading irrelevant operators should be reduced. To some extent the irrelevant basis vectors are a function of the position of H^* , so it is possible to simultaneously reduce the two coefficients. In QCD , there is an additional freedom -- all possible Wilson loops form an overcomplete set. Therefore, in order to tune the RGT and to find an efficient improved action, it is necessary to determine the operators that can be eliminated because of the overcompleteness and the redundant combinations.

Swendsen [32] has conjectured that the fixed point can be moved anywhere on the critical surface by tuning the RGT . In particular, if the simulation point is made H^* , then that RGT is optimal. There is some support for this in spin systems, where by adding terms to the RGT , one can successively kill terms in the renormalized Hamiltonian. There are two things to check here: first whether the coefficients of the RGT terms fall off like the couplings, i.e. exponentially, and second whether the long range untuned couplings continue to fall off at least as fast as before. In the $d = 2$ Ising model we find that all the couplings (other than the nearest-neighbor) in a 3×3 square of spins can be made small without affecting the long range couplings [33]. We have yet to test whether this is true in more complicated models which have non-analytic corrections to scaling.

The quantity to optimize in numerical simulations is the update complexity (embodied in the RGT or the hamiltonian) versus the de-

crease in the coefficient of the leading irrelevant operator. Swendsen [32] found that the eigenvalues for the $d = 3$ Ising model are significantly improved with a tuned 10 term *RGT*. A simulation that used a 10 term truncated renormalized hamiltonian determined by him did not work as well. I believe (based on tests in the $d = 2$ Ising model [22]) that this occurred because the Hamiltonian had large truncation errors and was not much closer to the H^* for the simple majority rule *RGT*. There is one additional anomaly in this approach: Tuning the *RGT* improved the thermal exponent but the results for the magnetic exponent deteriorated in quality. This is surprising because the fixed point is at zero odd couplings and these remain unchanged in tuning the *RGT*. The previous postulates (movement in redundant directions only versus killing all long range interactions), if true in general models are in conflict and the present results are ambiguous. Consequently, this subject is being explored further [33].

The criterion for an optimum *RGT* is to make the H^* and the *RT* as short ranged as possible. In critical phenomena, the improvement can be quantified by measuring the convergence of the exponents as a function of the blocking level. In *QCD* we are interested in continuum mass-ratios etc. These have so far been hard to measure so the improvement cannot be judged. The behavior of the *RT* for *QCD* is discussed at the end of section 5. For the moment let me conclude this section with the statement that we don't know how to optimize *MCRG* systematically and this subject is under investigation.

3: U(1) LATTICE GAUGE THEORY:

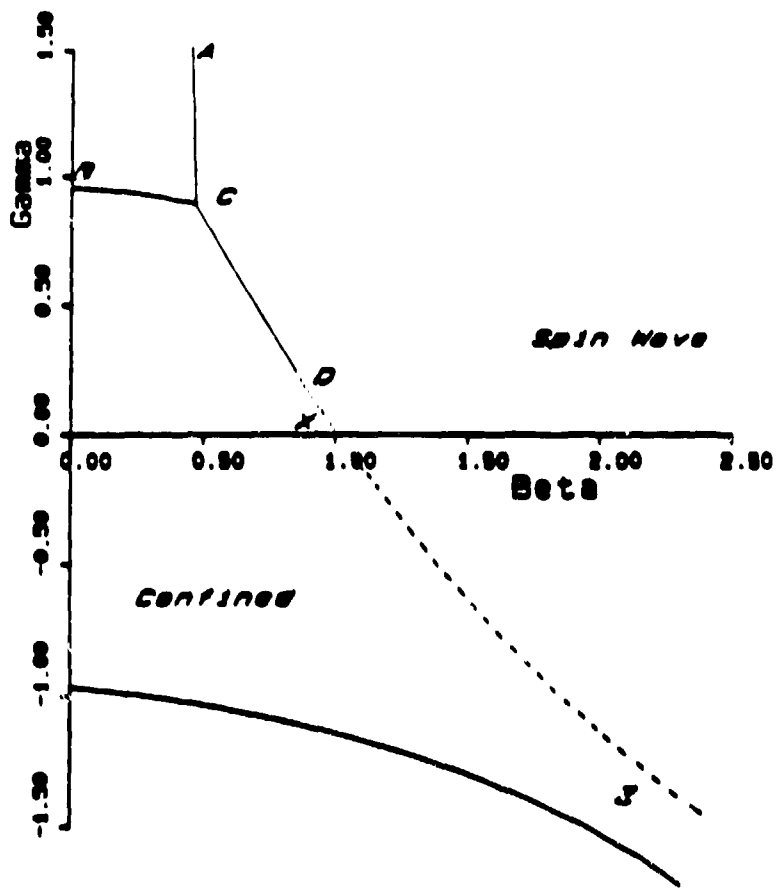
This model is a trivial limit of an eventual goal: To understand spontaneous symmetry breaking in the $SU(2) \times U(1)_Y$ theory of weak interactions. $U(1)$ has many of the technical complications one expects in the full theory, for example, large finite size effects, weak 1st order transitions with a possible tri-critical point (TCP) etc. So it is good starting place to test methods.

The phase diagram of the theory defined by the action

$$S = \beta \sum \cos\Theta_{\mu\nu} + \gamma \sum \cos 2\Theta_{\mu\nu} \quad (3.1)$$

where β (γ) is the charge 1 (charge 2) coupling is known to have a phase boundary separating the confining (strong-coupling) phase from the spin-wave (QED) phase [34] [35] [36]. The order of the transition along the boundary DXZ in Fig. 5 is not resolved. In particular it is not known if the gradually weakening first order transition along CD ends in a tricritical point, and if so what is its location. Evertz *et al.* [35] claim that the location of the TCP is at $\beta = 1.09 \pm 0.04$ and $\gamma = -0.11 \pm 0.05$ on basis of a scaling analysis of the discontinuity in the energy ΔE . The mechanism driving the transition are topological excitations [37] [38], *i.e.* closed loops of monopoles, whose density is observed to change at the transition [39] [40]. This change in density is caused by a growth in the size of the largest monopole loop which begins to span the finite lattices used in the calculations [39][41]. Thus, the usual difficulty of finite size effects near a TCP in determining the location of the TCP by an extrapolation of the latent heat ΔE along the phase boundary is here compounded by the presence of monopole current loops that are closed due to the lattice periodicity [39][41]. These contribute a fake piece to the ΔE which makes the extrapolation unreliable. One solution is to calculate and then subtract the contribution of these loops from ΔE before making the extrapolation. The more reliable method is $MCRG$ and in particular the 2-lattice method discussed in section 1.2 should be used to locate the TCP . A word of caution for the $U(1)$ model when using this method: There is a large shift in the critical coupling as a function of the lattice size [39] and consequently in the contribution of the fake monopole loops. One should therefore use a starting coupling for which both lattice simulations are on the same side of the transition.

The status of the order of the transition from $MCRG$ calculations using the T matrix is as follows: Along the Wilson axis [39] only one relevant exponent is found using the $\sqrt{3}$ RGT . Furthermore, the value of the exponent showed a variation with β . At $\beta = 1.0075$, $\nu \approx 0.32$



10
 11
 12

Fig. 5: The phase diagram of the $U(1)$ gauge theory in the two coupling plane. The order of the transition along the line DXZ needs to be resolved.

and this value changes to $\nu \approx 0.43$ (or even the classical value 0.5) at $\beta = 1.01$. One explanation is that the *TCP* lies above the Wilson axis and in simulations along the Wilson axis one measures first the tricritical exponent and then the critical one after going through the cross-over. The same conclusion is also reached in two $b = 2$ MCRG studies [42] [43] which extended the calculation to non-zero γ . Thus the only discrepancy between the MCRG studies and finite size scaling analysis is the precise location of the *TCP*.

The present status of the nature of the transition is confused. In all MCRG calculations in which the exponents are derived from the T matrix, one finds evidence for a second order transition on and below the Wilson axis. However, recently Decker *et al.* [44] have used the 2-lattice method (see eqn 4.3 in section 4) to calculate the leading exponent for a number of values of γ along the transition line and find the transition to be first order. We need to resolve this discrepancy if for no other reason but to understand the methods.

Our goal is to know whether there exists a non-trivial fixed point for the $SU(2) \times U(1)_\gamma$ model at which a continuum field theory can be defined. As the previous discussion shows, understanding even a simple limit model has been hard. To settle the important physics question requires considerable more work.

4: β -FUNCTION AND SCALING FOR $SU(3)$ LATTICE GAUGE THEORY

The non-perturbative β -function tells us how the lattice spacing goes to zero as $g_{bare} \rightarrow 0$. Since on the lattice all dimensionful quantities, like masses, are measured in units of the lattice spacing a , we need to know how a scales in order to take the continuum limit. One option is to use the 2-loop perturbative result provided it is demonstrated that this is valid at values of g_{bare} where the calculations are done. The other is to measure the non-perturbative β -function. Since the value of g_{bare} at which asymptotic scaling sets in is not *a priori* known, the

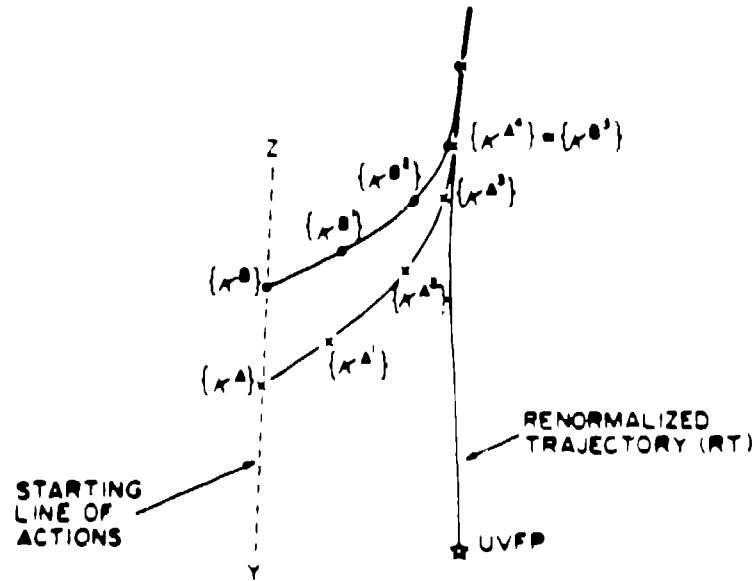


Fig. 6: The evolution of actions under a *RGT*. Due to long-distance matching, the correlation length on the two starting actions $\{K^A\}$ and $\{K^B\}$ differs by the scale factor b of the *RGT*.

calculation of the non-perturbative β -function is necessary.

There are two methods for calculating the non-perturbative β -function directly.

4.1) *MCRG* using Wilson's 2 lattice method [1][3]: There are 2 groups who have used this method for $SU(3)$; one with $b = \sqrt{3}$ *RGT* [45] and the second [28] with $b = 2$ proposed by Swendsen [24]. The outline of the method is: First a system of size $L = (b^n)^d$ is simulated with couplings K_α^A and the expectation values of Wilson loops are calculated on the original lattice and the n block lattices. A second system of size $S = (b^{n-1})^d$ is then simulated with couplings K_α^B chosen judiciously. Again the expectation values are calculated on the n lattices. The expectation values from the two simulations are then compared on the same size lattices, i.e. the ones from the

larger starting lattice L blocked one more time than those from the smaller lattice. The couplings K_α^B are adjusted (which requires a new simulation) until there is matching at the last, n^{th} , level. In practice it is sufficient to do two simulations S_1 and S_2 which bracket L and then use interpolation. The test for convergence of the two theories L^m and S^{m-1} is that the expectation values should match simultaneously at the last few levels. The ideal situation is shown in the coupling constant space in Fig. 6. At matching, the correlation length on L (starting couplings K_α^A) is larger than on S (K_α^B) by the scale factor b . If the starting trajectory is taken to be the Wilson axis (or any 1 parameter line specified by K) then the value of the β -function, $\Delta\beta$, for a scale change b is $(K^A - K^B)$. Note that finite size effects are minimized since the comparison is on approximately the same physical size lattices when matching occurs.

There is a one to one correspondence between the value of the couplings and the expectation values of Wilson loops. Under the assumption that the fixed point action is local (at any scale a few short range couplings are sufficient to characterize the action) matching the expectation values of a few small Wilson loops is sufficient to guarantee that the two actions are equal. Finite size effects in expectation values are irrelevant on blocked lattices that match because then the two theories are approximately identical and under further blocking continue to converge to a common trajectory. Thus it is sufficient to require that matching first take place on lattices which are large enough to accommodate the important couplings. Thereafter, the check can be on a 1^4 lattice too! It is the range of the couplings that controls finite size effects in *MCRG* and not the correlation length and this range falls off exponentially even on the critical surface. This is why *MCRG* has good control over finite size effects and is a powerful method.

For the simple plaquette $SU(3)$ action with $K_F \equiv \frac{6}{g^2}$, asymptotic scaling is defined by the 2-loop perturbative β -function,

$$\frac{\partial(g^{-2})}{\partial(\ln a)} = -\frac{11}{8\pi^2} - \frac{51}{64\pi^4}g^2 + \dots \quad (4.1)$$

The quantity calculated using *MCRG* is,

$$\Delta\beta = -\frac{\partial(6g^{-2})}{\partial(\ln a)} \cdot \ln b \quad , \quad (4.2)$$

i.e., the discrete β -function at K_F evaluated for a scale change b .

This 2-lattice method also gives the thermal exponent ν for transitions governed by a fixed point k^* . Let the RT be parameterized by K , then under a RGT

$$(K^2 - K^*) = b^{\frac{1}{\nu}} (K^1 - K^*) \quad (4.3)$$

where the flow is from K^1 to K^2 . So, from a sequence of matching couplings one can determine ν and K^* .

The results for $\Delta\beta$ from the $b = \sqrt{3}$ calculation [45] are shown in Table 1, while those for $b = 2$ are shown [28] in Table 2. The global data is shown in figure 8. There is clear evidence of a dip at $\frac{6}{g^2} \sim 6.0$ which is caused by the end point of the phase transition line in the fundamental-adjoint coupling space. The conclusion of these calculations is that there is no asymptotic scaling below $6/g^2 = 6.1$. Second, even though the results for $6/g^2 > 6.75$ have large statistical errors, they consistently fall below the 2-loop value.

For the $\sqrt{3}$ transformation we have made a finite size test [46]. The matching is done for a starting $(9\sqrt{3})^4$ lattice at $6/g^2 = 6.75$ with 9^4 lattices. The results for $\Delta\beta$ are 0.42(2), 0.47(1), 0.42(1), 0.44(2) for matching on the $3\sqrt{3}$, 3, $\sqrt{3}$ and 1 block lattices respectively. These values are consistent with previous numbers and show that the observed oscillations are a function only of the number of times blocking has been done and not on the starting lattice size. Also, note that the result on the 4th and additional step falls roughly in between the previous two. This supports our claim that convergence is oscillatory and asymptotic. For this reason, when using 9^4 starting lattices, we quote the mean value from matching on the $(\sqrt{3})^4$ and the 1^4 lattices as our best estimate, and for error we give the spread. This is much larger than the statistical and systematic errors in matching a few small loops on a given level.

Starting $9^4 K_F$	Matching on 3^4	Matching on $(\sqrt{3})^4$	Matching on 1^4	2-loop $\Delta\beta$
6.0	.337(5)	.323(5)	.308(6)	.489
6.125	.387(5)	.376(5)	.351(6)	.488
6.25	.421(4)	.424(5)	.401(5)	.488
6.35	.431(4)	.452(5)	.445(9)	.487
6.45	.432(4)	.464(6)	.423(12)	.487
6.5	.435(4)	.464(6)	.449(15)	.487
6.75	.430(4)	.485(5)	.443(9)	.485
6.75*	.42(2)	.47(1)	.42(1)	.44(2)*
7.0	.42(2)	.49(1)	.42(2)	.484
7.25	.41(2)	.51(2)	.46(2)	.483
7.50	.38(3)	.49(2)	.42(2)	.482

Table 1: The values of $\Delta\beta$ for $b = \sqrt{3}$ RGT from matching at different levels of blocking [46]. The couplings are for the starting 9^4 lattice along the Wilson axis. The matching K_F on $(3\sqrt{3})^4$ were determined by linear interpolation and the errors are based on a 1σ fit. For $K_F \geq 6.75$, the systematic errors may be larger than the estimates. Also shown are the values of $\Delta\beta$ corresponding to asymptotic scaling. The results at 6.75* are using a $9\sqrt{3}$ starting lattice, so there is an extra level of blocking for which the result is shown in the last column.

The results using the $b = 2$ RGT proposed by Swendsen and embellished with an optimized kernel are shown in table 2. For comparison, the 2-loop result is $\Delta\beta \approx 0.61$. The matching lattices used in the calculation are $L = 16^4$ and $S = 8^4$.

Wilson's 2-lattice method can also be used to measure the $\Delta\beta$ for a theory with dynamical fermions. All the steps are the same once the configurations are generated with the full action. There are two important differences: 1) in this case the couplings are not expected to fall off as fast as for the pure gauge theory, so larger loops may be necessary to obtain reliable matching [31]. 2) there is a second parameter, the quark mass that has to be fixed to the same physical value on the 2 lattices. A naive solution would be to use perturbation theory which

K_F	$b = 2$ MCRG method	$b = 2$ 1-loop Ratio method
6.0	0.35(2)	0.36(3)
6.3	0.43(3)	0.45(3)
6.6	0.55(9)	
6.9	0.51(6)	
7.2	0.51(7)	

Table 2: The values of $\Delta\beta$ for a scale change of $b = 2$. The results are from Bowler *et al.* [24]. The 2-loop perturbative result is 0.61. The matching is done on starting lattices 16^4 versus 8^4 .

unfortunately does not work well at $g \leq 1$. The other possibility is to match a physical quantity like the π mass extrapolated to zero quark mass. This is beyond our present computational power

4.2) Loop ratio method [47] [28]:

This method is based on the fact that the ratios of Wilson loops that cancel the perimeter and corner terms like

$$R(i, j, k, l) = \frac{W(k, l)}{W(i, j)} \quad \text{where } i + j = k + l . \quad (4.4)$$

satisfy an approximate homogeneous renormalization group equation

$$R(2i, 2j, 2k, 2l, g_a, 2L) = R(i, j, k, l, g_b, L) . \quad (4.5)$$

Using Monte Carlo data for ratios calculated on 2 lattices of size $2L$ and L , with couplings g_a and g_b respectively, gives the the desired answer $\Delta\beta = (6/g_a^2 - 6/g_b^2)$ for $b = 2$. Caveats: Eq. (4.5) is correct only as $i, j, k, l \rightarrow \infty$, otherwise there are corrections due to lattice artifacts. The quality of numerical results for large i, j, k, l are limited by statistics. To confirm the reliability of the results, we should show that the value of $\Delta\beta$ converges to a constant as a function of loop size.

The contribution of lattice artifacts can be reduced in perturbation theory. To do this consider Eq. (4.5) for a linear combination

of loop ratios with coefficients α_i . To determine these α_i , use the expectation values of loops calculated in perturbation theory and require that $\Delta\beta = 0$ (tree-level), 0.579 (1-loop) ... Having determined α_i perturbatively, use the monte carlo data for Wilson loops to calculate the non-perturbative $\Delta\beta$. The limitation of this improvement approach is that if two (or more) ratios representing different scales (say $i = 1$ and 4) are used then the difference in statistical errors becomes a problem. Second, at weak coupling each ratio roughly satisfies Eq. (4.5) so there is a loss of sensitivity in determining α_i . At strong coupling, perturbation theory calculation of α_i breaks down. So, at best, there exists a window in g where reliable results can be obtained. Hasenfratz *et al.* [28] claim that this is true for $\frac{6}{g^2}$ in the range [6,6.3]. In this interval their results are in agreement with their $b = 2$ MCRG results as shown in Table 2. A high statistics calculation of large loops in SU(2) by Gutbrod [48] shows that stability with respect to loop size is reached rather slowly. Therefore one has to be cautious of apparent convergence.

4.3) Results and Discussion:

For $\frac{6}{g^2} > 6.4$, the two MCRG results are consistent and fall about 10% below the 2-loop value. This situation seems to persist up to 7.5. It is very important to determine whether even at $\frac{6}{g^2} > 7.0$ we are $\approx 10\%$ below the 2-loop behavior. If the observed behavior is correct, then we should stop thinking in terms of asymptotic scaling. We need to perform a consistency check that demonstrates that the results for $\Delta\beta$ have converged and that the MCRG method is not limited by finite size effects.

It is hard to compare directly the results in the region of the dip of the $b = \sqrt{3}$ study with the $b = 2$ ones because of the different scale factor of the RGT. One check is to take the $\sqrt{3}$ data and fit it to a smooth function with the correct asymptotic behavior. This function can then be used to determine the discrete change $\Delta\beta$ in the couplings for any other scale factor b . Petcher [49] has carried out the following analysis: he constrains the function by a fit to the $b = \sqrt{3}$ data with matching on the $\sqrt{3}$ lattice (note that our preferred values are the

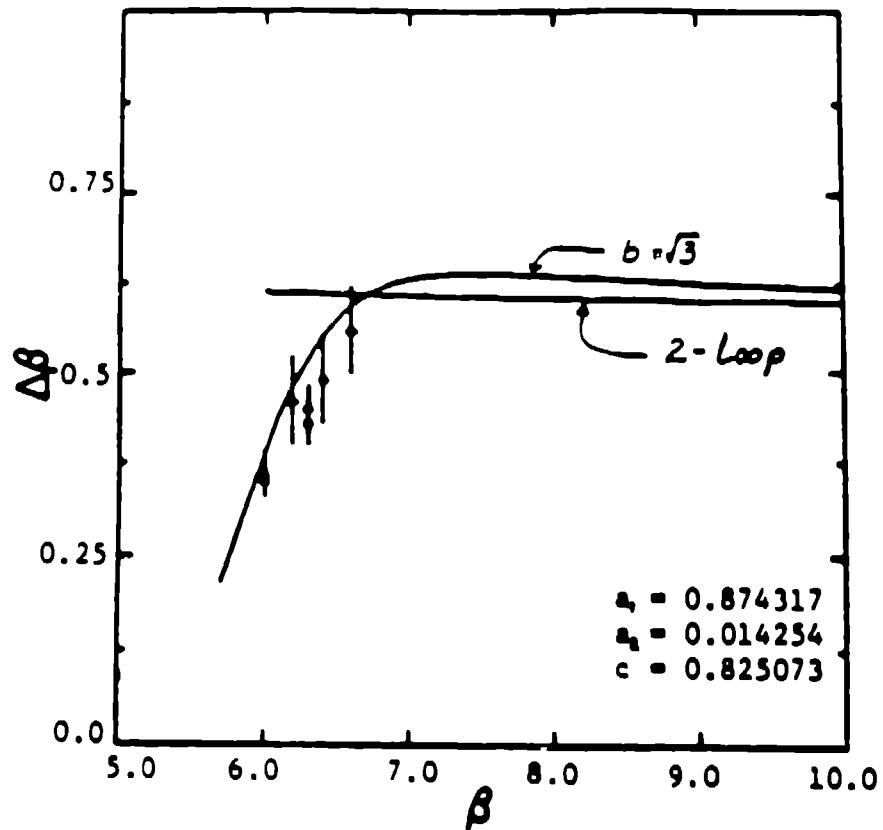


Fig. 7: Having used a fit to the $\sqrt{3}$ data to determine the parameters of a smooth β -function, the smooth $\Delta\beta$ for $b = 2$ is compared with the data. This analysis of D. Petcher is with old data. New results will be presented elsewhere [45].

mean of the matching value on the $\sqrt{3}$ and 1 lattices). As shown in Fig. 7 the smooth function he finds from the $\sqrt{3}$ data, rescaled to $b = 2$ compares well with the $b = 2$ MCRG data. Another test, which addresses the problem of finite lattice size effects, is for us to repeat the $9\sqrt{3}$ calculation in the region of the dip.

Next we would like to check if the $\Delta\beta$ calculated from MC determinations of different physical observables are identical and agree with the MCRG calculations. This comparison tests two things; 1) whether there exists scaling (constant mass ratios) before (larger g) asymptotic scaling and 2) whether the MC measurements are reliable. The lattice value of a mass ma calculated at two values of the coupling, $\frac{g}{g_1}$ and $\frac{g}{g_2}$, gives the $\Delta\beta$ for a scale change $\frac{a_1}{a_2}$. Unfortunately the values of couplings are not selected to give the $\Delta\beta$ for a given constant scale change. This again introduces the problem of rescaling data. In Fig. 8 we only use pairs of data points with a scale factor close to $\sqrt{3}$. On close scrutiny of the data between $\frac{g}{g_1} = 5.9$ and 6.3 one sees two curves, the $b = \sqrt{3}$ MCRG data agrees with σ while $b = 2$ MCRG data is consistent with the T_c data. If this discrepancy is not due to finite size effects or our inability to measure long distance observables, then it implies that even scaling is violated until $\frac{g}{g_1} \approx 6.2$. We need more reliable data to settle this point. At $\frac{g}{g_1} = 6.0$, the 0^{++} glueball mass [50] string tension σ [51] and the deconfinement temperature T_c [52] [53] represent scales of 2, 5 and 8 lattice units respectively. Thus identical $\Delta\beta$ would be a reasonable test of scaling even though there is the problem of rescaling data. Unfortunately, there is no point at the moment from glueball data due to large uncontrolled finite size effects as discussed in my lecture on glueballs.

The onset of asymptotic scaling has also been checked by plotting $\frac{ma}{\Lambda_a}$ where m is the deconfinement temperature T_c and Λ is the 2-loop perturbative scale. The two groups doing this calculation [52][53] use a different criteria to fix the transition coupling. Their results for $N_f = 10, 12, 14$ coincide when the same criterion is used by both and give an accurate measurement of T_c . However, the results show a very broad transition region so more careful finite size studies are needed to fix the

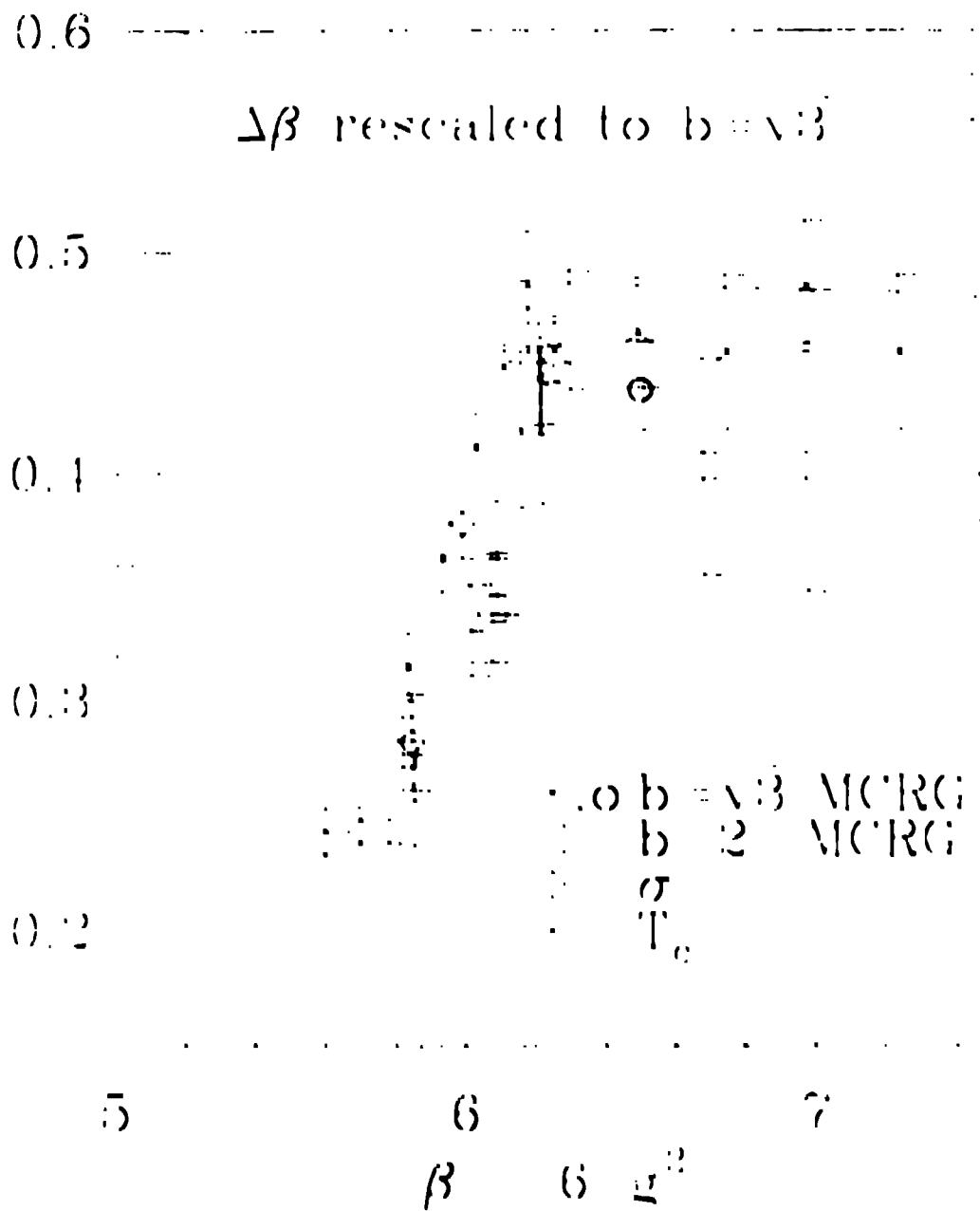


Fig. 8: Data for $\Delta\beta$ after rescaling to $b = \sqrt{3}$. The straight line is the two loop asymptotic value (mean ≈ 0.485).

infinite volume transition point. In figures 9a and 9b, I show the data for T_c/Λ with Λ defined both with the the 1-loop and 2-loop formula. In both cases this ratio is roughly constant for $N_\tau = 10, 12, 14$ and different from the value at $N_\tau \leq 8$. A closer inspection shows a small consistent decrease even at $N_\tau = 14$. The range of g between $N_\tau = 10$ and 14 is too small to deduce to better than 10% whether the curves have reached their asymptotic behavior. Even so, we cannot distinguish whether there is scaling for $\frac{6}{g^2} > 6.15$ according to 1-loop or the 2-loop behavior. This exposes one kind of $O(g^2)$ problems. Second, there are possible large, i.e. $(1 + O(g^2))$, regularization scheme dependent terms in the 2-loop Λ for $g \sim 1$. Because of these uncertainties, it is not possible to test asymptotic scaling to better than 10% by this method yet. Thus these calculations should be used as a guide and the goal should always be to attain constant mass-ratios.

To conclude this section: *MCRG* calculations have provided us with a definitive statement on the approach to the continuum limit. This is non-trivial. The present MC determination of σ and the glueball masses need improvement before a definite statement of scaling can be made. The largest lattice calculation of σ by de Forcrand [54] show deviations from asymptotic scaling i.e. $\sqrt{\sigma} = 92 (79) \Lambda_L$ at $\frac{6}{g^2} = 6.0$ (6.3). Since these calculations have already taxed the power of a Cray XMP-48, it leads us to the question whether improved actions can help. This is discussed next.

5: DETERMINATION OF THE IMPROVED ACTION.

The advantage of using an improved action in MC simulations is to reduce the effect of operators that lead to scaling violations. In QCD this means that corrections to mass-ratios determined from small lattices can be reduced. Second, we want to avoid regions near singularities where universality (continuum mass-ratios) is violated. A known example is the end point of the phase structure in the fundamental-adjoint plane.

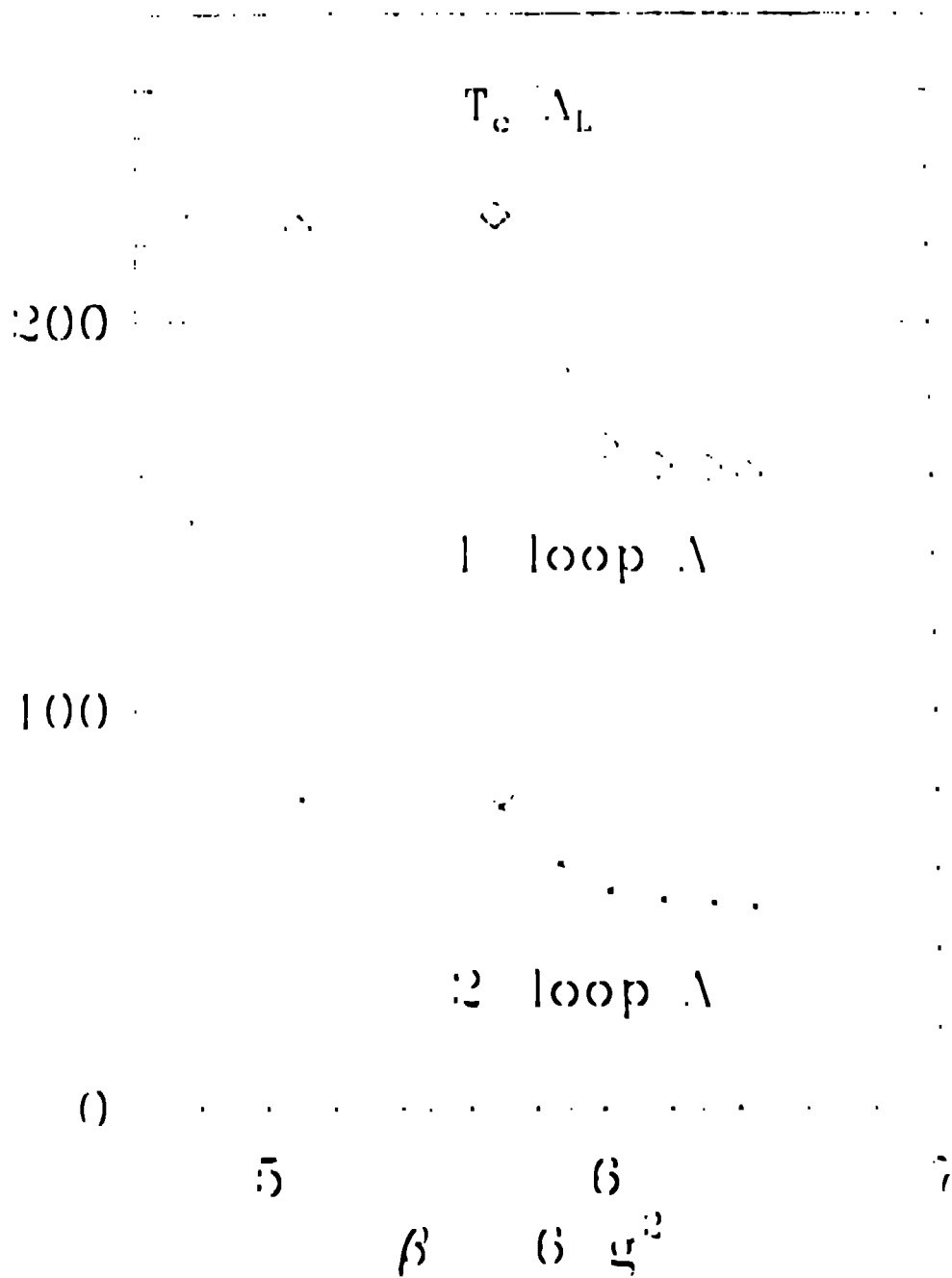


Fig. 9a: A plot of T_c/Λ to check for asymptotic scaling. The data is from Gottlieb et al. [51] who use the "3/4 deconfined" criterion for determining g_r .

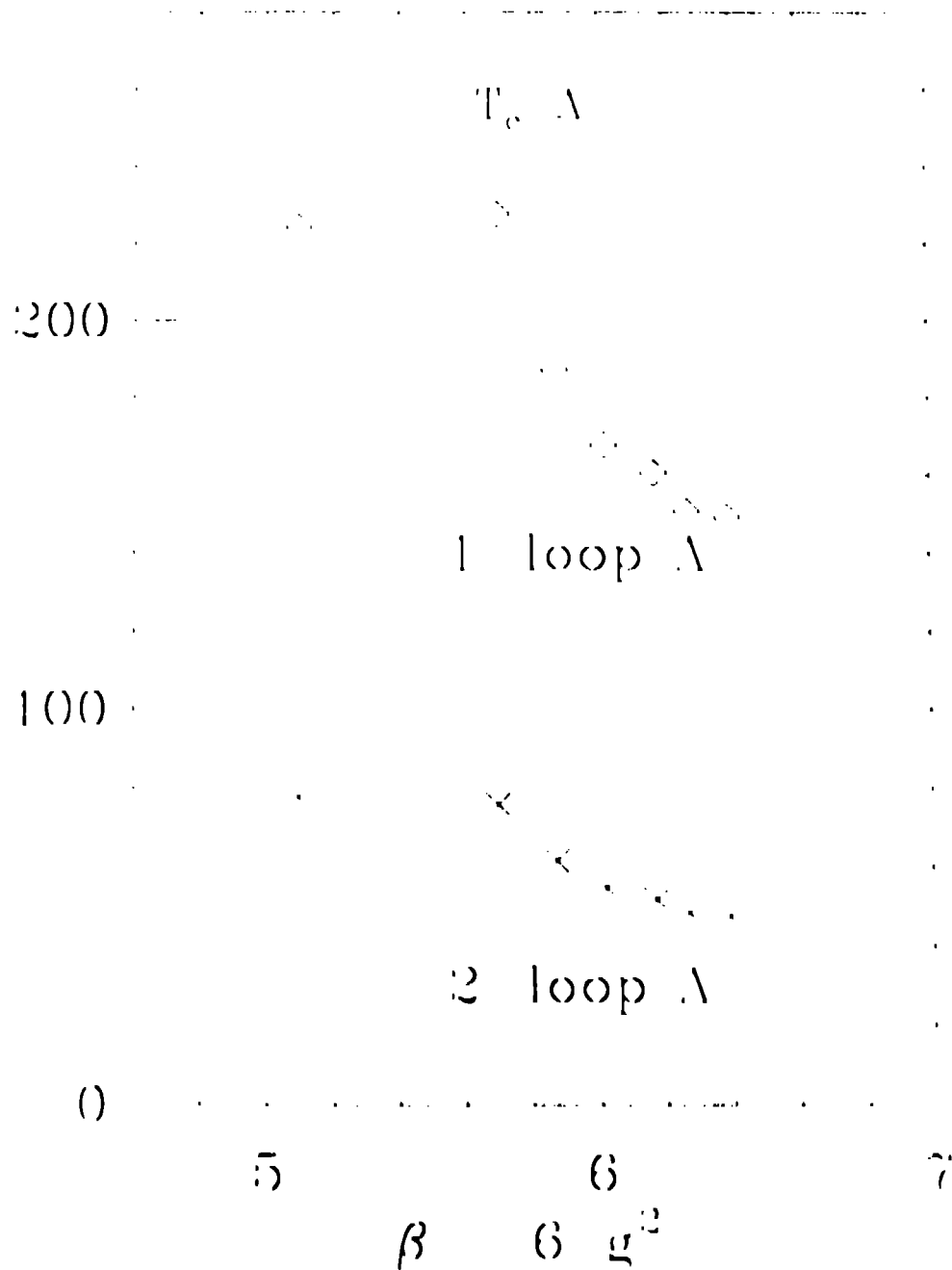


Fig. 9b: A plot of T_c/Λ to check for asymptotic scaling. The data is from Christ et al. [52] who use the "1/2 deconfined" criterion for determining g_c .

There are at least 11 methods in existence to calculate the renormalized couplings. All, except for those using perturbation theory (and therefore only valid near $g = 0$ where scheme dependence is negligible), are based on *MCRG*. In fact, since the fixed point and the Renormalized trajectory is a function of the *RGT*, an improved action is content-free unless the *RGT* is specified. I shall briefly describe the methods, state their advantages and disadvantages and mention results obtained with them. The generic problem of systematic errors in the estimate of the couplings due to a truncation in the number of couplings kept in the analysis will be referred to as "truncation errors". This is a serious drawback because the errors can be very large and there is no way of estimating them without a second long simulation. In order to consider this truncated ansatz to be the best "fit", a criterion to judge the improvement has to be established [31]. This is discussed after a brief description of the methods. To fix the notation, the pure gauge $SU(2)$ action is written as

$$S = K_F \sum \text{Tr} U_p + K_{6p} \sum \text{Tr} U_{6p} + K_A \sum \left\{ \frac{4}{3} (\text{Tr} U_p)^2 - \frac{1}{3} \right\} + K_{\frac{3}{2}} \sum \{ 2(\text{Tr} U_p)^3 - \text{Tr} U_p \} \quad (5.1)$$

while the $SU(3)$ action is

$$S = \text{Re} \left[K_F \sum \text{Tr} U_p + K_{6p} \sum \text{Tr} U_{6p} + K_6 \sum \left\{ \frac{3}{2} (\text{Tr} U_p)^2 - \frac{1}{2} \text{Tr} U_p \right\} + K_A \sum \left\{ \frac{9}{8} |\text{Tr} U_p|^2 - \frac{1}{8} \right\} \right] \quad (5.2)$$

Here the higher representations have been constructed from U_p , all the traces are normalized to unity and the sums are over all sites and positive orientations of the loops.

5.1) Symanzik Program [55] : This is a perturbation theory method to remove all $O(a^2)$ corrections in physical observables. At the tree level, at 1-loop [56] and in the leading log [57] analysis, the $O(a^2)$ corrections are removed by including the 6-link planar loop with strength

$$\frac{K_{6p}}{K_F} = -0.05 \quad (5.3)$$

There have been some $SU(3)$ calculations [58] done with this action, but they are inconclusive and no statement for an improvement in mass-ratios can be made as of now.

5.2) Block Spin Renormalization Group (perturbation theory): The first work in this direction is by Wilson [1] who wrote down the ansatz (for details see [31])

$$\frac{K_{6p}}{K_F} = -0.0576 \quad , \quad \frac{K_{6t}}{K_F} = -0.0388 \quad , \quad (5.4)$$

where K_{6t} is the twisted 6-link coupling. No calculation of physical observables has been done with this action. The group of Iwasaki *et al.* [59] have made a large independent effort in this direction of improvement. They find that near $g = 0$ the action after 3 *RGT* can be approximated by including the 6-link planar loop with strength

$$\frac{K_{6p}}{K_F} = -\frac{0.331}{3.648} \quad . \quad (5.5)$$

They show that for both the Wilson ansatz, Eq. (5.4), and for this action instantons are stable on the lattice. Since this is not true of the simple plaquette action, they regard it as another criterion for improvement. They have recently calculated the string tension and the hadron masses in the quenched approximation using the improved gauge action of Eq. (5.5) and the standard Wilson action for the quark propagator on a $12^3 \times 24$ lattice at an effective $\frac{6}{g^2} \sim 5.9$. Their results for mass ratios are very good. We need to ascertain if these impressive results are really due to the improved action.

5.3) Migdal-Kadanoff Recursion Technique: This calculation [60] is limited to the plaquette in the fundamental and higher representations. The integration over links is done by expanding the action in terms of the characters and then using the recursion formula. In the improved action, the effect of the singularity in the fundamental-adjoint plane is reduced but the leading irrelevant coupling K_{6p} is not included. For $SU(2)$ [60], the convergence in the character expansion

was good, the recursion was stable on keeping 20 characters. The improved action is dominated by the spin 1 and 3/2 representations, and the K-M improved trajectory was approximated by

$$\frac{K_A}{K_F} = -0.24 \quad . \quad (5.6)$$

It was later shown by Bitar *et al.* [61] that the heat Kernal action works very well in the recursion scheme and in fact is the solution in the perturbative limit. For a SU(2) calculation of the β -function along the K-M improved trajectory $K_A = -0.24K_F$, and for an analysis of the improved action see Ref. [23].

5.3b) Phenomenological (Lines Of Constant String Tension): The continuum limit is taken along directions perpendicular to the lines of constant string tension in the negative fundamental-adjoint plane. Rebbi *et al.* [62] have measured the $q\bar{q}$ potential, while Samuel [63] has promoted a calculation with scalar quarks. The effective coupling for comparison on the Wilson axis is defined by using the large N resummation technique [64] [65]. Since no direct comparison has been made it is hard to state if better mass ratios are obtained.

5.4) Swendsen's method [66] using the Callen representation: The block expectations values of Wilson loops are calculated in two ways. First as simple averages over block configurations, and second using the Callen representation [67] with a guess for the block couplings. From these two estimates, the block couplings are determined iteratively. The method is fast and easy to implement. It does have undetermined truncation errors. Lang [68] has used this method to show that the quartic coupling $\lambda\phi^4$ in the self-interacting scalar field theory renormalizes to zero. Recently Lang [42] and Burkitt [43] have used it to map the flow of the action under the $b = 2 RGT$ (section 2.2) for the U(1) model. From a difference in the flows they can estimate the transition point on the Wilson axis. It would be instructive to extend the U(1) analysis to $\pm\gamma$ coupling values along the phase transition line and check if there exists a *TCP*.

5.5) Callaway-Petronzio-Wilson method [69] [70] of fixed block spins: This method is useful for discrete spin systems like the Ising model and models in the same universality class. A MCRG calculation is modified by fixing all the block spins except one such that only a controllable few block interactions are non-zero. The system is simulated with the RGT used as an additional weight in the Metropolis algorithm. The ratio of probability of this unfixed spin being up to it being down is equal to a determined function of a certain number (depending on how many block interactions are non-zero) of block couplings. By using different configurations of fixed block spins a system of linear equations is set up from which the block couplings are determined. The drawback of this method, even for the Ising model, is that it is hard to set up the block spins so that only a few (≈ 10) block interactions are nonzero. Wilson showed that this can be done if one uses the lattice gas representation i.e. 0 or 1 for spin values. The couplings in the ± 1 representation are then given by an expansion in the lattice gas couplings. The second improvement due to Wilson is that instead of a MC determination of the ratio of probabilities, the exact result can be obtained in the transfer matrix formalism. In the $d = 2$ Ising model, the convergence of the ± 1 couplings in terms of the lattice gas couplings is slow [70]. About a 1000 lattice gas couplings were necessary for an accuracy of $\approx 10^{-4}$. However, the calculation is non-statistical and very fast.

5.6) Character Expansion method of Bitar [71] : I will describe this method with a restriction to simple plaquette actions. The character expansion for the action is $\sum_p \sum_r K_r \chi_r(U_p)$ where χ_r is the character in the r^{th} representation and K_r is the corresponding coupling. Similarly the Boltzmann factor F_p for each plaquette p can be expanded in a character expansion $F_p = \sum_r d_r f_r \chi_r(U_p)$ where d_r is the dimension and f_r the coefficient for r^{th} representation. The couplings K_r are given by

$$K_r = \int d(U_p) \ln F_p(U_p) \chi_r(U_p). \quad (5.7)$$

The crucial step is that the ratio $d_r f_r / f_1$ can be calculated as a ratio of

expectation values over block configurations. From this the Boltzmann factor F_p and consequently K_r can be determined. The method is sensitive to the convergence of the character expansion i.e. the number of terms in r needed to determine F_p accurately. After this there are no truncation errors in determining K_r . The method grows in complexity if larger loops are to be included in the analysis. The first results [71] for the simple plaquette action in $SU(2)$ are encouraging.

5.7) The Schwinger-Dyson Equation method [72] [73] : In this method the lattice Schwinger-Dyson equations (equations of motion for expectation values of n -point functions) are used to write down a set of inhomogeneous linear equations for the couplings. The coefficients and the inhomogeneous term are given in terms of expectation values of n -point functions. In deriving these equations the action has to be truncated to the subspace of couplings to be determined. Thus the method has truncation errors. Preliminary results for the abelian-higgs models and the $O(3)$ non-linear σ -model in $d = 2$ are encouraging.

5.8) 2-Lattice MCRG method [74] [7]: The calculation steps are the same as Wilson's 2-Lattice method to determine the β -function. The method consists of expanding the block expectation values (with unknown couplings) about those from a simulation with known couplings. Keeping just the linear term in the expansion gives the difference between the two sets of couplings. The main advantage is that this comes free with the calculation of the β -function. The method has a statistical drawback that it requires two different simulations so there is no possibility of cancellation of statistical errors. Also, far from the RT , only the first renormalized couplings can be determined accurately. There exist extensive calculations for both the $SU(2)$ and the $SU(3)$ models using the $\sqrt{3}$ RGT. The estimate for the improved action in a 4-parameter space for $SU(2)$ is [23]

$$\frac{K_{6p}}{K_F} = -0.06 \quad , \quad \frac{K_A}{K_F} = -0.19 \quad , \quad \frac{K_{\frac{1}{2}}}{K_F} = 0.03 \quad (5.8)$$

and for SU(3) is [45]

$$\frac{K_{6p}}{K_F} = -0.04 \quad , \quad \frac{K_8}{K_F} = -0.12 \quad , \quad \frac{K_6}{K_F} = -0.12 \quad . \quad (5.9)$$

The truncation errors are known to be large and the reliability of the results is being tested by using the estimated improved action in the update and repeating the calculation of the β -function and the improved action [31]. The results for the ratio m_{0++}/σ with this action are given in my lecture on glueballs. At present it is hard to evaluate the improvement because we do not have control over finite size effects in glueball masses. A detailed comparison of the renormalized action obtained with this method and with the microcanonical method is made in table 3.

5.9) Microcanonical (Creutz's Demon) Method [75] : This method is very efficient if from a previous *MCRG* calculation expectation values of n block Wilson loops at each of the l block levels are determined. To determine the corresponding couplings at the l^{th} level, a microcanonical simulation is then done (on a same size lattice as on which the block expectation values were calculated) with the corresponding n energies fixed and with one demon per interaction. The desired n couplings are then determined from the distribution of demon energies. P. Stolorz [76] used the block expectations values for SU(2) obtained after two applications of the $\sqrt{3}$ *RGT* for a starting 18^4 lattice. From these he obtained the second, ($l = 2$), renormalized action in a truncated coupling constant space (four couplings of Eq(5.1)). The results are shown in Table 3 and compared with the first renormalized couplings obtained from the 2-Lattice *MCRG* method described above. The results show a rapid convergence of the action to the *RT* consistent with the estimates given in Eqs (5.8). This is evidence that the $\sqrt{3}$ *RGT* transformation has good convergence properties after two steps. In this calculation it was easy to thermalize the four energies. The simulation is faster than the 2-Lattice method and has better statistical properties. Also the block couplings at all levels

Initial Action K_F	K_F	K_A/K_F	$K_{3/2}/K_F$	K_{6p}/K_F
2.50 (W)	2.57(1)	-0.195(01)	0.043(01)	-0.004(3)
	2.06(1)	-0.186(06)	0.038(03)	-0.01(2)
2.75 (W)	3.16(1)	-0.199(03)	0.042(02)	-0.02(2)
	2.82(4)	-0.214(11)	0.044(06)	-0.02(4)
3.00 (W)	3.69(1)	-0.190(04)	0.040(02)	-0.031(7)
	3.47(5)	-0.211(12)	0.039(04)	-0.03(3)
3.25 (W)	4.12(2)	-0.160(05)	0.025(03)	-0.037(4)
	4.00(4)	-0.182(10)	0.032(06)	-0.04(3)
3.50 (W)	4.71(2)	-0.168(05)	0.028(03)	-0.040(4)
	4.40(7)	-0.150(15)	0.007(06)	-0.05(2)
4.35 (MK)	3.42(1)	-0.211(02)	0.044(01)	-0.03(1)
	3.10(3)	-0.235(12)	0.055(04)	-0.03(3)

Table 3. Projection of the renormalized SU(2) action onto the $[K_F, K_A, K_{3/2}, K_{6p}]$ space for several starting actions. For each starting action, the first row shows the couplings after one $b = \sqrt{3} RGT$ with starting lattices of size 9^4 calculated by the 2-lattice method [23]. The second row shows the couplings after two RGT calculated using the microcanonical demon method [76]. The last set, $K_F = 4.35$, is with the action given by the MK trajectory Eq. (5.6).

can be determined once the block expectation values are known. The truncation errors are the same as in the 2-Lattice method.

5.10) Block Diagonalization method of Mütter and Schilling [26]: This is at present the only method that attempts to improve both the gauge and the fermion action. The main idea is that quark propagators are calculated on blocked gauge configurations using a blocked fermion action. The blocked fermion action is calculated as follows: Let the starting action be the Wilson action

$$\bar{\Psi} M \Psi , \quad (5.10)$$

where M is the interaction matrix. The lattice is now divided into

blocks which for the $\sqrt{3}$ RGT contain 9 sites each. The site action is then cast into a block action

$$\Xi \Gamma \Xi \quad (5.11)$$

where Ξ is a 9 component Dirac fermion field and Γ is the interaction matrix set up to reproduce Eq. (5.10). The part of Γ that corresponds to the mass term, Γ_m , is diagonalized to provide the non-interacting fermion basis vectors. For the $\sqrt{3}$ RGT, the 9 eigenvalues of Γ_m are 0 and 8 degenerate ones with value $9/a$. Only the light mode is kept on the blocked lattice. The interaction between the light and heavy modes is calculated in perturbation theory and these terms are added to the Wilson action to give the improved fermion coupling matrix for the light mode. This is like the standard construction of effective field theories. This fermion diagonalization is approximate. Thus lattice masses will not a priori change by the scale factor b between the original and the blocked lattice. It is therefore necessary to first check how good the transformation is in preserving mass-ratios of the unblocked system. The results on a twice blocked set of configurations using $b = 2$ are encouraging [77]. Results of a test of preservation of mass ratios under blocking should be available soon for both the $b = 2$ and $b = \sqrt{3}$ RGT. At this point it is worth mentioning that the following advantages were observed in the diagonalization process for the $\sqrt{3}$ RGT in comparison to $b = 2$.

- (a) The separation between the light modes $m \sim 0$ and the heavy modes is better i.e. $9/a$ versus $2/a$, so the perturbative corrections are more reliable.
- (b) Rotational invariance is not broken as is in the $b = 2$ transformation.
- (c) No closed gauge loops which manifest themselves as additional contact terms in the fermion operators arise. This implies that the value of the Wilson parameter r does not get modified and κ_c remains the same on the blocked lattice for Wilson fermions if the exact fermion coupling matrix is derived.
- (d) The blocking of gauge links is the same as defined in section 2.3.

Discussion: There are some features of the improved action that seem common to the various analysis done. The details will certainly depend on the specific *RGT*.

- (a) The leading irrelevant operator is dominated by K_{6p} , the 6-link planar Wilson loop. Thus a *RGT* that kills it is an improvement.
- (b) From the $\sqrt{3}$ *RGT* analysis, one gets an estimate of $K_A/K_F \sim K_6/K_F \sim -0.12$. Thus near $\frac{6}{g^2} = 6$, the phase structure in the $\{K_F, K_A\}$ plane is avoided. This is necessary because in the vicinity of the end point of the phase structure universality is violated.
- (c) The *RT* for the $b = \sqrt{3}$ *RGT* shows significant deviations from linearity in the region accessible to Monte Carlo. The ratios given in Eqs. (5.8) and (5.9) are an estimate of the asymptotic behavior.
- (d) The *RT* out of the fixed point is local i.e. dominated by small loops. The Wilson axis is tangent to the strong coupling *RT* at the trivial fixed point at $K_\alpha = 0$. The change from the weak coupling *RT* to flow close to the Wilson axis takes place in the region where current Monte Carlo calculations have been done i.e. between 5.7 and 6.5. This feature needs to be investigated since current mass-ratios show a behavior that is in between strong coupling and the expected continuum one.

It is still necessary to evaluate whether constant mass-ratios in the quenched approximation are obtained significantly earlier with an improved action. The results have to justify the factor of ~ 5 by which the gauge update slows down when the above four couplings are used. The key lies in improving the fermion sector. For dynamical quarks, the gauge update is a small fraction of the update time. So, an investment in improving the gauge action is justified.

6: IMPROVED MONTE CARLO RENORMALIZATION GROUP METHOD [78]

I shall describe the Gupta-Cordery MCRG method (*IMCRG*) in

some detail. In this method too, the Renormalized Hamiltonian and the Linearized Transformation Matrix, T , are determined in some truncated space of interactions. However, in this sub-space they have no additional truncation errors i.e. the determined quantities have their infinite component values. Second, there are no long time correlations even on the critical surface and the block n -point correlation functions like $\langle S_\alpha^1 S_\beta^1 \rangle - \langle S_\alpha^1 \rangle \langle S_\beta^1 \rangle$ are calculable numbers. Because of these properties, the method allows a careful error analysis in the determination of the exponents from a truncated T .

In the *IMCRG* method the configurations $\{s\}$ are generated with the weight

$$P(s^1, s) e^{-H(s) + H^\theta(s^1)} \quad (6.1)$$

where H^θ is a guess for H^1 . Note that both the site and block spins are used in the update of the site spins. In analogue to Eq. (1.2), the distribution of the block spins is given by

$$e^{-H^1(s^1) + H^\theta(s^1)} = \sum P(s^1, s) e^{-H(s) + H^\theta(s^1)} \quad (6.2)$$

If $H^\theta = H^1$, then the block spins are completely uncorrelated and the calculation of the n -point functions on the block lattice is trivial.

$$\langle S_\alpha^1 \rangle = 0 \quad \langle S_\alpha^1 S_\beta^1 \rangle = n_\alpha \delta_{\alpha\beta} \quad \dots \quad (6.3)$$

where for the Ising model (and most other models) the integer n_α is simply a product of the number of sites times the multiplicity of the interaction type S_α . When $H^\theta \neq H^1$, then to first order

$$\langle S_\alpha^1 \rangle = \langle S_\alpha^1 S_\beta^1 \rangle_{H^\theta = H^1} (K^1 - K^\theta)_\beta \quad (6.4)$$

Using Eqs. (6.3,6.4), the renormalized couplings $\{K_\alpha^1\}$ are determined with no truncation errors

$$K_\alpha^1 = K_\alpha^\theta + \frac{\langle S_\alpha^1 \rangle}{n_\alpha} \quad (6.5)$$

This procedure can be iterated -- use H^{n-1} as the spin H in Eq. (6.1) to find H^n . If the irrelevant eigenvalues are small, then after two

or three repetitions of the *RGT*, the sequence H^n converges to the fixed point Hamiltonian H^* which is assumed to be short ranged. For the $d = 2$ Ising model, the method has been shown to be extremely stable [79]. The linearity approximation, Eq. (6.4), is under control. An iteration process using a few thousand sweeps suffices to determine successively improved H^g up to an accuracy of $O(10^{-4})$. Beyond that the errors fall as \sqrt{N} and the number of interactions that have to be included grows rapidly.

The one remaining approximation is in the use of a truncated H^{n-1} for the spin Hamiltonian in the update to find H^n . This is solved formally in a straightforward manner: In Eq. (6.1) use H^g as the guess for H^n . The update now involves the original spins and all block spins up to the n^{th} level in the Boltzmann weight

$$P(s^n, s^{n-1}) \dots P(s^1, s) e^{-H(s) + H^g(s^n)} \quad (6.6)$$

The four Eqs. (6.2-6.5) are unchanged except that the *level* superscript is replaced by n , i.e. the n^{th} level block-block correlation matrix is diagonal and given by Eq. (6.3). With this modification, the H^n is calculated directly. The limitation on n is the size of the starting lattice. The other practical limitation is the complexity of the computer program. I have made the following comparison in the $d = 2$ Ising model [22]: H^2 was calculated using Eqn (6.2) and by iterating i.e. $H_2 \leftarrow H^1 \rightarrow H^2$ in which case all interactions of strength $> 5 \times 10^{-4}$ are retained in H^1 . The statistical accuracy in both cases is $O(10^{-5})$. I find that the iterated answer is good to only 10^{-4} . Thus the truncation errors do conspire and get magnified. The lesson learned from the simple case of $d = 2$ Ising model is that in order to get couplings correct to one part in 10^{-5} at $n = 2$, it is necessary to include all couplings of strength $\sim 10^{-5}$ in H^1 .

The calculation of the T matrix proceeds exactly as in the standard *MCRG* i.e. Eqs. (1.4) to (1.6). However, in the limit $H^g = H^1$, the block-block correlation matrix D is diagonal and given by Eq. (6.3). Thus it has no truncation errors, can be inverted with impunity and the final elements of T are free of all truncation errors. This is the key

feature of *IMCRG*. The only error comes from finding the eigenvalues from a truncated T matrix. These errors can be estimated and the results improved perturbatively as explained in section 6.1.

In addition to the advantages mentioned above, simulating with *IMCRG*, the system does not have critical slowing down. The correlation length ξ can always be made of $O(1)$, so finite size effects are dominated by the range of interactions, which by assumption of a short range H^* fall off exponentially. Thus, critical phenomenon can be studied on small lattices with no hidden sweep to sweep correlations that invalidate the statistical accuracy of the results. Using H^0 as the known nearest-neighbor critical point $K_{nn}^c = 0.4406868$, I find that the *IMCRG* results [79] for H^1 are independent (within the statistical accuracy $\approx 10^{-5}$) of finite size effects for lattice sizes 16, 32, 64 and 128. Again, only those couplings that fit into a 3×3 square were included.

A technical point. When $H^\theta = H^1$, the block spin configurations are such that all values of the field variable become equally likely. For Ising like systems this poses no problems because near criticality all discrete values are equally likely. For non-abelian gauge theories, the important configurations in the continuum limit are fluctuations about the identity. Thus *IMCRG* will be inefficient. This can be fixed by adding an integrable factor in addition to H^θ in eqn. (6.1) that restricts the block variable to near the identity. What this factor is has to be worked out depending on the model.

IMCRG is in practice very similar to *MCRG* though a little more complicated because it requires a simultaneous calculation of a many term $H(s)$ and H^θ at update. However, conceptually it is very different and powerful.

6.1: Truncation Errors In The *LTM*

Consider the matrix equation for T in block form

$$\begin{pmatrix} D_{11} & D_{12} \\ D_{21} & D_{22} \end{pmatrix} \begin{pmatrix} T_{11} & T_{12} \\ T_{21} & T_{22} \end{pmatrix} = \begin{pmatrix} U_{11} & U_{12} \\ U_{21} & U_{22} \end{pmatrix} \quad (6.7)$$

where D_{11} and U_{11} are the 2 derivative matrices calculated in some truncated space of operators that are considered dominant. The elements of the sub-matrix T_{11} will have no truncation errors provided we can calculate

$$T_{11} = D_{11}^{-1} \{U_{11} - D_{12}T_{21}\}. \quad (6.8)$$

In the *IMCRG* method the matrix D is diagonal and known, so D_{12} is 0. Thus elements of T_{11} determined from U_{11} have no truncation errors. The errors in the eigenvalues and eigenvectors arise solely from diagonalizing T_{11} rather than the full matrix T . Calculations in the $d = 2$ Ising model have shown that these errors are large (of order 10%), and the convergence is not systematic i.e. the result fluctuates about 2. This may be because all operators of a given range are not included. An open problem therefore is a robust criterion for classifying operators into sets such that including successive sets decreases the truncation error geometrically by a large factor.

The errors arising from using a sub-matrix T_{11} can be reduced significantly by diagonalizing

$$T_{11} + T_{11}^{-1}T_{12}T_{21} = D_{11}^{-1}U_{11} + \{-D_{11}^{-1}D_{12} + T_{11}^{-1}T_{12}\}T_{21} \quad (6.9)$$

as shown by Shankar, Gupta and Murthy [80]. The correction term $T_{11}^{-1}T_{12}T_{21}$ is the 2nd order perturbative result. It is valid for all eigenvalues that are large compared to those of T_{22} . The matrix $T_{12}T_{21}$ is approximately equal to $(T^2)_{11} - (T_{11})^2$ and can be calculated approximately in *IMCRG*. The errors which I have ignored are due to the *RG* flow, i.e. T^2 is evaluated at a different point than T . These errors depend on how close to H^* the calculation is done. For the $d = 2$ Ising model I find that the perturbative correction significantly ~~decreases~~ truncation errors in the relevant eigenvalues [22]. Second, when multilevel *IMCRG* is used, Eq. (6.6), the exponents have much smaller fluctuations at earlier levels and are close in value to those from *MCRG*. So *MCRG* results (obtained with with far less effort) are of the same quality as *IMCRG* with the perturbative improvement. Another thing we have learned from this study is that the difference

between the calculated eigenvalue at $n = 1$ ($1.97 \pm .01$) and the exact result, 2, does not seem to be due to truncation errors or statistics. The reason is that with the same subset of operators one gets the correct exponent after one blocking. Thus the deviation is most likely due to irrelevant operators causing corrections to scaling.

In standard *MCRG*, the calculations with $T = D_{11}^{-1}U_{11}$ have shown good convergence once few operators, $O(5 - 10)$, are included. The reason for this is an approximate cancellation between the two types of truncation errors. To show this use Eq. (6.7), ignore terms with T_{22} and approximate T_{11} by $D_{11}^{-1}U_{11}$. Then the correction term in eqn. (6.9) is

$$-D_{11}^{-1}D_{12} + T_{11}^{-1}T_{12} \sim -D_{11}^{-1}D_{12} + U_{11}^{-1}U_{12} .$$

In most calculations, the derivative matrices are roughly proportional, i.e. $U \sim \lambda_i D$ with corrections that fall off as the ratio of non-leading eigenvalues to the leading one λ_i . This statement can be checked by expanding operators in term of eigenoperators. Thus Swendsen⁷ by calculating just $D_{11}^{-1}U_{11}$ and ignoring all truncation problems was in effect canceling a large part of the truncation error (2nd term in Eq. (6.9)) against the error arising from diagonalizing a truncated matrix (perturbative correction, 3rd term in Eq. (6.9)). This explains the success of his method. Shankar [81] has found a correction term to further decrease the truncation effects in *MCRG*. Given the assumptions, the flow under a *RG* and the success of the procedure as it exists, an improvement may be hard to evaluate. However, the check needs to be made for the $d = 3$ Ising model.

To summarize, the best way to get accurate results is to use *IMCRG* to calculate the renormalized couplings and Swendsen's *MCRG* method to calculate the eigenvalues.

Let me also summarize some of the other results obtained from the study of the $d = 2$ Ising model and the open problems.

[1] In models examined so far we can arrange T to look like

$$\begin{pmatrix} A & B \\ \epsilon & D \end{pmatrix} \quad (6.10)$$

with A the minimal truncated $n \times n$ block matrix that should be calculated. The case $x = 0$ is simple; there are no truncation errors in either *MCRG* or *IMCRG* and diagonalizing A gives the n largest eigenvalues. Otherwise, the truncation error depends on the dot product of terms in ϵ and B . From a study of the $d = 2$ Ising model we know that the T matrix has elements that grow along rows and fall along columns [80]. An estimate of the rate of growth in the elements along the rows of the T matrix is given by the elements of the leading left eigenvector. For two spin interactions in the $d = 2$ Ising model, these grow like $x^{3/4}$. Therefore, a priori, the matrix T is badly behaved. Furthermore, the requirement of absolute convergence in the dot product of elements in ϵ and B only guarantees that this product is finite but it may be arbitrarily large i.e. $O(1)$. The reason one gets sensible results is because the elements along the columns are observed to fall off faster (presumably exponentially). So, for each model a careful study of the signs and magnitude of the elements in ϵ as a function of the *RGT* is necessary. This should also give a handle on the generation of long range interactions with bad *RGT*. So we need to develop a theory for how the elements along the columns fall-off.

- 2 The non-leading eigenvalues are not very accurately determined in either method. The matrix T starts developing complex eigenvalues after ≈ 8 operators are included.
- 3 The results for H^2 using *IMCRG* converged up to an accuracy of a few parts in 10^{-5} provided the couplings in H^2 were correct to $O(10^{-3})$. This initial accuracy can be achieved [79] with a few thousand sweeps on a 128^2 lattice.
- 4 The statistical errors in *IMCRG* can be evaluated very reliably [79]. Detailed binning analysis showed that each sweep is approximately independent and an accuracy of 10^{-5} is obtained in all couplings with $\sim 2 \cdot 10^6$ sweeps on a 64^2 lattice. This could be achieved with 3000 Vax 11.780 hours. In *MCRG*, we find that the errors in the leading eigenvalue show no critical slowing down. In

fact they are smaller than in *IMCRG*. Thus there is a remarkable cancellation of errors in the construction of T from U and D .

- [5] A reliable classification scheme for interactions into complete sets is needed so that we have control over truncation errors.
- [6] A quantitative understanding of the tuning of the *RGT* is lacking.

To conclude, I believe that *MCRG* and *IMCRG* provide a complete framework to analyze the critical behavior of spin and gauge models. With the increased availability of supercomputer time we shall have very accurate and reliable results.

7: RENORMALIZATION GROUP INSPIRED MULTIGRID UPDATE

A multigrid update algorithm is aimed at overcoming critical slowing down in lattice gauge theories and critical phenomenon. The method described here uses the critical 2-dimensional Ising model as a test case. Once it is shown to work, the next model to try is the $O(3)$ non-linear sigma model in 2-dimensions. This model has many features in common with non-abelian gauge theories for which we desperately need an efficient update algorithm.

For a multigrid cycle to work, there are three essential ingredients. I list them and a proposed solution.

- 1) Fine to coarse grid operator P : This operator should preserve the long distance, slowly varying part of the field distribution. The solution is a renormalization group block spin transformation. Let this be defined as

$$P(s, s') = e^{-\lambda(s' - \sum s)^2}$$

where $\sum s$ is the block average of spins in the block cell and the s' can be restricted to have unit norm like s . The strength λ is a free parameter and needs to be determined by numerical optimization. For most models, unlike a gaussian model, the couplings on the blocked lattice are not known *a priori*. The success of any multigrid

algorithm will depend on our ability to calculate a simple truncated action that preserves physics at many length scales simultaneously.

- [2] The Hamiltonian on the coarse lattice $H'(s')$: In principle the blocked Hamiltonian includes all possible couplings. However if the fixed point is local, then these couplings fall off exponentially (essential assumption of the renormalization group). The precise form of the H' depends on P . If we restrict ourselves to preserving only one correlation length (which we will choose to be the largest one), then we can work with a much simpler action, the nearest neighbor action with temperature as the single coupling. To find the sequence of H , we can use Wilson's 2-lattice method (which preserves a single correlation length) or use scaling. Let me ignore scaling violations and assume that the temperature is the relevant field. Then $(t^2 - t^c) = b^{\frac{1}{\nu}} (t^1 - t^c)$ gives the relation between the couplings on two successive lattices. The restriction, if we use perturbation theory, is that the coarsest lattice coupling has to lie in the weak coupling region where scaling holds. The ideal situation is to know the sequence of H along the renormalized trajectory. However, in this case the correct mass-ratios are given on the coarsest lattice and multigrid is not needed. One could improve the scaling behavior by using a truncated approximation to the RT. This will allow more than one correlation length to be held fixed. Such an approximate renormalized trajectory has been worked out for gauge theories (see section 5, especially eqns. 5.8 and 5.9), the $O(3)$ model by Shenker and Tobochnik [3] and in more detail by A. Hasenfratz and A. Margaritis [82], etc. Again, the couplings along this trajectory at two successive points differing by one block transformation can be calculated by Wilson's 2-lattice method for the β function.
- [3] The coarse to fine grid inverse operator R : This is the crucial step in the algorithm. Given a configuration on the coarse lattice, we would like to generate the spins on the next finer level which preserve the longest correlation length. The solution is to generate

spins on the fine grid with the probability weight

$$R(s', s) = e^{-\beta(s' - \sum s_i)^2} \cdot e^{H(s)}$$

where $H(s)$ the Hamiltonian (or action) on the fine lattice and calculated as described above. Said another way, given a distribution of spins $\{s'\}$, the new fine spins are generated according to R . Even if the initial $\{s\}$ are random, thermalization will be fast since R forces strong correlation with $\{s'\}$. To guarantee that the distribution of spins on the fine lattice are distributed according to $H(s)$, a certain number of standard updates should be done. Here I anticipate using fourier acceleration to improve convergence. For Ising like systems (few discrete states) a heat bath algorithm can be written for K^2 . For others one can use either heat-bath or Metropolis depending on the ease in implementation.

One method for generating independent configurations is as follows: Thermalize on the coarsest lattice L^n and then use R to generate configurations on L^{n-1} . Now, do a few sweeps to equilibrate the high frequencies on L^{n-1} since all correlation lengths are not preserved by the interpolation. Repeat this process recursively until the finest scale is reached. To generate the next decorrelated lattice, start again on the coarsest scale with an independent lattice. The method is useful if at each level n the number of smoothing sweeps necessary to produce the correct distribution do not grow as ξ_n^2 . This is because the auto-correlation length for standard update algorithm grows roughly as ξ^2

If H^n were chosen along the exact renormalized trajectory, then none of the above would be necessary. Calculation of the physics on the coarsest grid would give the continuum mass-ratios. What we are proposing is to use simple local actions at all levels and preserve only the largest correlation length. The final smoothing sweeps on the finest grid then give the correct distribution.

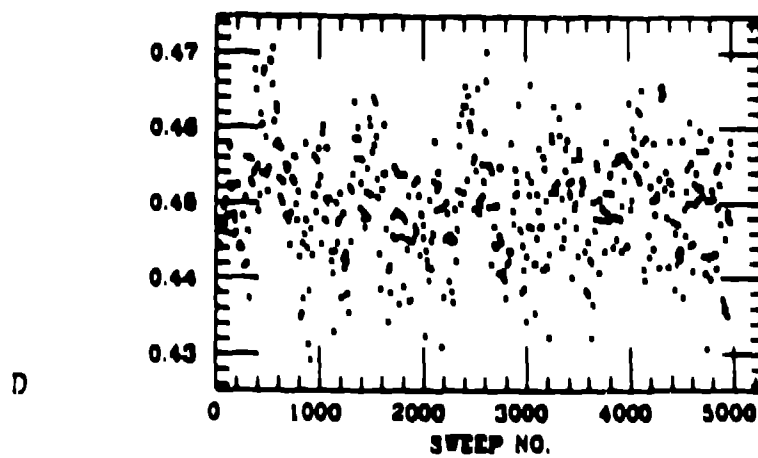
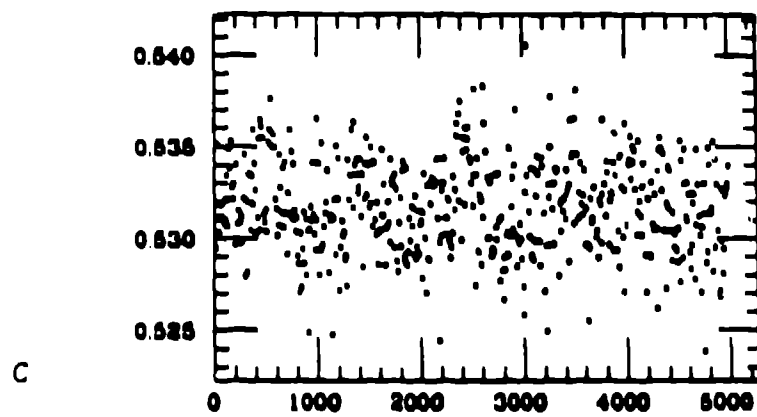
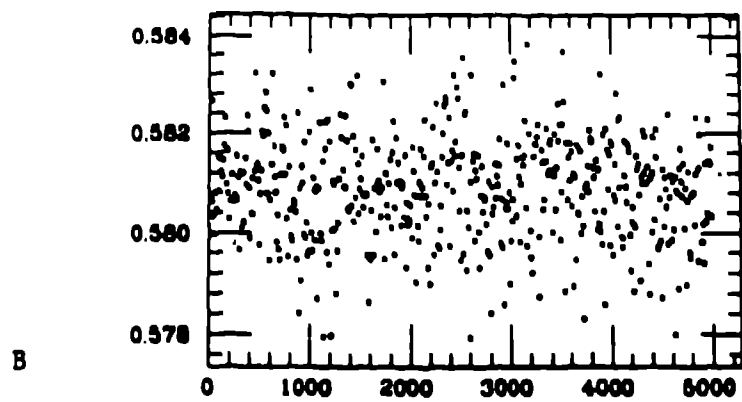
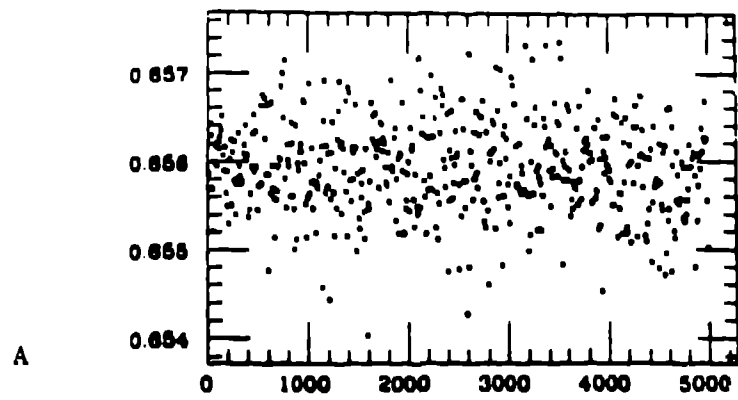
This method deviates from standard multgrid used, for example, in solving differential equations which have a unique solution. In that case it is the error vector, which has long range correlations, that is

processed on increasingly coarse grids and the corrections are boosted to correct the iterate at the next fine level. In update, we want to generate statistically independent configurations, so the method proceeds from coarse to fine grid alone and then starts all over again. We don't want to transfer long wavelength information from fine to coarse grid.

For the matrix inversion problem in Lattice gauge theories, the standard V cycle [20] can be used. However, one has to determine the Wilson (or Staggered) action on the block lattice derived for the particular block spin transformation used to project the gauge fields. Also, the coarse to fine grid interpolating operator has to be constructed carefully to preserve the long wavelength properties of the background gauge fields. A step in this direction is the "block diagonalization" scheme of Mütter and Schilling [26].

8: MEASURING AUTO-CORRELATIONS

The method we propose is to use block operators. The process of blocking explicitly gets rid of the high frequency components. After a sufficient number of blocking steps, the long correlations are discernable by eye in a Monte Carlo time history of simple observables - Wilson loops. In figure 10, we [83] show the plaquette as a function of the sweep number on a sequence of blocked lattices $9\sqrt{3} \rightarrow 9 \rightarrow 3\sqrt{3} \rightarrow 3 \rightarrow \sqrt{3} \rightarrow 1$ at $\beta = 6.75$ for our 20 hit Metropolis algorithm. Note, it is only on lattices 3^4 or smaller (6×6 renormalized loops) that one begins to see the long auto-correlation. Methods like binning or measuring auto-correlation coefficients on the original lattice would have failed to expose the auto-correlation length of ≈ 500 from a measurement of 6×6 unblocked loops over 5000 sweeps. The MCRG method is also faster than measuring large unrenormalized loops because blocking and measuring the plaquette are trivially vectorized. Lastly, the method highlights the amount of ultra-violet contamination that exists in lattice measurements.



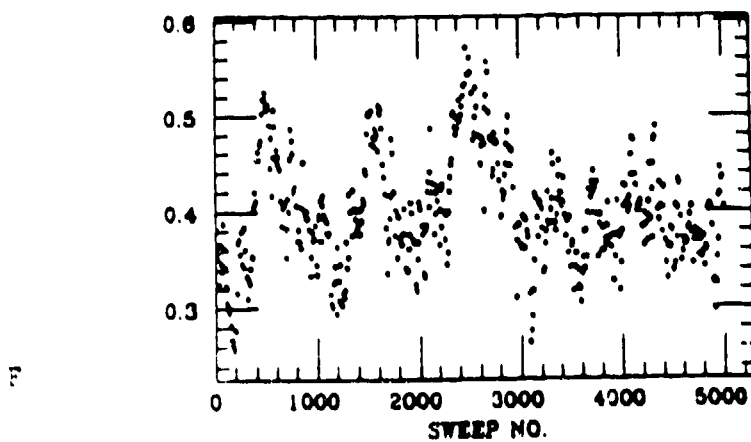
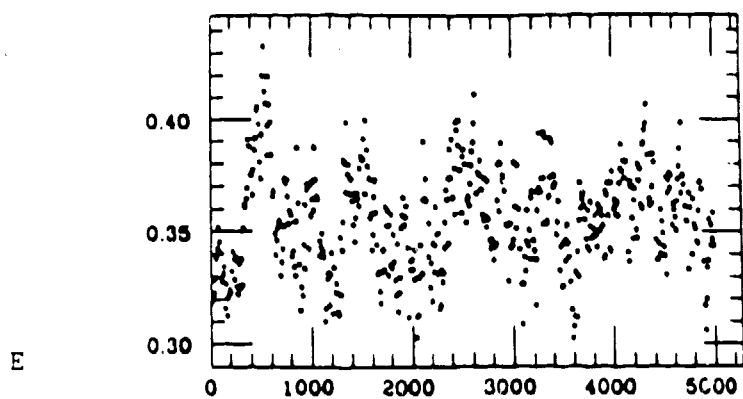


Fig. 10: Demonstration of auto-correlations using block loops. a) Plaquette on $(9\sqrt{3})^4$ lattice shows random behavior. b) Blocked plaquette (BP) on 9^4 lattice shows random behavior. c) Twice BP on $(3\sqrt{3})^4$ lattice shows almost random behavior. d) Thrice BP on 3^4 lattice starts to show correlations. e) Four times BP on $(\sqrt{3})^4$ lattice shows correlations. f) Five times BP on 1^4 lattice shows an auto-correlation length of ≈ 500 .

9: EFFECTIVE FIELD THEORIES

The point of effective field theories is that physical phenomena at some given length scale can be described by some effective/composite degrees of freedom. The couplings between these variables are determined by the underlying microscopic theory. Thus we would like to know these effective degrees of freedom and the corresponding couplings. So far the discussion of *MCRG* has focused on the change of scale without a change of variables. To make full use of its power, a transformation of variables at the appropriate scale should be added *i.e.* in addition to a *RGT* that just averages over degrees of freedom, consider a change from the microscopic theory to an effective theory with new variables at some give length scale. These variables can be composite (as is the case in going from QCD to a theory where the degrees of freedom are hadrons) or represent a freezing as in $SU(2)$ at high temperatures where the interaction between the Wilson lines is described by an effective $d = 3$ Ising model. Here one transforms from link variables to Wilson lines to Ising spins.

Once the effective theory has been constructed, it is important to know the universality class to which it belongs. This would provide a detailed knowledge of the critical/long distance behavior. Little work has been done in actually exploring universality classes by mapping flows that incorporate a change of variables.

The way to do this in standard *MC* is to define the composite degrees of freedom and their n -point functions in terms of the microscopic variables. From the expectation values of these n -point correlation functions calculated as simple averages, the corresponding couplings can then be determined by a Microcanonical simulation as described in section 5.9. One such calculation is by Ogilvie and Gocksch [84] in which they determine the nearest neighbor couplings between the Wilson lines in $SU(2)$.

In *MCRG*, the transformation from the microscopic degrees of freedom to the composite variables is made on the original lattice (same as in *MC*). The *RGT* is defined on the composite variables and the

critical exponents of the effective theory are calculated from the *LTM*. The couplings can be determined by one or more of the methods of section 5, but keep in mind that these methods have truncation errors. The optimum way to determine the effective couplings is *IMCRG* with H^g a guessed Hamiltonian for the effective theory. This process maps the universality class of the model.

One of the goals of this approach is to fix the parameters of the effective chiral lagrangian.

References

- 1] K. G. Wilson, in *Recent Developments in Gauge Theories*, Cargese (1979), eds. G. t' Hooft, *et al.* (Plenum, New York, 1980).
- 2] R. H. Swendsen, *Phys. Rev. Lett.* **42**, (1979) 859.
- 3] S. H. Shenker and J. Tobochnik, *Phys. Rev.* **B22** (1980) 4462.
- 4] S. K. Ma, *Phys. Rev. Lett.* **37**, (1976) 461.
- 5] L. P. Kadanoff, *Rev. Mod. Phys.* **49**, (1977) 267.
- 6] K. G. Wilson, in *Progress in Gauge Field Theories*, edited by G. t' Hooft *et al.*, (Plenum, New York 1984).
- 7] R. H. Swendsen, in *Real Space Renormalization, Topics in Current Physics*, Vol 30, edited by Th. W. Burkhardt and J. M. J. van Leeuwen (Springer, Berlin, 1982) pg. 57.
- 8] J. M. Drouffe and C. Itzykson, *Phys. Reports* **38** (1978) 133. ;
J. B. Kogut, *Rev. Mod. Phys.* **51** (1979) 659 and **55** (1983) 775. ;
M. Creutz, L. Jacobs and C. Rebbi, *Phys. Rep.* **95**, (1983) 201. ;
M. Creutz, *Quarks, Gluons and Lattices* , Cambridge Univ. Press (1984). ;
J. M. Drouffe and J. B. Zuber, *Phys. Reports* **102** (1983) 1.
- 9] K. Binder, in *Monte Carlo Methods in Statistical Physics*, edited by K. Binder (Springer, Berlin, 1979) Vol 7 , and in *Applications of Monte Carlo Methods in Statistical Physics*, (Springer Verlag, Heidelberg, 1983).
- 10] I have taken the liberty to use as synonymous the terms action and Hamiltonian since the meaning is clear from the context.
- 11] K. G. Wilson and J. Kogut, *Phys. Rep.* **12C**, (1974) 76.
- 12] P. Pfeuty and G. Toulouse, *Introduction to the Renormalization Group and Critical Phenomenon*, (John Wiley & Sons, New York 1978).
- 13] D. Amit, *Field Theory, the Renormalization Group and Critical Phenomenon*, (World Scientific, 1984).
- 14] N. Metropolis, A. W. Rosenbluth, M. N. Rosenbluth, A. H. Teller and E. Teller, *J. Chem. Phys.* **21** (1953) 1087.
- 15] M. Creutz, *Phys. Rev. D* **21** (1980) 2308.

- 16 D. Callaway and A. Rehman, *Phys. Rev. Lett.* **49** (1982) 613; ;
M. Creutz, *Phys. Rev. Lett.* **50** (1983) 1411; ;
J. Polovni and H. W. Wyld, *Phys. Rev. Lett.* **51** (1983) 2257.
- 17 G. Parisi and Wu Yongshi, *Sci. Sin.* **24** (1981) 483.
- 18 G. G. Batrouni, G. R. Katz, A. S. Kronfeld, G. P. Lepage, B. Svetitsky, and K. G. Wilson, *Phys. Rev.* **D32** (1985) 2736.
- 19 M. Fisher in 'Advanced Course in Critical Phenomenon'; Lecture Notes in Physics, Vol 186, Springer Verlag 1983.
- 20 A. Brandt, in *Multigrid Methods*, Lecture Notes in Math 960, (Springer Verlag 1982) and references therein.
- 21 The idea was first discussed by G. Parisi in *Progress in Gauge Field Theories*, edited by G. 't Hooft, *et al.*, (Plenum, New York, 1984).
- 22 R. Gupta, Work in Progress.
- 23 R. Gupta and A. Patel, *Nucl. Phys.* **B251** (1985) 789.
- 24 R. Swendsen, *Phys. Rev. Lett.* **47** (1981) 1775.
- 25 R. Cordery, R. Gupta and M. A. Novotny, *Phys. Lett.* **128B** (1983) 425.
- 26 K. H. Mütter and K. Schilling, *Nucl. Phys.* **B230** [FS10] (1984) 275.
- 27 D. Callaway and R. Petronzio, *Phys. Lett.* **149B** (1984) 175; ;
This transformation was also known to R. Gupta, B. Svetitsky and K. G. Wilson but not pursued in favor of the first three.
- 28 K. C. Bowler, A. Hasenfratz, P. Hasenfratz, U. Heller, F. Karsch, R. D. Kenway, I. Montvay, G. S. Pawley, and D. J. Wallace, *Nucl. Phys.* **B257** (1985) [FS14] 155; and *Phys. Lett.* **179B** (1987) 375; ;
A. Hasenfratz, P. Hasenfratz, U. Heller and F. Karsch, *Phys. Lett.* **140B** (1984) 76.
- 29 M. E. Fisher and M. Randeria, *Phys. Rev. Lett.* **56** (1986) 2332.
- 30 R. Gupta, *Proceedings of the Wuppertal Conference on Lattice Gauge Theory*, Academic Press (1986).
- 31 A. Patel and R. Gupta, *Phys. Lett.* **183B** (1987) 133.
- 32 R. H. Swendsen, *Phys. Rev. Lett.* **52** (1984) 2321.
- 33 R. Gupta, C. Umrigar and K. G. Wilson, work under progress.
- 34 G. Bhanot, *Nucl. Phys.* **B208** (1982) 168.

- [35] H. G. Evertz, J. Jersák, T. Neuhaus and P. M. Zerwas, *Nucl. Phys.* **B251** (1985) 279.
- [36] The presence this phase transition was shown analytically by A. Guth, *Phys. Rev.* **D21** (1980) 2291; and by J. Frölich and T. Spencer, *Commun. Math. Phys.* **83** (1982) 411.
- [37] T. Banks, R. Mayerson and J. Kogut, *Nucl. Phys.* **B129** (1977) 493.
- [38] T. A. DeGrand and D. Toussaint, *Phys. Rev.* **D22** (1980) 2478.
- [39] R. Gupta, M. A. Novotny and R. Cordery, Northeastern Preprint 2654 (1984); and *Phys. Lett.* **172B** (1986) 86.
- [40] J. Barber, *Phys. Lett.* **147B** (1984) 330.
- [41] V. Grösch, K. Jansen, J. Jersák, C. B. Lang, T. Neuhaus and C. Rebbi, *Phys. Lett.* **162B** (1985) 171.
- [42] C. Lang, *Nucl. Phys.* **B280**(1987) 255 .
- [43] A. N. Burkitt, *Nucl. Phys.* **B270** (1986) 575.
- [44] K. Decker, A. Hasenfratz and P. Hasenfratz, *Talk at the BNL Lattice conference, 1986.*
- [45] R. Gupta, G. Guralnik, A. Patel, T. Warnock and C. Zemach, *Phys. Rev. Lett.* **53** (1984) 1721. ;
R. Gupta, G. Guralnik, A. Patel, T. Warnock and C. Zemach, *Phys. Lett.* **161BB** (1985) 352.
- [46] R. Gupta, G. Guralnik, G. Kilcup, A. Patel and S. Sharpe, in preparation.
- [47] M. Creutz, *Phys. Rev.* **D23** (1981) 1815.
- [48] F. Gutbrod, *Phys. Lett.* **186B** (1985)389.
- [49] D. Petcher, *Nucl. Phys.* **B275** [FS17] (1986) 241.
- [50] R. Gupta, Lecture on glueballs; *ibid.*
- [51] R. Gupta, Lecture on $\bar{q}q$ Potential; *ibid.*
- [52] S. Gottlieb, A. D. Kennedy, J. Kuti, S. Meyer, B. J. Pendleton, R. Sugar and D. Toussaint, *Phys. Rev. Lett.* **55** (1985) 1958; ;
D. Toussaint, *Talk at the BNL Lattice Conference, 1986.*
- [53] N. Christ, Private Communications.
- [54] P. De Forcrand, *Proceedings of the Metropolis Conference, Los Alamos* (1985), *J. Stat. Phys.* **43** (1986) 1077; and private com-

munications.

- [55] K. Symansik, in *Proceedings of the Trieste workshop on non-perturbative field theory and QCD (dec. 1982)*, World Scientific (1983) 61.
- [56] P. Weisz and R. Wohlert, *Nucl. Phys.* **B236** (1984) 397.
- [57] G. Curci, P. Menotti and G. P. Paffuti, *Phys. Lett.* **130B** (1983) 205.
- [58] P. de Forcrand and C. Roiesnel, *Phys. Lett.* **137B** (1984) 213, and *Phys. Lett.* **143B** (1984) 453. ;
P. de Forcrand, Ecole Polytechnique preprint A615.0784 (July 1984).
- [59] Y. Iwasaki, preprint UTHEP-118 (1983) ;
S. Itoh, Y. Iwasaki and T. Yoshie, *Phys. Lett.* **183B** (1987) 351 and *Phys. Lett.* **185B** (1987) 390.
- [60] K. M. Bitar, S. Gottlieb and C. Zachos, *Phys. Rev.* **D26** (1982) 2853.
- [61] K. Bitar, D. Duke and M. Jadid, *Phys. Rev.* **D31** (1985) 1470.
- [62] D. Barkai, K. J. M. Moriarty and C. Rebbi, *Phys. Rev.* **D30** (1984) 2201.
- [63] O. Martin, K. Moriarty and S. Samuel, *Nucl. Phys.* **B261** (1985) 433.
- [64] B. Grossmann and S. Samuel, *Phys. Lett.* **120B** (1983) 383.
- [65] A. Gonzales Arroyo and C. P. Korthals Altes, *Nucl. Phys.* **B205** [FS5] (1982) 46. ;
R. K. Ellis and G. Martinelli, *Nucl. Phys.* **F135** [FS11] (1984) 93.
- [66] R. H. Swendsen, *Phys. Rev. Lett.* **52** (1984) 1165.
- [67] H. B. Callen, *Phys. Lett.* **4B** (1961) 161.
- [68] C. Lang in *The Proceedings of the Tallahassee Conference on Advances in Lattice Gauge Theory*, (World Scientific, 1985).
- [69] D. Callaway and R. Petronzio, *Phys. Lett.* **139B** (1984) 189.
- [70] K. G. Wilson and C. Umrigar, unpublished.
- [71] K. Bitar, *Phys. Rev.* **D35** (1987) 691.
- [72] D. Callaway and R. Petronzio, *Nucl. Phys.* **B240** [FS12] (1984) 577.

- [73] M. Falcioni, G. Martinelli, M. L. Paciello, G. Parisi, B. Taglienti, *Nucl. Phys.* **B265** (1986) [FS15] 187.
- [74] R. Gupta and A. Patel, *Phys. Rev. Lett.* **53** (1984) 531 ;
R. Gupta and A. Patel, *Proceedings of the Argonne Conference on Gauge Theory On a Lattice*, (1984).
- [75] M. Creutz, A. Gocksch, M. Ogilvie and M. Okawa, *Phys. Rev. Lett.* **53** (1984) 875.
- [76] P. Stolorz, *Phys. Lett.* **172B** (1986) 77.
- [77] A. Konig, K. H. Mütter and K. Schilling, *Nucl. Phys.* **B259** (1985)33, and in the *Proceedings of BNL conference on Lattice Gauge Theory*, (1986).
- [78] R. Gupta and R. Cordery, *Phys. Lett.* **A105** (1984) 415.
- [79] R. Gupta in *Proceedings of the Tallahassee Conference on Advances in Lattice Gauge Theory*, World Scientific (1985).
- [80] R. Shankar, R. Gupta and G. Murthy, *Phys. Rev. Lett.* **55** (1985) 1812.
- [81] R. Shankar, *Phys. Rev.* **B33** (1986) 6515.
- [82] A. Hasenfratz and A. Margaritis, *Phys. Lett.* **133B** (1983) 211 ;
A. Hasenfratz and A. Margaritis, *Phys. Lett.* **148B** (1984) 128.
- [83] R. Gupta, G. Guralnik, G. Kilcup, A. Patel and S. Sharpe; Unpublished.
- [84] A. Gocksch and M. Ogilvie, *Phys. Rev. Lett.* **54** (1985) 1985.